AD-A048 852 JOHNS HOPKINS UNIV LAUREL MD APPLIED PHYSICS LAB F/G 20/12
INDIRECTLY FUNDED RESEARCH AND EXPLORATORY DEVELOPMENT AT THE A--ETC(U)
JUL 77 R W HART N00017-72-C-4401
UNCLASSIFIED APL/JHU/SR-77-2 NL

1 OF 3
AD
A048852

APL/JHU
SR 77-2
JULY 1977

(12)
B.S.

Special Reports

INDIRECTLY FUNDED RESEARCH AND EXPLORATORY DEVELOPMENT AT THE APPLIED PHYSICS LABORATORY

FISCAL YEAR 1976

THE JOHNS HOPKINS UNIVERSITY ■ APPLIED PHYSICS LABORATORY

Unclassified

SECURITY CLASSIFICATION OF THIS PAGE

PLEASE FOLD BACK IF NOT NEEDED FOR BIBLIOGRAPHIC PURPOSES

REPORT DOCUMENTATION PAGE

1. REPORT NUMBER: APL/JHU/SR-77-2 (14)	2. GOVT ACCESSION NO.
3. RECIPIENT'S CATALOG NUMBER	
4. TITLE (and Subtitle): INDIRECTLY FUNDED RESEARCH AND EXPLORATORY DEVELOPMENT AT THE APPLIED PHYSICS LABORATORY, FISCAL YEAR 1976. (6)	5. TYPE OF REPORT & PERIOD COVERED: Annual Report. 1 Oct 75 - 30 Sep 76 (9)
	6. PERFORMING ORG. REPORT NUMBER
7. AUTHOR(s): R. W. Hart Editor (10)	8. CONTRACT OR GRANT NUMBER(s): N00017-72-C-4401 (15)
9. PERFORMING ORGANIZATION NAME & ADDRESS: The Johns Hopkins University Applied Physics Laboratory, Johns Hopkins Rd., Laurel, MD 20810	10. PROGRAM ELEMENT, PROJECT, TASK AREA & WORK UNIT NUMBERS: ~~NA~~
11. CONTROLLING OFFICE NAME & ADDRESS: Naval Plant Representative Office, Johns Hopkins Rd., Laurel, MD 20810 (11) Jul 77	12. REPORT DATE: Fiscal Year 1976
	13. NUMBER OF PAGES: 194 (3 blank)
14. MONITORING AGENCY NAME & ADDRESS: Naval Plant Representative Office, Johns Hopkins Rd., Laurel, MD 20810 (12) 193p.	15. SECURITY CLASS. (of this report): Unclassified
	15a. DECLASSIFICATION/DOWNGRADING SCHEDULE: NA
16. DISTRIBUTION STATEMENT (of this Report): Approved for public release; distribution unlimited.	
17. DISTRIBUTION STATEMENT (of the abstract entered in Block 20, if different from Report)	
18. SUPPLEMENTARY NOTES	

19. KEY WORDS (Continue on reverse side if necessary and identify by block number)

Basic research
Fundamental research
Indirectly funded research
Research Center annual report

20. ABSTRACT (Continue on reverse side if necessary and identify by block number)

This report summarizes the Indirectly Funded Research and Exploratory Development activities of The Johns Hopkins University Applied Physics Laboratory during fiscal year 1976 (1 October 1975-30 September 1976).

DD FORM 1 JAN 73 1473

031 650

Unclassified

SECURITY CLASSIFICATION OF THIS PAGE

LB

APL/JHU
SR 77-2
JULY 1977

Special Reports

INDIRECTLY FUNDED
RESEARCH AND EXPLORATORY DEVELOPMENT
AT THE APPLIED PHYSICS LABORATORY
FISCAL YEAR 1976

R. W. HART, Editor

THE JOHNS HOPKINS UNIVERSITY ■ APPLIED PHYSICS LABORATORY
Johns Hopkins Road, Laurel, Maryland 20810
Operating under Contract N00017-72-C-4401 with the Department of the Navy

2

THE JOHNS HOPKINS UNIVERSITY
APPLIED PHYSICS LABORATORY
LAUREL, MARYLAND

ABSTRACT

This report summarizes the Indirectly Funded Research and Exploratory Development activities of The Johns Hopkins University Applied Physics Laboratory during fiscal year 1976 (1 October 1975-30 September 1976).

Preceding Page Blank - Filmed

CONTENTS

subject areas reported on include:

THE RESEARCH CENTER

(cont fr p 5)

and

EXPLORATORY DEVELOPMENT --

(cont on p 7)

(cont fr p 6)

PUBLICATIONS

Preceding Page Blank - Filmed

THE INDIRECTLY FUNDED RESEARCH AND DEVELOPMENT PROGRAM

The need to adapt to the future conflicts with the day-to-day tasks of research and development engineering laboratories. On the one hand, the Laboratory must exercise innovative capabilities and advance the state of the art if it is to avoid obsolescence. On the other hand, the engineering tasks of the Laboratory require commitment to prescribed completion dates and therefore must involve essentially state-of-the-art technology. The Indirectly Funded Research and Development (IR&D) Program provides for innovation and technological advances that cannot be supplied within directly funded engineering development tasks.

The central objective of the IR&D program is to enhance the present and future vigor of the Laboratory. Accordingly, the IR&D efforts continue to be aimed at

1. Providing current, in-depth understanding of technical fields of importance to the Laboratory's applied tasks,

2. Originating and exploring new concepts of potential importance to the solution of national problems, and

3. Providing a window into science to cultivate the technical competence of the Laboratory as an organization devoted to development and engineering tasks.

The research component of the IR&D program is carried out in the Research Center of the Laboratory; the exploratory development component of the IR&D program is performed by project initiators in the task divisions of the Laboratory. The Research Center program, coordinated by the Director, the Program Review Board of the Laboratory, and the Chairman of the Research Center, looks mainly toward advancing science and the transfer of new concepts into the Laboratory's technology. Exploratory development projects are primarily short-term explorations of the feasibility of new ideas applicable to hardware systems, components, and materials and must be specifically authorized by the Director.

The IR&D program continues to be productive. Among its more notable contributions is the concept of doppler navigation by satellite that led to the Navy Navigation Satellite System. Other contributions, as described in previous reports, include development of the concepts of detection and tracking of aircraft that led to the Navy's AN/SYS-1 automated system, dual-mode Redeye, electrostatic stabilization of aircraft, and the box-type launching system.

This year, the importance of the box launcher was recognized by the award of the Navy Distinguished Public Service Medal to Mr. S. Kongelbeck, who conceived and led the project at the Laboratory.

Since the Laboratory is primarily engaged in work for the Navy and the Department of the Defense (DoD), the IR&D program is mainly concerned with Navy- and DoD-related problems. However, with the encouragement of the Secretary of Defense and the Department of the Navy, the Laboratory also works on urgent problems for other agencies, including the National Aeronautics and Space Administration, the National Institutes of Health, the Energy Research and Development Administration, the Federal Aviation Administration, and the State of Maryland. This year, as for the previous year, about 15% of the Laboratory's efforts were directly funded by civilian agencies. Accordingly, IR&D projects are carried out in appropriate non-DoD areas.

The IR&D program summarized in this report makes significant contributions to the Laboratory and to the scientific and technological community.

THE RESEARCH CENTER

INTRODUCTION

The central purpose of the Research Center is to enhance the scientific and technological vigor of the Laboratory. Accordingly, research is carried out to explore and advance new concepts of present and potential importance and to stimulate the technological application of new developments in basic science.

The IR&D program continues to comprise about two-thirds of the work of the Research Center. It is this program that provides the long-term continuity essential to in-depth research and innovative competence in fields that are important to the present and that are expected to be important for the future. The remaining fraction of the Research Center's efforts is devoted to investigations and counsel in support of non-Research Center tasks and to research projects funded by agencies external to the Laboratory. To disseminate information to the general scientific and technological community, the research results are presented in addresses at regularly scheduled scientific meetings and at academic and institutional seminars, and are published in the professional literature. To disseminate information within the Laboratory, seminars are held to report on relevant national and international professional meetings, as well as on current investigations within the Research Center.

In part, the facilities for advanced research include a microwave physics laboratory, a laser laboratory, a solid-state laboratory (with a sputter ion mass spectrometer), a mass spectrometry laboratory, a molecular free radical laboratory, a gas kinetic laboratory (with a fast-flow reactor), a scanning electron microscope laboratory (with an ultrahigh vacuum for surface studies), and a spectroscopy laboratory equipped for work in the ultraviolet, visible, and infrared regions of the spectrum.

The size of the Research Center remains essentially constant. The professional staff consists of 40 senior physicists, chemists, mathematicians, and engineers, assisted by six associate investigators and a supporting staff of 14 technicians, machinists, and secretaries. The work of these investigators is augmented, in effect, by collaboration with many colleagues at other institutions, including universities, government, industrial, and nonprofit laboratories.

The Research Center is structured into the following eight groups: (a) the Theoretical Problems Group, devoted primarily to applied analysis in diverse topics; (b) the Applied Mathematics

Group, devoted primarily to the development of analytical and numerical techniques for partial differential equations and spectral theory; (c) the Electronic Physics Group, devoted primarily to improved understanding of energy-transfer mechanisms at the atomic and molecular level; (d) the Chemical Physics Group, aimed primarily at improved understanding of the kinetics of gas-phase interactions; (e) the Microwave Physics Group, aimed toward the development of improved understanding of electromagnetic behavior of condensed phase materials; (f) the Quantum Electronics Group, devoted mainly to increased understanding of electromagnetic mechanisms important to lasers and to organic conductors; (g) the Excitation Mechanisms Group, concerned with laser excitation mechanisms and applications; and (h) the Solid State Physics Group, concerned primarily with developing the properties of disordered semiconductors.

Nontechnical Highlights

Throughout the year, as in the past, the efforts of the Research Center continued as an orderly unfolding of the work of the past, modulated by changing Laboratory needs and new advances in science and technology. One indication of productivity and professional competence is the fact that during the year 52 Research Center manuscripts were published in the professional literature and an additional 13 manuscripts were accepted for publication. It is also noteworthy that Dr. V. O'Brien of the Research Center's Theoretical Problems Group was invited to serve on a National Academy of Sciences National Research Council Associateship Evaluation Panel and also that she was elected a Fellow of the American Physical Society. Other items worthy of mention include that Dr. L. Monchick of the Chemical Physics Group served as the William S. Parsons Visiting Professor in the Chemistry Department of The Johns Hopkins University during the academic year 1975-76, and that Dr. D. M. Silver of the Theoretical Problems Group was invited to give the Chemistry Department's Research Seminar on Theoretical Chemistry for this academic year. Dr. D. W. Fox, head of the Applied Mathematics Group, was appointed the William S. Parsons Visiting Professor in the University's Department of Mathematical Sciences for the academic year 1976-77. Also, Dr. M. H. Friedman, head of the Theoretical Problems Group, was appointed Visiting Scholar at Stanford University in their Department of Ophthalmology. Dr. K. Moorjani of the Solid State Physics Group was invited and supported by the Centre de la Recherche Scientifique to attend the International Colloquium on Metal-Nonmetal Transitions (Autrans, France). Among the more distinguished invited talks, it is to be noted that Dr. F. J. Adrian, head of the Microwave Physics Group, has been asked to lecture at the NATO Advanced Study Institute on Chemically Induced Magnetic Polarization, scheduled for April 1977.

Technical Highlights

Research in laser mechanisms and applications continues to be carried out in the Quantum Electronics and Excitation Mechanisms Groups. One of the most potentially significant developments of the past year is the development of a new concept for a supersonic-flow CW laser to avoid most of the serious aerothermodynamic problems of conventional high-powered chemical lasers. The concept, initiated and being explored by the Excitation Mechanisms Group, is now directly funded by the Navy. It is also noteworthy that a collaborative research project has been developed to assist the Naval Surface Weapons Center (NSWC) in the diagnostics of electrical discharge CO_2 lasers intended ultimately for shipboard high-resolution laser radar.

Increasing emphasis continues to be placed on selected aspects of the mechanics of fluids. The area of focus concerns the effects of water flow past submerged or partially submerged bodies, a most important hydrodynamic problem area for the Navy. The development of sophisticated new techniques for stratified flows has proceeded apace through a second year of fruitful activity in the Applied Mathematics Group. A study of the electromagnetic effects of such flows and a study of the influence of a submerged body on the surface wave structure (nonstratified flow) have been completed in the Theoretical Problems Group.

A general trend continues toward increased concern with interfacial and near-surface physics and chemistry, in concert with generally increasing levels of such activity elsewhere and increasing expectations for improved technology in electronics and energy-related areas. In the Electronics Physics Group, a new research project dealing with corrosion of surfaces was initiated, following the installation last year of the ultrahigh vacuum scanning electron microscope. Pitting under an almost intact protective oxide layer has been conclusively demonstrated under certain conditions.

A second new surface-research project concerns corrosion and electrochemistry of electrolyte-semiconductor interfaces and the potential use of such "junctions" as inexpensive solar cells or solar batteries. This small-scale collaborative effort involves members of three groups: the Solid State Physics Group, the Quantum Electronics Group, and the Theoretical Problems Group.

A third new surface-science study was initiated in the Microwave Physics Group to apply the newly developing technique of photoacoustic spectroscopy to the study of gas-solid surface phenomena. This study has already led to significant new insights, especially with respect to mechanisms whereby light incident on a surface is absorbed and reemitted as fluorescent or phosphorescent radiation.

Vacuum-deposited thin films continue as the center of interest in the Solid State Physics Group, where research deals primarily with realizing advantageous polycrystalline solar cells. Significant improvements have been achieved with respect to film thickness, grain size, and solar cell efficiency. In this context, a unique nondestructive technique for estimating certain impurities was conceived and demonstrated.

Finally, it is interesting to note that results of electron spin resonance investigations carried out in past years by the Research Center have become a focus of interest in astrophysics. The data facilitate identification of free radicals newly discovered in interstellar space by radio astronomers at other laboratories.

APPLIED ANALYSIS

The Applied Analysis component of the IR&D program is characterized by the development of theoretical techniques and their application to a range of problems of interest to the Laboratory and its Naval and civilian sponsors.

In addition to continuing a number of ongoing research studies, several new projects have been initiated this year. The activity in theoretical chemistry on molecular structure and reactivity is continuing with the addition of a new study on the application of Padé approximants to perturbation theory. Further progress has been made on phase transitions, viscous flow, and transport theory and laser intensity correlation spectroscopy. New projects in the area of wave phenomena include analysis of the scattering of surface waves by a submerged sphere and scattering from rough surfaces. In addition, hydromagnetism in the ocean and interfacial transport across structured membranes represent further new areas of interest. The research is carried out through the part-time efforts of nine senior scientists, in several instances with the collaboration of scientists in other divisions and at other institutions not funded by the APL IR&D program.

Eight unclassified journal publications were issued during the present reporting period, and nine others were accepted for future publication. Dr. V. O'Brien, a member of the Group, was elected to Fellowship in the American Physical Society and invited to be a member of the National Research Council Research Associateship Evaluation Panel. Dr. M. H. Friedman, Supervisor of the Group, was invited to Stanford University for two months as a Visiting Scholar; he continues to serve as (part-time) Associate Professor of Ophthalmology in the Johns Hopkins School of Medicine.

THEORETICAL CHEMISTRY: MOLECULAR STRUCTURE AND REACTIVITY

Diagrammatic techniques of many-body perturbation theory have been exploited for the determination of the electronic structure of atoms and molecules. Classical dynamical trajectory calculations have been performed to examine reactive and inelastic collisions between two hydrogen molecules.

The electronic structure of atoms and molecules plays a dominant role in chemical reactivities. Since chemical reactions pervade the fields of combustion, propulsion, and other energy-related phenomena, a detailed understanding of these processes is important for future DoD and civilian applications. The studies in theoretical chemistry are a continuing effort to develop methods

for quantitative considerations of molecular structures and reactivities.

One of the goals of atomic and molecular collision studies is the calculation of cross sections and rate constants for inelastic and reactive chemical processes with sufficient accuracy to predict or reproduce results of experimental measurements. In a chemical collision system, the second Born-Oppenheimer approximation is usually invoked to separate the equations governing the motions of nuclei from those of electrons. Thus the motion of the nuclei, which comprise the dynamical system under study, is assumed to be governed by a potential energy function or surface corresponding to the quantum mechanical solution of the appropriate molecular electronic problem. Since, as we have shown, the results of collision or scattering calculations are usually quite sensitive to the detailed nature and properties of the potential energy surface employed (Ref. 1), it is essential that the most accurate and realistic potential surfaces be generated for use in dynamical studies. One solution to this problem is our application of many-body perturbation theory to the electronic structure of molecules (Ref. 2).

We have developed the technique of applying many-body perturbation theory to determine the structure of molecules from preliminary calculations restricted to two-body interactions (Refs. 3, 4, and 5). We truncate the perturbation series after third order with higher order contributions included by means of denominator shifts (Ref. 6). In the many-body approach, the correlation energy is developed in terms of several diagrams representing the various types of interelectronic interactions. Such diagrams are particularly useful for translating algebraic expressions into extremely efficient computational schemes for use on the computer.

Our subsequent calculations (Refs. 7 and 8) encompass the rigorous evaluation of all diagrams in the many-body perturbation series for the energy through third order, including all the many-body effects that arise. In addition to achieving a balanced description of the system, the inclusion of all many-body effects permits the development of rigorous variational many-body perturbative schemes for constructing upper bounds to the energy. The absolute accuracy of the results obtainable is directly dependent on the quality of the basis sets employed. However, the agreement with singly and doubly excited configuration interaction results for neon is within 1.1% for our perturbation scheme and within 2.3% for our variational scheme (Ref. 9). This demonstrates the inherent power of the diagrammatic perturbation method.

In developing the many-body methods for molecular applications, a number of aspects must be considered. One of these involves

the use of modified potentials, rather than the standard Hartree-Fock potential, for the determination of excited state orbitals. Although it is possible to tailor these orbitals to some physical feature of the system under study by using a modified potential, we find (Ref. 3) that the modified and standard potentials yield total electronic energies within 1 kcal/mole of one another when the perturbation calculations are performed through third order with shifted denominators. This shows that the costly integral transformation, required when a modified potential is used, can be avoided without significant sacrifice of accuracy. By including three-body and four-body contributions to the energy, we have strengthened these results by providing an upper-bound criterion with which the results can be judged (Ref. 10).

Currently, this work is being extended to include applications to excited state species, open-shell configurations, and degenerate energy levels. These extensions should bring the diagrammatic many-body perturbative scheme into use for the calculation of potential energy surfaces corresponding to collisions between molecules in ground states or excited states.

<u>Principal Investigators</u>: D. M. Silver, S. Wilson, N. J. Brown, and R. J. Bartlett. Dr. Silver is a senior chemist in the Theoretical Problems Group of the Research Center. Dr. Wilson held a postdoctoral appointment at the Applied Physics Laboratory during this year. Drs. Brown (University of California, Berkeley) and Bartlett (Batelle Memorial Institute) are not funded by the program.

<u>References</u>

1. N. J. Brown and D. M. Silver, "Reactive and Inelastic Scattering of $H_2 + D_2$ using a London-Type Potential Energy Surface," <u>J. Chem. Phys.</u>, Vol. 65, No. 1, 1 July 1976, pp. 311-325.

2. D. M. Silver, "Calculation of Potential Energy Surfaces Using Many-Body Perturbation Theory" in "Report of Workshop on Collisions on Potential Energy Surfaces of Excited States," C. Moser (ed.), Centre Européen de Calcul Atomique et Moléculaire, Université de Paris XI, Orsay, France, 31 May 1976, pp. 235-253.

3. D. M. Silver and R. J. Bartlett, "Modified Potentials in Many-Body Perturbation Theory," <u>Phys. Rev. A</u>, Vol. 13, January 1976, pp. 1-12.

4. R. J. Bartlett and D. M. Silver, "Many-Body Perturbation Theory Applied to Electron Pair Correlation Energies. II. Closed-Shell Second-Row Diatomic Hydrides," J. Chem. Phys., Vol. 64, No. 11, 1 June 1976, pp. 4578-4586.

5. R. J. Bartlett and D. M. Silver, in Quantum Science, Plenum Press, New York, 1976, pp. 393-408.

6. R. J. Bartlett and D. M. Silver, "Some Aspects of Diagrammatic Perturbation Theory," Int. J. Quantum Chem. Symp., Vol. S9, December 1975, pp. 183-198.

7. S. Wilson and D. M. Silver, "Diagrammatic Perturbation Theory: Many-Body Effects in the $X^1\Sigma^+$ States of First-Row and Second-Row Diatomic Hydrides," J. Chem. Phys. (to be published).

8. S. Wilson, R. J. Bartlett, and D. M. Silver, "Many-Body Effects in the $X^1\Sigma^+$ States of the Hydrogen Fluoride, Lithium Fluoride and Boron Fluoride Molecules," Mol. Phys. (to be published).

9. S. Wilson and D. M. Silver, "Algebraic Approximation in Many-Body Perturbation Theory," Phys. Rev. A, Vol. 14, December 1976.

10. D. M. Silver, S. Wilson, and R. J. Bartlett, "Modified Potentials in Many-Body Perturbation Theory: Three-Body and Four-Body Contributions," Phys. Rev. A (to be published).

APPLICATION OF PADÉ APPROXIMANTS TO PERTURBATION THEORY

The analytic continuation techniques of Padé approximants are applied to the Rayleigh-Schrödinger perturbation theory for the energy of atoms and molecules. It is demonstrated that the use of the [N+1/N] Padé approximants eliminates a certain arbitrariness in the splitting of the known exact Hamiltonian into unperturbed and perturbed parts.

Rayleigh-Schrödinger perturbation theory provides a convenient method for describing the corrections to independent particle models of the electronic structure of atoms and molecules. Although the exact Hamiltonian is known for these systems, the corresponding wave functions are not known. The perturbation theory approach to these problems is to choose a suitable zeroth order

Hamiltonian, H_0, whose eigenfunctions are known and to consider systems described by Hamiltonians $H_0 + \lambda H_1$. For problems where the exact Hamiltonian, $\mathcal{H}$, is known, one chooses $H_1 = \mathcal{H} - H_0$ so that the exact Hamiltonian is recovered at $\lambda = 1$. Considerable freedom exists in the choice of H_0; for example, one might modify a given H_0 to produce a change of scale and a shift of origin in the zeroth-order energy spectrum, provided H_1 is suitably modified so that $\mathcal{H}$ is recovered at $\lambda = 1$. The exact energy for these systems is written as a power series in the variable λ. In practical applications, the power series must be truncated at some finite order, M, omitting a residual contribution of order $O(\lambda^{M+1})$.

We have found that [P/Q] Padé approximants provide useful alternative representations of the energy. If P + Q = M, these approximants can be determined from the Mth order series, and, moreover, each of these approximants also only omits residual contributions of order $O'(\lambda^{M+1})$. Thus, the question arises as to which of these approximants one should use to estimate the energy. The first suggestion that an appropriate representation could be selected on the basis of the behavior of the various approximants under arbitrary changes of scale and/or origin in the zeroth-order operator became apparent to us during some exploratory numerical studies. As noted above, the exact Hamiltonian is recovered at $\lambda = 1$ so that these changes will not affect the exact energy. However, truncation at a finite order can produce an apparent dependence of the energy on these changes. In fact, numerical analysis of the 41-term series for the H^- ion shows that the only entries that do not depend on these changes belong to the class of [N+1/N] approximants for all the values of N available. We also demonstrate that this invariance is a direct consequence of the transformation relations among the coefficients in the unmodified Hamiltonian and those in the shifted-and-scaled Hamiltonian and are totally independent of the actual values of the coefficients. Thus, the use of the [N+1/N] Padé approximant eliminates a certain arbitrariness in the splitting of the Hamiltonian into unperturbed and perturbed parts, which suggests the appropriateness of this representation. This work has been submitted for publication (Ref. 1).

<u>Principal Investigators</u>: R. A. Farrell, D. M. Silver, and S. Wilson. Drs. Farrell and Silver are senior physicists of the Theoretical Problems Group of the Research Center. Dr. Wilson held a postdoctoral appointment at the Applied Physics Laboratory during this year.

<u>Reference</u>

1. S. Wilson, D. M. Silver, and R. A. Farrell, "Special Invariance Properties of the [N+1/N] Padé Approximant to the Rayleigh-Schrodinger Perturbation Expansion," submitted for publication in <u>Proc. R. Soc.</u>

SCATTERING OF SURFACE WAVES BY A SUBMERGED SPHERE

The problem of the scattering of surface waves in a nonviscous, incompressible fluid of infinite depth by a fully submerged, rigid, stationary sphere has been solved in this work. The solution is expressed in terms of an infinite set of linear algebraic equations for the expansion coefficients in spherical harmonics of the velocity potential. The scattering cross section has been evaluated numerically and is shown to peak for values of the product of radius and wave number somewhat less than unity. Also, the Born approximation to the cross section is obtained in closed form and compared with the exact solution.

The problem of determining the influence of a submerged body on the ambient surface wave structure (and the converse problems of the influence of surface waves on a submerged body) is an old one, going back almost a century to Sir W. Thomson and Sir H. Lamb. But while a great deal of effort has been devoted since then to the solution of various special cases and the development of a variety of approximation methods, one of the simplest and most important cases has remained unsolved: the modification (i.e., scattering) of a surface wave by a completely submerged, rigid, stationary sphere.

The present work (Ref. 1) provides an exact solution to this problem for a homogeneous, incompressible, nonviscous fluid of infinite depth and infinite extent. The approach is to cast the equation for the velocity potential into the form of an integral equation. The integral extends over the surface of the sphere and has as its kernel an appropriate Green's function; an explicit expression for this function was obtained in Kochin's pioneering work (Ref. 2), rederived independently by John (Ref. 3), and further developed by Wehausen and Laitone (Ref. 4). Expansion in spherical harmonics of the Green's function and the velocity potentials of the known incident and unknown modified wave permits us to evaluate the integrals analytically and leads to an infinite set of linear algebraic equations for the unknown expansion coefficients. As long as the center of the sphere is submerged by more than about a sphere diameter, only the first few harmonics contribute significantly, and the corresponding coefficients are readily found by truncating the expansion. The equation of the free surface, which embodies the desired modification of the incident wave, is obtained directly from this modified velocity potential. This approach makes it easy to calculate both the total and the partial scattering cross sections of such a submerged sphere.

We have also calculated (Ref. 1) the Born approximation to the scattering cross section. In this approximation, the unknown velocity potential in the integrand (on the surface of the spherical scatterer) is approximated by the known velocity potential of the

incident wave, thereby reducing the problem from an integral equation to the evaluation of an integral. This integral can be evaluated in closed form as a very simple expression involving modified Bessel functions, and we show that it leads to a good approximation to the exact scattering cross section. In addition to providing a simpler method for calculating the cross section when great accuracy is not required, the Born approximation can also be used to interpret physically the qualitative features of the dependence of the cross section on the two dimensionless parameters: The ratio of the depth of the sphere center to the radius, a, and the ratio of a to the surface wavelength.

One of the most striking characteristics of the cross section for the scattering of a surface wave by a submerged sphere is that, as a function of the product of wavenumber and radius, it has a single pronounced peak. This is in sharp contrast to the many well known cases of acoustic and electromagnetic waves scattered by spheres, where the cross section has an oscillatory structure caused by diffraction. The reason that these oscillations are largely washed out in the present case of surface wave scattering lies in the exponential decay of surface waves with depth.

The same approach that has produced these results is likely to succeed if the sphere is in uniform, horizontal motion under laminar flow conditions and if the sphere is replaced by a spheroid. This work will be presented to the November meeting of the American Physical Society at Eugene, Oregon, 22-24 November 1976, and has been submitted for publication.

Principal Investigator: E. P. Gray. Dr. Gray is a senior physicist in the Theoretical Problems Group of the Research Center.

References

1. E. P. Gray, "Scattering of a Surface Wave by a Submerged Sphere," submitted to J. Eng. Math.

2. N. E. Kochin, "The Theory of Waves Generated by Oscillations of a Body Under the Free Surface of a Heavy, Incompressible Fluid," Uchenye Zapiski Moskov. Gos. Univ., Vol. 46, No. 85, 1940, transl. in Soc. Nav. Arch. Marine Eng., Tech. Res. Bull. No. 1-10, 1952.

3. F. John, "On the Motion of Floating Bodies. II. Simple Harmonic Motion," Comm. Pure App. Math., Vol. 3, No. 45, 1950.

4. J. V. Wehausen and E. V. Laitone, "Surface Waves," in Handbuch der Physik, Vol. 9, Pt. 3, Fluid Dynamics, S. Flugge, ed., 1960, pp. 445-778.

SCATTERING FROM ROUGH SURFACES

A variational principle is developed for predicting the scattering of electromagnetic radiation from random rough surfaces such as the ocean. This principle provides a technique for improving the results of other predictive methods and also provides a quantitative measure of their accuracy.

The theoretical description of the scattering of waves by statistically rough surfaces continues to be of interest in many areas, including satellite altimetry, radar, sonar, characterization of amorphous surfaces, and characterization of optical surfaces. Considerable progress has been achieved in recent years, but it remains true that analytical treatments continue to be approximate. As in the case of smooth surfaces, an integral equation relates the field at an arbitrary point to the field and/or its derivatives on the surface. In general, two kinds of approximations are involved: (a) the field and/or its derivatives at the surface, and (b) the statistical (roughness) properties of the surface. We regard the statistics of the surface as given and develop an expression for the scattered amplitude that is insensitive to (small) errors made in approximating the surface field.

The initial step is to note that for fixed (nonstatistical) surfaces one can write a variational principle for the scattered amplitude, T, in the form

$$T = \frac{N_1 N_2}{D} , \tag{1}$$

where N_1, N_2, and D are surface integrals whose integrands depend on the fields. If the exact surface fields are used and the amplitude of the incident plane wave is set equal to (-i), $T = N_2$. Thus the closeness of N_1/D to unity (for incident amplitude (-i)) is a measure of the quality of any approximate surface field. Straightforward application of Eq. 1 to statistical surfaces would require evaluation of averages of the form $\langle N_1 N_2 \rangle$, which would be formidable. Fortunately, we have been able to circumvent this difficulty by demonstrating that the expression

$$\langle N_1 \rangle \langle N_2 \rangle / \langle D \rangle \tag{2}$$

provides a variational principle for the ensemble average T, and that when the amplitude of the incident wave is set equal to -i, the closeness of $\langle N_1 \rangle / \langle D \rangle$ to unity is a quantitative measure of

accuracy. Evaluation of the ensemble averages in expression 2 are straightforward, although nontrivial, and applications of 2 to specific problems are currently underway.

We illustrate the method for a scalar field whose normal derivative vanishes on the boundary. The initial results of this investigation have been submitted for publication (Ref. 1).

<u>Principal Investigators</u>: R. A. Farrell, E. P. Gray, and R. W. Hart. Drs. Farrell and Gray are senior physicists in the Theoretical Problems Group of the Research Center, and Dr. Hart is Chairman of the Research Center.

<u>Reference</u>

1. R. W. Hart and R. A. Farrell, "A Variational Principle for Scattering from Rough Surfaces" (submitted for publication to <u>IEE-AP</u>).

INTERFACIAL TRANSPORT ACROSS STRUCTURED MEMBRANES

Membrane transport is important to a wide variety of disciplines, ranging from desalination and energy conversion to general physiology. An essential feature of membranes, whose importance has not always been recognized, is their heterogeneity. The objectives of this research are to identify and solve important structure-related problems in membrane characterization, the prediction of membrane performance, and the design of interfacial devices. During the past year, a mathematical analysis of transport across series-parallel structures has been developed. In addition, based on earlier theoretical studies of transport across heteroporous membranes, a novel and versatile membrane transport cell has been developed.

In developing a model of structured membranes, a trade-off must be made between fidelity (the representation of the system as a highly interconnected network of paths whose transport properties may vary) and characterizability (the availability of experimental data that can be used to evaluate the parameters of the model). For systems of practical interest, experimental data are available to support only the most primitive structural models. Accordingly, the simplest model possessing both series and parallel organization was selected for initial study. The model consisted of two dissimilar membranes in series, in parallel with a third membrane. The questions posed were: What is the best experimental protocol for characterizing the individual components of this system, what information is available from conventional characterization techniques, and how can the model be used to predict transport behavior?

It is convenient to couch the discussion in terms of a biological cell layer, to which the initial model is apparently similar. Here, the two series membranes bound the cytoplasm, and the parallel element is the intercellular pathway. The system is ideally suited for examination because it is known to be asymmetric and because considerable experimental effort has been expended to characterize such layers. To date, we have constructed a model of an "epithelium" and examined the ability of experiments to yield transport properties for the specific case of corneal epithelium. We find that (a) despite the numerous experiments that have been run on this tissue, not all of the parameters of the model can be unambiguously evaluated; (b) structure cannot be ignored when interpreting the results of experiments using radioactive tracers; and (c) in spite of the above limitations, the model exhibits predictive capabilities that it would lack were it unstructured.

We have developed a novel membrane transport cell to determine experimentally membrane phenomenological coefficients as well as a "heteroreflectivity" coefficient (Ref. 1) that corrects for possible errors in the predicted flux across heteroporous parallel pathway membranes. Laser interferometry is used to measure the refractive index and, therefore, relative solute concentrations on either side of the membrane. The time courses of both volume flow (measured using capillary tubes) and solute flow are measured simultaneously. The experimental protocol employs a constant pressure head across the membrane, and thus volume flow and solute flow are linearly dependent on the concentration difference across the membrane. Phenomenological coefficients obtained during preliminary experiments on dialysis tubing with sucrose as the solute are comparable to published data. For this particular membrane and solute, the solute flux error due to neglecting heteroreflectivity is found to be negligible. Experiments with other solutes and membranes are planned.

<u>Principal Investigators</u>: M. H. Friedman and R. A. Meyer. Dr. Friedman is the Group Supervisor of the Theoretical Problems Group of the Research Center. Mr. Meyer is a senior engineer with the Theoretical Problems Group.

<u>Reference</u>

1. M. H. Friedman, "The Effect of Membrane Heterogeneity on the Predictability of Fluxes, with Application to the Cornea," J. Theoret. Biol., Vol. 61, 1976, pp. 307-328.

VISCOUS FLOW AND TRANSPORT THEORY

Reliable estimates of flow and transport parameters are necessary in many technical applications but are often difficult to obtain when they necessitate complete viscous solutions to the Navier-Stokes equation and the convective transport equation. Combining analytic and numerical techniques, we have successfully addressed problems involving separation in steady and unsteady flow, pulsatile flow through orthogonal branches, and velocity and scalar transport fields in noncircular ducts.

Our analytic investigation of two-dimensional (2D) steady separation in Stokes flows between eccentric cylinders, either of which is fixed while the other rotates, produces insight into separation phenomena on rounded surfaces of either concave or convex curvature. The recirculation regions, including the angle of separation streamline departure, are functions of the cylinder pairs, not the radius of curvature of the stationary wall per se. However, there are universal relations among the separation streamline angle, the null vorticity curve, and the null along-wall velocity component curve, and these 2D relations apply to other laminar curved boundary flows, including those at a higher Reynolds number. This work has been submitted for publication (Ref. 1).

Unsteady separation is less well characterized theoretically, but numerical simulations of oscillatory flow in simple 2D geometries show features often revealed in more complex flow situations. The local results near the stagnation points of the recirculation regions are fully consistent with our steady separation theory, even though the stagnation points may migrate along the solid surfaces, as described in one of our recent publications (Ref. 2).

We have also used our "unsteady" numerical method to calculate pulsatile flow through an orthogonal trifurcation; this study is being written now for publication. A series of calculations was made for a simple pulsatile flow with the same dynamic parameters, Reynolds number, and Stokes number as those we used previously (Ref. 3) for a symmetric bifurcation so that comparisons could be made. The width of the orthogonal side branches and the outflow through them were varied. Although there are quantitative differences due to geometry and flux partition, certain similarities of wall shearing stress distribution at the branch corners and near divider tips were made evident.

Velocity fields in fully developed parallel flow in straight ducts of simple cross-sectional shape can be found analytically, for steady flow or unsteady flow in some cases. Other shapes

are intractable analytically, but we have obtained the velocity solution by finite difference approximation, as described in detail in Ref. 4. We tested the accuracy of the finite difference approach by comparison to analytic solutions in the simple ducts, and we obtained new solutions for a variety of noncircular ducts. The advantage of the numerical technique for oscillatory flow is a considerable saving in computer time. By Fourier superposition, any periodic flow in an arbitrary duct can be synthesized.

Fully developed steady thermal fields for straight ducts of arbitrary section with constant longitudinal mean temperature gradient can be derived from the steady velocity field determined above. The convective transport equation takes a relatively simple form, and we have evaluated the solution numerically for a variety of wall-temperature distributions, as described in Ref. 5. Uniform wall temperature results duplicate analytic results for simple shapes quite accurately, and the thermal field in arbitrary section shapes can be found as readily. Extended surfaces, achieved by attaching a longitudinal fin within the duct, have produced some surprising heat transfer results, particularly if the temperature distribution on the fin is not uniform.

By the well-known analogy between heat and mass transfer, the numerical techniques are equally applicable to concentration fields. The fully developed mass concentration field theory may lead to improved blood-dialysis devices and/or heart-lung machines, as described in Ref. 6.

Principal Investigators: V. O'Brien and L. W. Ehrlich. Dr. O'Brien is a senior physicist in the Theoretical Problems Group, and Dr. Ehrlich is a senior mathematician in the Applied Mathematics Group of the Research Center.

References

1. V. O'Brien, "Analytic Description of Steady Separation from Curved Surfaces," 1976 (submitted to Phys. Fluids).

2. V. O'Brien, "Reply by Author to D. P. Telionis," AIAA J., Vol. 13, 1975, p. 1680.

3. V. O'Brien, L. W. Ehrlich, and M. H. Friedman, "Unsteady Flows in a Branch," J. Fluid Mech., Vol. 75, 1976, pp. 315-336.

4. V. O'Brien, "Steady and Unsteady Flow in Non-Circular Straight Ducts," 1976 (accepted for publication in the ASME J. Appl. Mech.).

5. V. O'Brien, "Developed Convective Thermal Fields in Non-Circular Ducts," APL/JHU TG 1303, 1976.

6. V. O'Brien, "Convective Field Theory to Predict Dialysis/Oxygenator Efficiency," Proc. 29th Ann. Conf. Eng. Med. Biol., Boston, 6-10 November 1976.

HYDROMAGNETISM OF THE OCEAN

Ocean motions across ambient magnetic fields induce electric currents in the sea and associated magnetic fields in the environment that are readily measurable, though small, and of interest for various geophysical, oceanographic, and Naval problems. The ocean motions may be either those of natural origin or ones associated with moving bodies; the ambient magnetism is the earth's field and that of the body if magnetizable. The resulting wide varieties of oceanic hydromagnetism have been surveyed and estimated theoretically in order to isolate potentially significant phenomena for detailed study.

Seawater has a moderate electrical conductivity such that the interaction between oceanic flowfields and ambient magnetic fields induces small but significant hydromagnetic effects in the ocean environment. A multitude of such oceanic hydromagnetic phenomena arise from the diversity of possible natural or body-related flows interacting with the earth or body magnetism. In consultation with the SSBN Security Program, we have assayed to survey the manifold of possible effects and to estimate numerically the importance of each from a fundamental theoretic standpoint. The basic physical principles are well established and mathematically formulated in the combined Maxwell-Navier-Stokes equations of hydromagnetism.

Oceano-magnetism (OM) differs from more familiar variants of hydromagnetism in that the conductivity, ambient magnetism, and flow scales fall far from the extremes encountered in usual laboratory or cosmic applications. The majority of OM effects are purely inductive, but we have also considered the possibility of radiative and other phenomena. We discuss only the inductive effects here.

We consider the OM induction phenomena arising from the natural ocean motions:

1. Surface gravity waves (SW), from local winds (sea) or distant storms (swell);

2. Internal gravity waves (IW);

3. Ambient acoustic waves (AW); and

4. Sea currents and tides;

and those related to passage of a body through the sea:

5. Mean flow of seawater through the body magnetic field;

6. Potential flow due to hull displacement;

7. Wake flow, from turbulent growth near the body to collapse in the far region; and

8. Propagated disturbances, due to body-generated SW, IW, and AW.

These phenomena include both nonpropagating effects and inductive effects propagated purely mechanically via the ocean wave motions (SW, AW, IW above). The propagating induction, termed "OM pseudoradiation," will be presented here as an example of the general survey and results.

The OM pseudoradiation (1, 2, 3, 8 above) expressed in terms of plane waves can be categorized in terms of the dispersion relation of the generating ocean wave (SW, IW, AW), as shown in Fig. 1. To the left of the diagonal dashed line a quasi-static approximation holds, while to the right a nonstatic limit obtains for long wavelengths. A simple estimator for the size of the OM effects is derived for either limit that smoothly interpolates through the transition region. In this way, the SW- and IW-induced OM effects of import for geophysical studies, for example, are discussed in a simple and unified manner. Further, the AW-induced OM wave, or "sonomagnetic" pseudoradiation, is found to be of peculiar interest in the infrasound regime (Fig. 1). Whereas the purely sonic field (AW) is essentially confined within the ocean, the sonomagnetic pseudowave radiates into the air above the sea, particularly at infrasonic frequencies. Considering the utility of airborne observations (e.g., Project Magnet, cf. Ref. 1), we have analyzed the sonomagnetic field in detail in a paper in preparation.

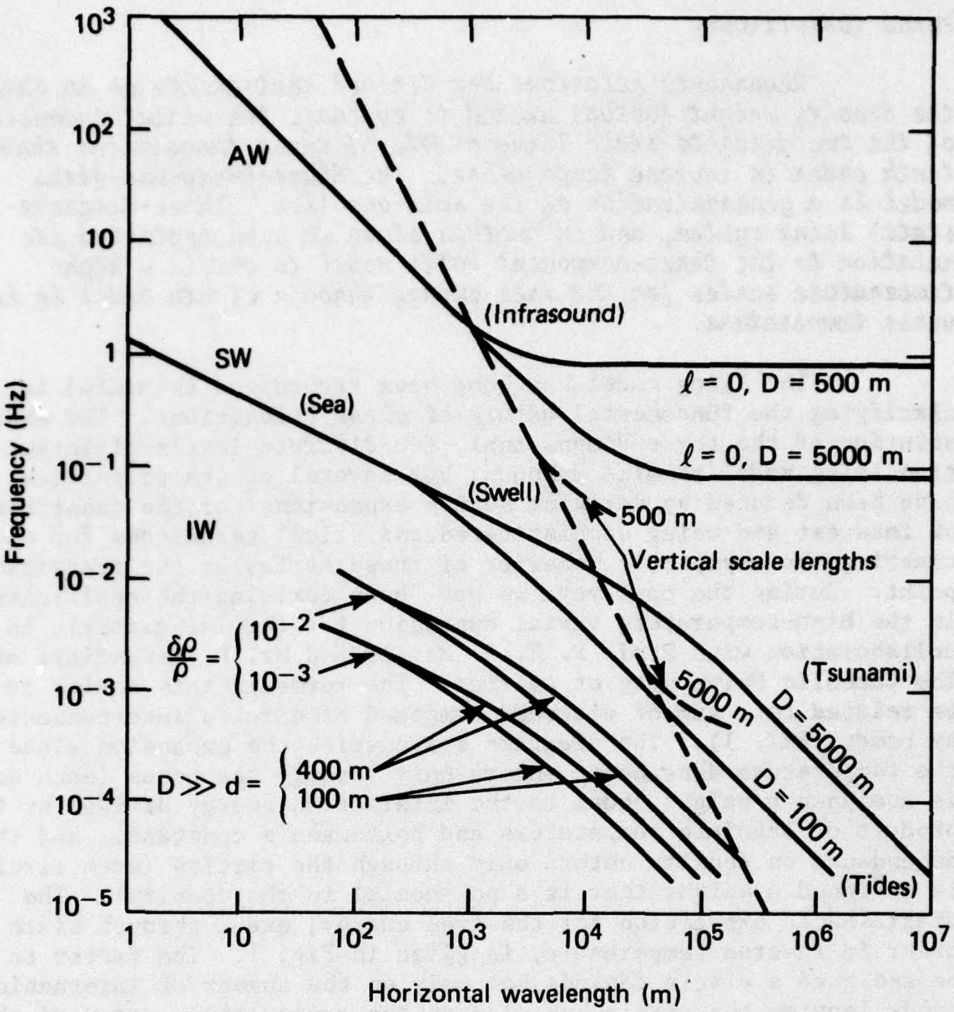

Fig. 1 Acoustic (AW), Surface (SW), and Internal (IW) Ocean Waves. The various waves are represented by their dispersion relations (solid lines) for ocean depth (D), pycnocline depth (d), density change ($\delta\rho$), sonic mode (ℓ), with IW curves truncated at the Brunt-Vaisala frequency for 25-m-thick pycnocline. The dashed line separates quasi-static (left) and nonstatic (right) regimes of OM pseudoradiation.

Principal Investigator: J. F. Bird, in consultation with H. Ko. Dr. Bird is a senior physicist in the Theoretical Problems Group of the Research Center. Dr. Ko is not supported by the IR&D program.

Reference

1. A. J. Zmuda (ed.), World Magnetic Survey 1957-1969, IUGG Publication Office, Paris, 1971.

PHASE TRANSITIONS

Recurrence relations are derived that enable us to obtain the density weight factors needed to evaluate the virial expansion of the two discrete-state Ising models of phase transitions through tenth order in inverse temperature. The Blume-Emery-Griffiths model is a generalization of the spin-one (i.e., three-discrete-state) Ising system, and in another study we have exploited its relation to the three-component Potts model to obtain a high-temperature series for the free energy through eighth order in inverse temperature.

The Ising model has long been recognized as useful in clarifying the fundamental nature of phase transitions. The exact solution of the three-dimensional, two-discrete-levels-of-interaction Ising model remains unknown, but several of its properties have been deduced by deriving series expansions for the quantities of interest and using sophisticated analytical techniques for extracting the asymptotic behavior of these series at the transition point. During the past year we have been deriving the coefficients in the high-temperature virial expansion for the Ising model, in collaboration with Prof. P. H. E. Meijer and Mr. P. Esfandiari of The Catholic University of America. The terms in this series can be related to a sum of diagrams composed of circles interconnected by bonds (Ref. 1). The diagrams systematize the expansion since the temperature dependence enters only through the bonds (each bond is assigned a weight equal to the interaction energy divided by the product of absolute temperature and Boltzmann's constant), and the dependence on density enters only through the circles (each circle is assigned a weight that is a polynomial in the density). The diagrammatic expression for the free energy, exact through sixth order in inverse temperature, is given in Fig. 1. The factor to be assigned a circle depends not only on the number of interaction bonds leaving the circle but also on the articulation order of the circle. The diagrams with articulation circles in Fig. 1 are contained within the square brackets, and a kth order articulation circle is one that upon its removal from a (connected) diagram causes the diagram to separate into k disjoint parts.

During the past year, we have extended Eq. 1 (Fig. 1) to include all diagrams needed to calculate the free energy to order $(T)^{-10}$ and have determined the appropriate density factors (Ref. 1). The first task was to list the 428 topologically distinct diagrams with 10 or fewer bonds. The primary difficulty involves recognizing diagrams that are in fact topologically equivalent but appear to be distinct because of the way they are drawn. The connectivity of a diagram can be represented by a matrix, and certain invariants of these matrices are used to recognize topological equivalence.

$$-\beta F = -L\left(\rho \ln(\rho) + (1-\rho)\ln(1-\rho)\right)$$

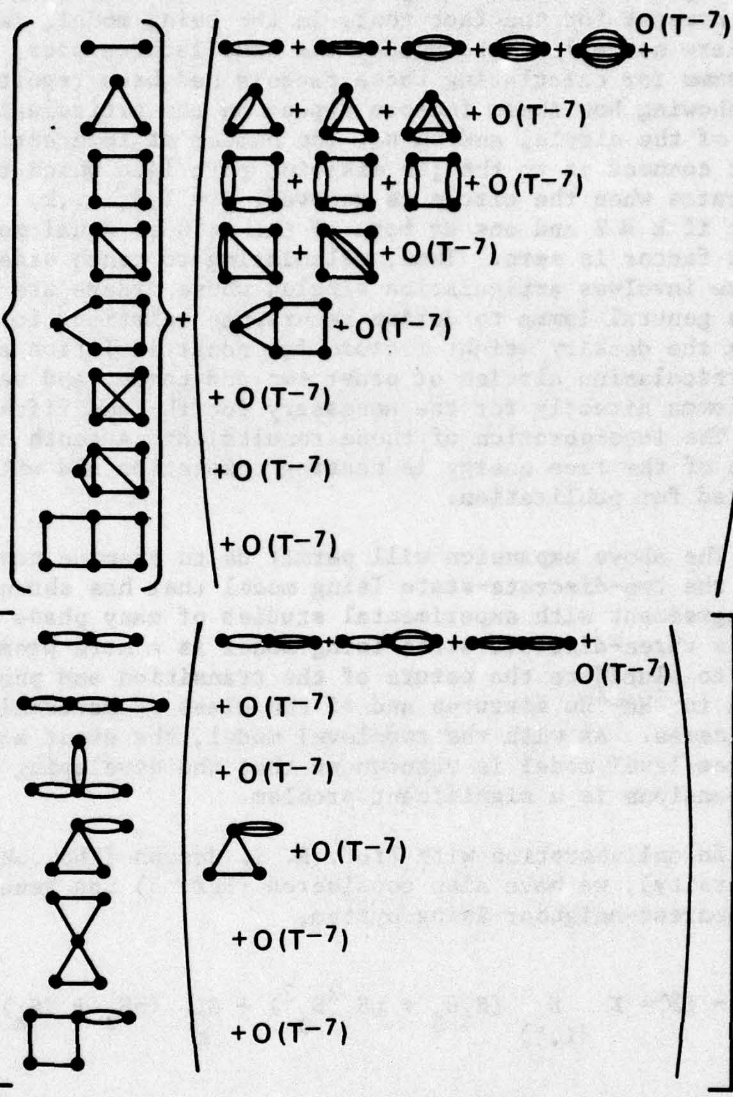

Fig. 1 Diagrammatic Expression for the Virial Expansion of the Free Energy (F) of the Lattice Gas. Here L is the number of lattice sites, ρ is the number density of occupied sites, β is the usual Boltzmann temperature factor, and $O(T^{-7})$ denotes that the next terms are of order temperature to the minus seventh power. The weight assigned an articulation circle (cf. text) is zero if one of the pieces of the diagram that it interconnects has but one line connecting the piece to the diagram. This fact has been used to eliminate diagrams such as , , , etc. from the list.

Our most difficult task in evaluating the free energy from the diagrams is determining (Ref. 2) the density weight factors that account for the fact that, in the Ising model, two particles are not allowed to occupy the same lattice site. A general lemma for calculating these factors had been reported (Ref. 3) showing how these factors depend on the articulation order, k, of the circle, and on n_j, the number of interaction bonds that connect it to the jth disjoint part into which the diagram separates when the circle is removed, $j = 1,2,\ldots,k$. It was shown that if $k \geqq 2$ and one or more of the n_j's is equal to one, the weight factor is zero. Thus, calculating to tenth order in temperature involves articulation circles whose orders are $\geqq 5$. We use the general lemma to derive recurrence relations for evaluating the density weight factors for nonarticulation circles and for articulation circles of order two and three, and we evaluate the lemma directly for the necessary fourth- and fifth-order circles. The incorporation of these results into a tenth order expression of the free energy is nearing completion and will then be submitted for publication.

The above expansion will permit us to examine new properties of the two-discrete-state Ising model that has shown remarkable agreement with experimental studies of many phase transitions. The three-discrete-state Ising model is a more promising candidate to elucidate the nature of the transition and phase separation in ^3He-^4He mixtures and of the class of materials known as spin glasses. As with the two-level model, the exact solution to the three-level model is unknown so that the developing of series expansions is a significant problem.

In collaboration with Prof. R. I. Joseph (The Johns Hopkins University), we have also considered (Ref. 5) the generalized spin-one nearest-neighbor Ising system,

$$-\beta\mathcal{H} = K \sum_{\langle i,j\rangle} (S_i S_j + \eta S_i^2 S_j^2) + \beta\sum_k (hS_k + \Lambda S_k) , \quad (2)$$

where $\mathcal{H}$ is the Hamiltonian, β is the Boltzmann temperature factor, $K = \beta J$ with J the interaction energy, S is the spin (state) variable that takes on the values ± 1 and 0, η is the biquadratic exchange, h is the "field," Λ is the anisotropy, and $\langle i,j\rangle$ denotes that the sum is over nearest-neighbor pairs. This system is called the Blume-Emery-Griffiths model, since these authors studied it in the mean-field approximation to elucidate the transition and phase separation in ^3He-^4He. The Potts model corresponds to Eq. 2 with $\eta = 3$, and several terms are available in the series expansion of

its free energy in the variable $u = e^{2K} - 1$. As with the spin 1/2 Ising system, the coefficients in these series derive from a specific set of diagrams. We have related the Hamiltonian of Eq. 4 for general η to this same set of graphs and have shown that factors of the form $\{u^{\ell}[1 + g(m)]\}$ in the Potts model are replaced by factors $\{[e^{K(\eta-1)} - 1]^{\ell} + u^{\ell}g(m)\}$. These factors are associated with diagrams having ℓ lines and m points. Taking this into account, we are able to write down the first seven terms in the Blume-Emery-Griffiths series on loose-packed lattices by inspection of the Potts model series and with a modest amount of recalculation obtain the eighth-order term. This eight-term series will allow us to examine the behavior of the model throughout most of (h,Λ,η,K) space, although the series may be too short to study behavior in the immediate neighborhood of critical points. The initial work has been accepted for publication; further analysis and extensions of the series will be the subject of future studies.

Principal Investigators: R. A. Farrell, P. Esfandiari, R. I. Joseph, and P. H. E. Meijer. Dr. Farrell is a senior physicist in the Theoretical Problems Group of the Research Center. Mr. Esfandiari was a graduate student at The Catholic University of America, Dr. Joseph is Professor of Electrical Engineering at The Johns Hopkins University, and Dr. Meijer is Professor of Physics at The Catholic University of America; these investigators were not funded by the program.

References

1. P. Esfandiari, Ph.D. thesis, The Catholic University of America, Washington, DC, 1976.

2. P. H. E. Meijer, P. Esfandiari, and R. A. Farrell, "A Diagrammatic Expansion of Ising Models in Terms of Strong Lattice Contents," Bull. Am. Phys. Soc., Vol. 21, 1976, p. 686.

3. R. A. Farrell, T. Morita, and P. H. E. Meijer, "Cluster Expansion for The Ising Model," J. Chem. Phys., Vol. 45, No. 1, 1966, pp. 349-363.

4. R. I. Joseph and R. A. Farrell, "High Temperature Series for the Spin-One Ising Model for Arbitrary Biquadratic Exchange, Field and Anisotropy" (accepted by Physics for publication).

LASER INTENSITY CORRELATION SPECTROSCOPY OF MACROMOLECULES

New methods are described for extracting useful descriptions of polydisperse scattering systems from intensity correlation data. The application of these versatile methods is illustrated for human-serum very-low-density lipoproteins.

Laser intensity correlation spectroscopy (ICS) has become a standard method of measuring the diffusion coefficient and therefore the effective hydrodynamic diameter of particles in solution. Measurements of this kind are important in the characterization of polymer solutions and in colloid science. Our capabilities with the ICS technique have been developed for application to human-serum low- and very-low-density lipoproteins (LDL and VLDL) in collaboration with Dr. S. Margolis of the Johns Hopkins Medical Institutions. The Heart and Lung Institute of the National Institutes of Health began support of the work on 1 June 1976.

In the intensity correlation method, macromolecular diffusion coefficients are determined from the autocorrelation function of the intensity fluctuations in the light scattered from the molecules. These fluctuations arise from the Brownian motion of the scatterers. The general form of the correlation function is $C(\tau) = A|g^{(1)}(\tau)|^2 + B$, where A, B, and τ are the amplitude, background, and delay time, respectively. For a single-sized molecular species, $g^{(1)}(\tau) = \exp(-Dq^2\tau)$, where D is the translational diffusion coefficient. The factor q^2 is an instrumental parameter equal to $(16\pi^2 n^2/\lambda_0^2)\sin^2(\theta/2)$, in which n is the refractive index of the solvent, λ_0 is the vacuum wavelength of the incident laser radiation, and θ is the scattering angle. ICS is presently the most rapid and accurate means of determining the diffusion coefficient in monodisperse systems.

The cumulant method (Ref. 1) has extended the usefulness of ICS to polydisperse systems and provides a completely general description of such systems. This method yields the z-average diffusion coefficient (which is related to the first cumulant K_1 by $K_1 = D_z q^2$) and its variance σ^2 (which is related to the first two cumulants by $\sigma^2 = K_2/K_1^2$). We have obtained the cumulants for solutions of LDL and VLDL (Ref. 2). Our results for VLDL, listed at the top of Table 1, are in general agreement with known properties.

Often it would be desirable to know more about the distribution than just the first two cumulants. Unfortunately, light scattering measurements lack sufficient precision to determine the exact distribution form. However, in many instances these methods, supplemented by model size distribution functions, can provide additional information. Previously, we investigated the use of a

Gaussian model distribution to describe VLDL size (Refs. 2 and 3). This description was inadequate because, although the mean radius, a_0, was found to be reasonable, the standard deviation, σ, was not (c.f. Table 1). We concluded that other distribution forms were required to describe VLDL.

Recently we have found that the Pearson Type V distribution for the radius a,

$$N(a) = \frac{\gamma^{p-1}}{\Gamma(p-1)} a^{-p} e^{-\gamma/a} \tag{1}$$

(Ref. 4), provides a good description of VLDL size. Moreover, the two distributional parameters p and γ are readily calculated from K_1 and K_2. In this distribution the most probable radius (where the maximum value of N(a) occurs) is $a_{mp} = \gamma/p$. The moments of the size distribution $\langle a^r \rangle \equiv \int_0^\infty a^r N(a)da$, can also be used to

TABLE 1

RESULTS OF THE ANALYSIS OF VLDL DATA TAKEN AT $\theta = 90°$ AND $T = 299.3°K$

Cumulant Analysis (Refs. 1 and 2)				
$K_1^{20°}(s^{-1})$*	K_2/K_1^2	$\overline{D}_z^{20°}\ \frac{cm^2}{s} \times 10^8$*	Diameter (nm)†	
2124 ± 19	0.0635 ± 0.02	6.1 ± 0.1	71.0 ± 1.0	
Gaussian Parameters (Refs. 2 and 3)				
	Radius a_0(nm)	σ(nm)		
	20.5	10.0		
Pearson Type V Parameters				
p	γ	a_{mp}(nm)	$\langle a \rangle$(nm)	σ(nm)
22.75	5583.1	24.5	26.9	6.0

*K_1 and the z-average diffusion coefficient have been corrected to 20°C.

†The diameter is calculated from $\overline{D}_z^{20°}$ assuming spherical particles.

obtain the mean particle radius $\langle a \rangle$ and the variance $\sigma^2 = [\langle a^2 \rangle - \langle a \rangle^2]$. Using this definition for $\langle a^r \rangle$, we find that $\langle a \rangle = \gamma/(p-2)$ and $\sigma = \langle a \rangle/(p-3)^{\frac{1}{2}}$. The Pearson V distribution leads to

$$g^{(1)}(\tau) = (1 + \frac{C\tau}{\gamma})^{7-p} \quad , \tag{2}$$

where $C = kTq^2/6\pi\eta$. Here k, T, and η are Boltzmann's constant, absolute temperature, and solvent viscosity, respectively. We find that the cumulants can be readily calculated and are given by

$$K_1 = (\frac{C}{\gamma})\ (p-7)$$

and (3)

$$K_2 = (\frac{C}{\gamma})^2\ (p-7) \ .$$

The values of p, γ, a_{mp}, $\langle a \rangle$, and σ for the sample of VLDL are presented at the bottom of Table 1. Figure 1 is a plot of a Pearson Type V distribution with these parameters. This distribution gives a good description of the known properties of VLDL.

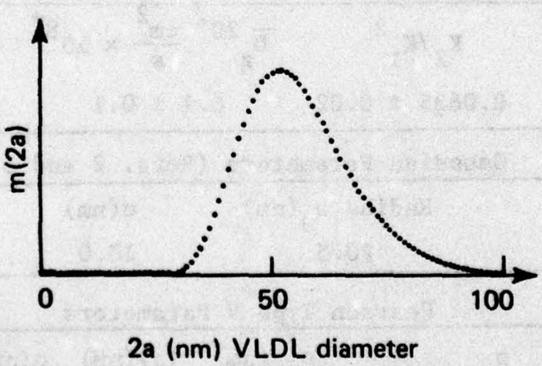

Fig. 1 The Pearson Type V Distribution of Diameter (2a) for the Parameters Shown in Table 1. VLDL are known to be spherical particles whose diameters range from 30 nm to greater than 90 nm in electron micrographs.

Knowledge of the form of $g^{(1)}(\tau)$ for the Pearson V size distribution affords the opportunity to perform numerical experiments to determine the optimum means of processing ICS data on such polydisperse systems. Preliminary results, obtained after adding appropriate noise to the artificially generated correlation function, indicate that K_1 is easily measured to better than 1% accuracy; however, K_2 is difficult to measure with less than 10% error.

A complete description of the relationship between the cumulants and the parameters of the Pearson V size distribution as well as for several other useful size distributions is being prepared for publication.

Principal Investigator: R. L. McCally. Mr. McCally is a senior physicist with the Theoretical Problems Group of the Research Center.

References

1. D. E. Koppel, "Analysis of Polydispersity in Intensity Correlation Spectroscopy: The Method of Cumulants," J. Chem. Phys., Vol. 57, No. 11, 1 December 1972, pp. 4814-4820.

2. C. B. Bargeron, R. L. McCally, M. H. Friedman, and S. Margolis, "Particle Size Distributions of Human Plasma Lipoproteins by Intensity Correlation Spectroscopy," Biophys. J., Vol. 15, Part 2, 1975, p. 215a (abstract).

3. C. B. Bargeron, "Measurement of a Continuous Distribution of Spherical Particles by Intensity Correlation Spectroscopy: Analysis by Cumulants," J. Chem. Phys., Vol. 61, No. 5, 1 September 1974, pp. 2134-2138.

4. W. P. Elderton and N. L. Johnson, Systems of Frequency Curves, Cambridge University Press, 1969.

APPLIED MATHEMATICS

The Applied Mathematics Group specializes in areas of classical and modern analysis of concern to the Laboratory. The group supports various Laboratory programs in addition to conducting research in support of and funded by the Research Center's IR&D program. The group consists of four senior mathematicians, each recognized as a significant contributor to his field through his published original researches. Active areas include numerical analysis and the development of computational algorithms, analysis of the behavior and of approximation of solutions of partial differential equations, and the development of estimation techniques in special theory. Applications have included improved computational procedures in numerous program areas involving particularly structural and fluid mechanics.

During the present year significant results have been obtained in the stratified flow studies, our newest area of investigation. Continuing important progress has been achieved in our ongoing effort toward development of general approximation methods in differential equations and estimation techniques in spectral theory. Results are summarized in the following individual research reports and are described in detail in five papers that have been accepted for publication. Near the end of this reporting period, Dr. D. W. Fox, Supervisor of the Applied Mathematics Group, began his appointment as William S. Parsons Visiting Professor in the Department of Mathematical Sciences at The Johns Hopkins University for the academic year 1976-77. During his appointment, Dr. V. G. Sigillito will be Acting Group Supervisor. At the invitation of the Board of Editors, Dr. Sigillito is preparing a monograph covering his research for publication by Pitman Publishing Limited.

STEADY STATE OSCILLATIONS IN A STRATIFIED FLUID

We consider the fluid motion induced by small steady oscillations of a body immersed in a vertically stratified fluid. Our treatment of this problem has several aspects. The first is the formulation and transformation of the problem for quite arbitrary bodies and general boundary motions. The second is the solution of a number of simple problems in two and three dimensions. Explicit solutions have been found, and their limiting behavior for high frequency and at the buoyancy frequency has been studied in detail. This leads to some new observations and to conjecture about the velocity field at the buoyancy frequency.

The study of stratified fluids is motivated by the need to understand the behavior of atmospheric and oceanographic flows in which the stratification and gravity introduce significant

buoyant forces. Of special practical interest is the study of flows caused by the displacement of submerged bodies in the ocean. The results described herein are of importance because they allow us to explicitly describe the flows induced by various submerged bodies in a stratified fluid. The graphs that illustrate the nature of the flows as the frequency of oscillation of the body approaches the buoyancy frequency of the fluid from above are of particular interest.

In the present investigation, the differential equations are those of the linear first-order theory of disturbances about equilibrium with the additional approximations that the buoyancy frequency and the density distribution may be taken to be constant. The resulting mathematical problem is essentially the same as that for small steady oscillations in a uniformly rotating fluid.

When the frequency is higher than the buoyancy frequency, the resulting mathematical problem is transformed into a one-parameter family of Neumann problems for the Laplacian. These problems are solved exactly for oscillatory translations and expansions of spheres and of long horizontal cylinders. As the frequency is approached from above, the velocities become strongly vertical and approach strictly vertical limiting flows. This behavior is clearly shown in Figs. 1 to 3.

Figure 1 shows a slice through the stream surfaces for the vertical oscillation of a sphere. The cut is made by a plane through the x_3-axis (vertical direction). Figure 2 has two interpretations. First, it gives the streamlines in the plane containing the x_3-axis and the direction of motion for a horizontally oscillating sphere; second, it gives the streamlines for the horizontal circular cylinder with the axis along x_2 oscillating in the x_1 direction. The labels on the graphs are consistent with the second interpretation. For each graph, the values of the stream function of the streamlines shown are those taken on the body surface for values of r/R_0 or x_1/R_0 ranging from 0.05 to 0.95 in steps of 0.05, where R_0 denotes the radius of the cylinder or sphere.

Figure 3 shows the limiting velocities in the examples as ω, the ratio of the frequency of oscillation to the buoyancy frequency, approaches 1^+. The first graph shows that produced by the vertically moving sphere. It is uniform above the sphere and has a return flow outside the vertical cylinder generated by the sphere. The second shows the same kind of result for the vertically oscillating horizontal cylinder. The third graph has two interpretations. The first of these is the velocity above a horizontally oscillating sphere in the plane defined by its vertical

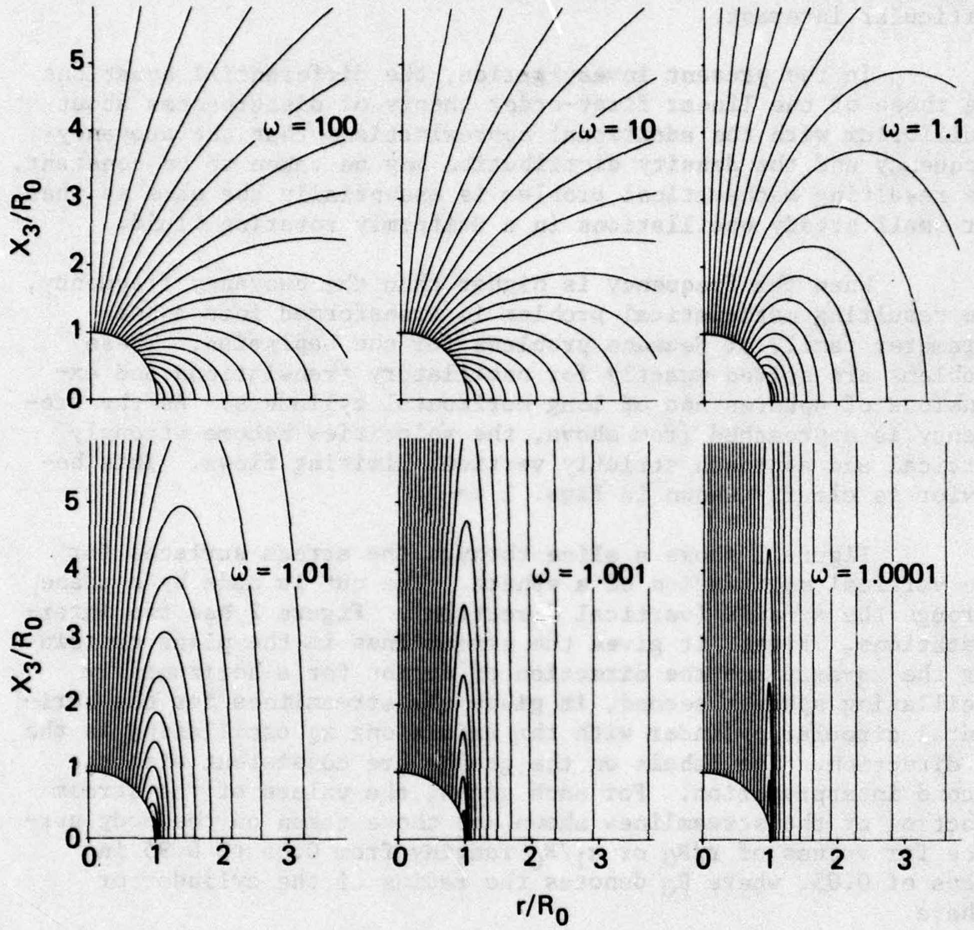

Fig. 1 Streamlines for Vertically Oscillating Sphere

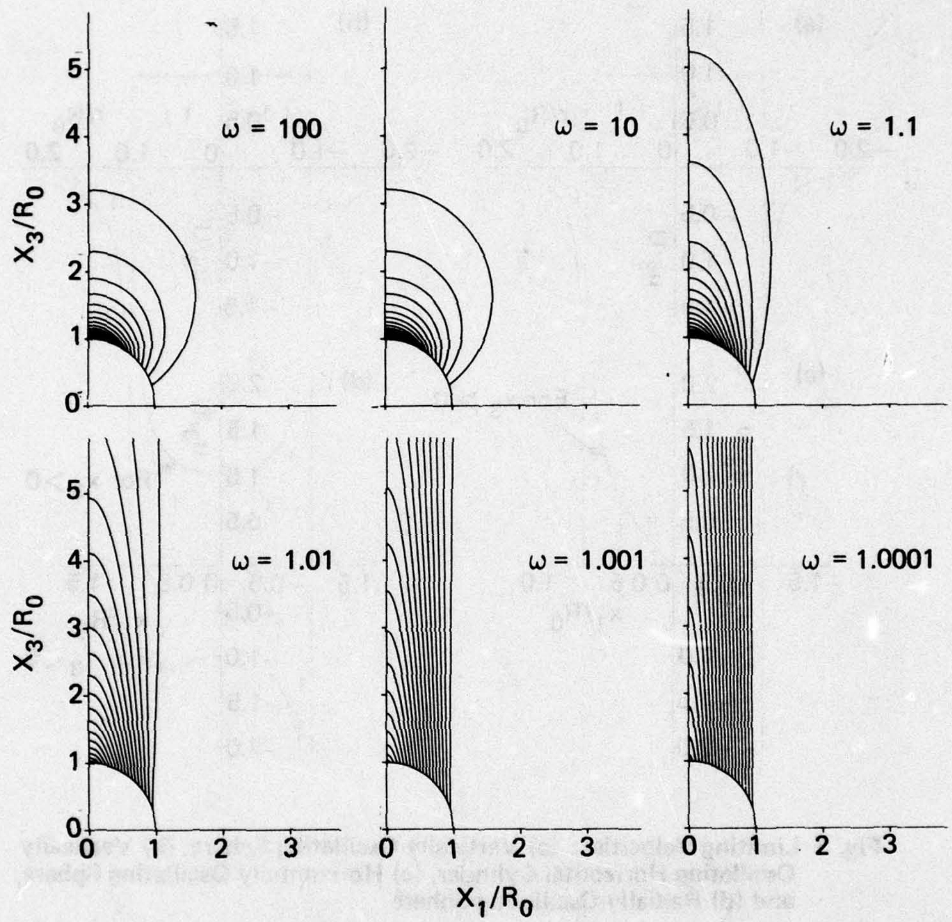

Fig. 2 Streamlines for Horizontally Oscillating Cylinder

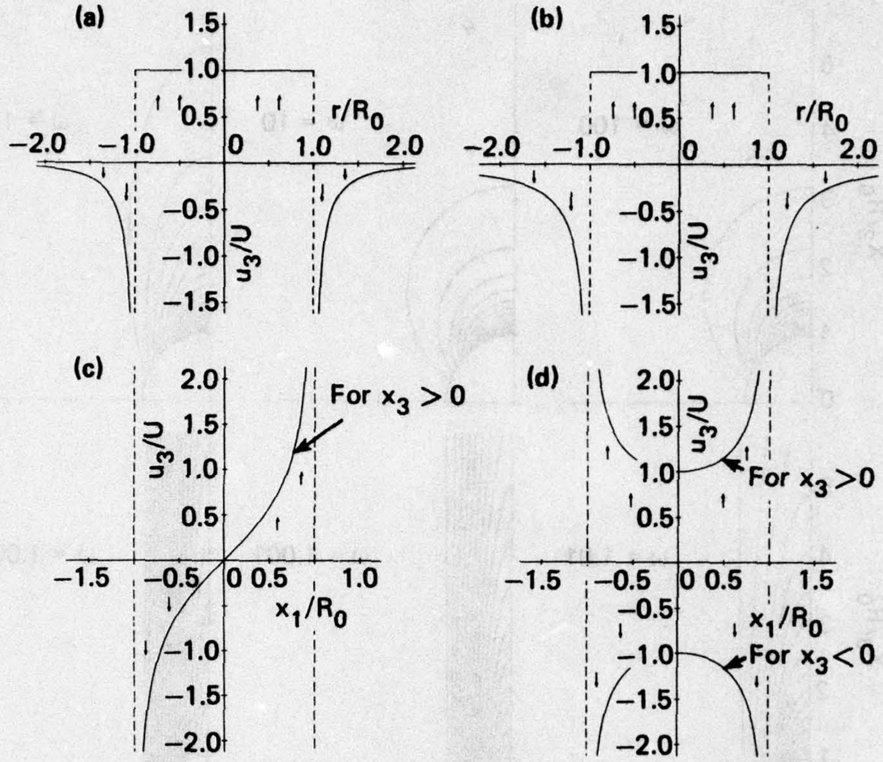

Fig. 3 Limiting Velocities: (a) Vertically Oscillating Sphere, (b) Vertically Oscillating Horizontal Cylinder, (c) Horizontally Oscillating Sphere, and (d) Radially Oscillating Sphere

axis and its direction of motion. The second is the velocity above a horizontal circular cylinder oscillating horizontally perpendicular to the axis of the cylinder. The velocities below the horizontally oscillating sphere and cylinder are the negative of those above. The last of the graphs also has two interpretations: the motion above and below the radially oscillating sphere in a vertical plane through the x_3-axis or the motion above and below the radially oscillating horizontal cylinder. In this figure, U denotes the magnitude of the prescribed velocity u^0.

These limiting flows suggest the following conjecture about the limiting vertical velocities above and below oscillating bodies.

The limiting vertical velocity u_3 above and below any body with prescribed velocity u^0 is independent of x_3 and is determined by the boundary condition,

$$u_3 n_3 = u^0 \cdot n \quad \text{on} \quad \partial G ,$$

whenever n_3 does not vanish. The flow outside the vertical cylinder generated by the body is zero if the prescribed velocities satisfy

$$\int_{\partial G^+} u^0 \cdot n \, dx = \int_{\partial G^-} u^0 \cdot n \, ds ,$$

in which ∂G^+ and ∂G^- are the top and bottom of the body, respectively.

Principal Investigators: D. W. Fox and V. G. Sigillito. Dr. Fox is Supervisor of the Applied Mathematics Group of the Research Center. He is William S. Parsons Visiting Professor in the Department of Mathematical Sciences for 1976-77. Dr. Sigillito is a senior mathematician of the Applied Mathematics Group of the Research Center. He is also an instructor in the Evening College of The Johns Hopkins University.

Reference

1. D. W. Fox and V. G. Sigillito, "Steady State Oscillations in a Buoyant Fluid, (to appear in J. Appl. Math. Phys.).

NUMERICAL SOLUTIONS OF PARTIAL DIFFERENTIAL EQUATIONS

The application of the conjugate gradient method with matrix splitting techniques to the iterative solution of elliptic finite difference equations has produced a method that allows a rapid solution of certain fluid flow problems.

One approach to solving a fluid flow problem involving a stenosis (or constriction) in an axisymmetric channel is the conformal transformation of the region to an infinite strip or rectangle. This in turn destroys the separability of the differential equation and precludes the use of direct methods on the resulting linear finite difference equation. To circumvent this, a conjugate gradient matrix splitting iterative technique is now being investigated. The method has been analyzed for problems that lead to symmetric positive definite matrices. However, some early results indicated that, with appropriate splitting, the method can be more widely applied (Ref. 1). Current investigation centers around studying optimal application and the matrix conditions needed to guarantee rapid convergence, thus allowing rigorous application of this efficient technique.

Principal Investigators: L. W. Ehrlich and J. R. Kuttler. Drs. Ehrlich and Kuttler are senior mathematicians of the Applied Mathematics Group of the Research Center. Dr. Ehrlich is also an instructor in the Evening College of The Johns Hopkins University, and Dr. Kuttler is also an instructor in the Evening College of the University of Maryland.

Reference

1. L. W. Ehrlich, "On Some Experience Using Matrix Splitting and Conjugate Gradient," presented at the 1975 SIAM Fall Meeting, San Francisco, CA.

ESTIMATING FREQUENCIES OF DIFFERENTIAL OPERATORS

We report on the results of several numerical experiments with a new method for estimating eigenvalues of elliptic partial differential operators. Such eigenvalue problems are of significant interest in naval structural engineering, since these equations describe the vibrational frequencies of beams, plates, rotors, and membranes. However, often only crude bounds are known for the eigenvalues, whereas more refined estimates are needed for design purposes.

In the last reporting period we described (Ref. 1) a new method, called the method of a priori — a posteriori inequalities, which takes crude estimates for eigenvalues and gives refined estimates using only elementary trial functions that need satisfy no boundary conditions (see also Ref. 2). Since then we have conducted several numerical experiments with the method to demonstrate its effectiveness.

The eigenvalue problem,

$$\Delta^2 u - \Lambda u = 0 \quad \text{in} \quad R, \qquad u = \frac{\partial u}{\partial n} = 0 \quad \text{on} \quad \partial R ,$$

describes the frequencies proportional to Λ of a plate R clamped on its boundary ∂R. Here Δ^2 is the biharmonic operator and $\partial/\partial n$ the normal derivative. Even for R, a rectangle, the problem cannot be solved exactly since Δ^2 is not separable.

For trial functions, we used products of even Legendre polynomials $P_{2m}(x)\ P_{2n}(y)$. The a priori inequality used was taken from Ref. 3. For a 2×2 square we obtain $\Lambda_1 = 80.910 \pm 0.056$; for a 2×2.5 rectangle, $\Lambda_1 = 55.826 \pm 0.009$ and $\Lambda_2 = 497.55 \pm 1.34$; for a 2×16 rectangle, $\Lambda_1 = 31.550 \pm 0.005$.

The eigenvalue problem,

$$\Delta u + \lambda u = 0 \quad \text{in} \quad R, \qquad u = 0 \quad \text{on} \quad \partial R,$$

describes the frequencies proportional to λ of a membrane R, fixed on its boundary ∂R. Here Δ is the Laplacian. For R, a nonsquare rhombus, the problem cannot be solved exactly.

For trial functions, even powers $x^{2m}y^{2n}$ were used with the a priori inequality from 1. For a 75° angle rhombus with unit side we obtain $\lambda_1 = 20.872 \pm 0.006$, $\lambda_2 = 79.047 \pm 0.024$, $\lambda_3 = 108.894 \pm 0.076$. For a 45° angle rhombus with unit side, we obtain $\lambda_1 = 34.779 \pm 0.078$, $\lambda_2 = 100.288 \pm 0.177$, $\lambda_3 = 185.47 \pm 2.17$.

The results described above are comparable with bounds obtained by other methods, although in some cases they are slightly worse than the best available bounds for each problem. More work needs to be done on solving the relative matrix eigenvalue problem that this method generates (Refs. 1 and 2). In contrast to other methods, the significant feature of the present method is its applicability to a wide variety of problems. This is a direct result of

the fact that the trial functions need not satisfy either the boundary conditions or the differential equation describing the problem.

Experiments are now being carried out on the fixed rhombical membrane problem using as test functions trigometrical functions that satisfy the equation $\Delta u_* + \lambda_* u_* = 0$.

Principal Investigators: J. R. Kuttler and V. G. Sigillito. Drs. Kuttler and Sigillito are senior mathematicians in the Applied Mathematics Group of the Research Center. Dr. Kuttler was an instructor at the University College (Evening College) of the University of Maryland from September 1975 through December 1975.

References

1. J. R. Kuttler and V. G. Sigillito, "Bounding Eigenvalues of Elliptic Operators," SIAM J. Math. Anal. (submitted for publication).

2. J. R. Kuttler and V. G. Sigillito, "Estimating Frequencies of Differential Operators," Indirectly Funded Research and Exploratory Development at the Applied Physics Laboratory, Fiscal Year 1975, APL/JHU SR 76-2, June 1976, pp. 41-43.

3. V. G. Sigillito, "A Priori Inequalities and Pointwise Bounds for Solutions of Fourth Order Partial Differential Equations," SIAM J. Appl. Math., Vol. 15, 1967, pp. 1136-1155.

ATOMIC, MOLECULAR, AND ELECTRONIC PHYSICS

Fundamental understanding of the interactions of atoms, molecules, electrons, and radiation with matter is important for improving technological capabilities in a wide variety of areas, such as lasers, computers, electromagnetic detectors, and propulsion. Research in atomic, molecular, and electronic physics continues as an important component of the Research Center's IR&D program, with emphasis on the development of improved experimental techniques and theoretical approaches for obtaining definitive information on reaction mechanisms and energy-transfer processes.

In the past year, the Electronic Physics Group has carried out research on a broad spectrum of topics, including (a) mass spectrometry of highly reactive species formed in elementary chemical reactions, (b) scanning electron microscopy, (c) structure of the ground states of the noble gas molecules KrF and XeF, and (d) measurement of mechanical properties of viscoelastic materials, such as solid propellants. Six papers have been submitted for publication, and others are now in preparation.

The work on viscoelastic materials is a new area of research concerned with the development of a nondestructive small deformation technique for measuring the tensile modulus of such materials, including solid propellants. The technique appears to be sufficiently promising that the Air Force Rocket Propulsion Laboratory is expected to provide funding for this project in the coming year.

In addition, the Electronic Physics Group has for more than 20 years collaborated with the Microwave Physics Group in research on the electron spin resonance of free radicals. A report on this activity is included in the IR&D report of the Microwave Physics Group.

Dr. S. N. Foner, Supervisor of the Electronic Physics Group, continues to serve as Chairman of the Editorial Board of the APL Technical Digest. He is an advisor to the Scientific Affairs Division of NATO. He also serves as Chairman of the Physics and Astronomy Panel of the Membership Committee of the Washington Academy of Sciences.

MASS SPECTROMETRY OF HIGHLY REACTIVE SPECIES

In atomic fluorine reactions, a considerable fraction of the available energy very frequently appears as internal excitation energy of the reaction products. Mass spectrometric studies with a crossed molecular beam reactor have provided information on the vibrational excitation of HF formed in F atom reactions with n-butane, isobutane, and ethylene.

Reactions involving atomic fluorine have a variety of potential applications in the fields of chemical lasers and high-energy fuels because large amounts of energy are released in the reactions and the reaction products are often very highly excited. Fluorine atom reactions have been studied in a high-intensity crossed molecular beam reactor at this Laboratory, as reported previously. It was shown that excitation of reaction products, particularly HF, could be deduced from appearance potential measurements, since the ionization potential of an excited state molecule is less than that of a ground state molecule. Such measurements provide valuable information on the initial distribution of energy among the products of exothermic reactions and complement that obtained from radiation measurement techniques, such as chemiluminescence and chemical laser experiments, and molecular beam experiments in which excitation energy is deduced from the measured angular distribution of the reaction products.

It has been found, for example, in the $F + H_2$ reaction (Ref. 1) that the total available reaction energy can be converted efficiently into internal excitation of the product HF molecule. The total energy available in this case is equal to the sum of the exothermicity of the reaction, $-\Delta H_0 = 31.5$ kcal mole^{-1}, the activation energy of the reaction 1.7 kcal mole^{-1}, the relative translational energy 3/2 RT(T = 300K) = 0.9 kcal mole^{-1}, and the H_2 internal energy RT = 0.6 kcal mole^{-1}, amounting to 34.7 kcal mole^{-1}, which is sufficient to populate the J = 6 rotational level in the v" = 3 vibrational level of HF; in fact, this excitation has been observed.

Some interesting complications occur in dealing with excited molecules in the mass spectrometer. While the theoretical minimum energy for ionization is $E_o - E_{exc}$, where E_o is the ionization potential of a ground state molecule and E_{exc} is the excitation energy, such a transition may have such low probability as to be unobservable. The reason is that if the internuclear distances for the vibrationally excited molecule and the ground state of the ion are significantly different, the transition probability, which is determined by the overlap integral or Franck-Condon factor for the two states, will be very small. From these considerations it follows that the measured decrease in the ionization potential of a molecule gives a lower bound on its excitation energy.

Mass spectrometric studies have been carried out on selected F atom reactions in which the HF molecule was produced with substantial internal excitation energy. Figure 1 shows appearance potential curves for the HF^+ ion for unexcited ground state HF, which is used as a reference, and for HF obtained from F atom reactions with n-butane, isobutane, and ethylene. It is

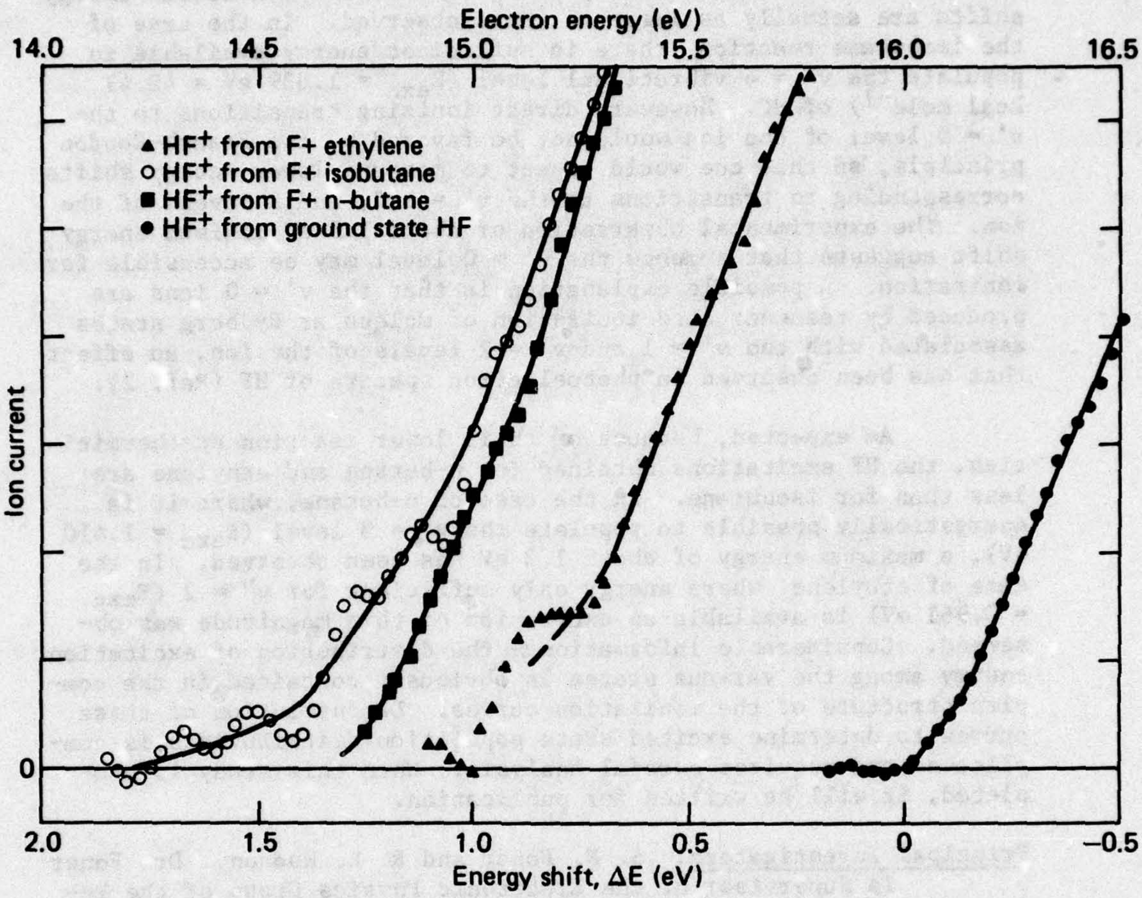

Fig. 1 Appearance Potential Curves for the HF^+ Ion for Ground State HF and for HF Produced by Reactions of F Atoms with n-Butane, Isobutane, and Ethylene. The energy scale shifts ΔE, with zero corresponding to ground state HF, give quantitative measures of excitation energies.

apparent from the magnitude of the scale shifts for the HF produced by reaction that some of the molecules are endowed with considerable energy.

What is somewhat surprising is that the ionization energy shifts are actually as large as those observed. In the case of the isobutane reaction, there is sufficient energy available to populate the v" = 4 vibrational level (E_{exc} = 1.839 eV = 42.41 kcal mole^{-1}) of HF. However, direct ionizing transitions to the v' = 0 level of the ion would not be favored by the Franck-Condon principle, so that one would expect to measure lower energy shifts corresponding to transitions to the v' = 1,2, and 3 levels of the ion. The experimental observation of about 1.8-eV maximum energy shift suggests that somehow the v' = 0 level may be accessible for ionization. A possible explanation is that the v' = 0 ions are produced by resonant auto-ionization of molecular Rydberg states associated with the v' = 1 and v' = 2 levels of the ion, an effect that has been observed in photoelectron spectra of HF (Ref. 2).

As expected, because of their lower reaction exothermicities, the HF excitations obtained for n-butane and ethylene are less than for isobutane. In the case of n-butane, where it is energetically possible to populate the v" = 3 level (E_{exc} = 1.410 eV), a maximum energy of about 1.3 eV has been observed. In the case of ethylene, where energy only sufficient for v" = 2 (E_{exc} = 0.961 eV) is available an excitation of this magnitude was observed. Considerable information on the distribution of excitation energy among the various states is obviously contained in the complex structure of the ionization curves. Deconvolution of these curves to determine excited state population distributions is complicated and requires careful analysis. When this study is completed, it will be written for publication.

Principal Investigators: S. N. Foner and R. L. Hudson. Dr. Foner is Supervisor of the Electronic Physics Group of the Research Center, and Mr. Hudson is a senior engineer in the Electronic Physics Group.

References

1. J. C. Polanyi and K. B. Woodall, "Energy Distribution Among Reaction Products. VI. F + H_2, D_2," J. Chem. Phys., Vol. 57, No. 4, 15 August 1972, pp. 1574-1586.

2. P. M. Guyon, R. Spohr, and W. A. Chupka, "Threshold Photoelectron Spectra of HF, DF, and F_2," J. Chem. Phys., Vol. 65, No. 5, 1 September 1976, pp. 1650-1658.

SCANNING ELECTRON MICROSCOPE INVESTIGATION OF POTENTIOSTATICALLY PITTED ALUMINUM

A stereoscopic scanning electron microscope investigation of potentiostatically pitted aluminum in chloride solutions has demonstrated that the oxide layer remains largely intact, occluding the growing pit from the bulk electrolyte. Defects in the central portion of the oxide are identified that apparently permit materials to enter and exit from the pit.

During the past decade, there has been considerable research performed in the area of localized corrosion (Ref. 1). In general, the goal of this research has been to find technological solutions to the problems of stress corrosion cracking and pitting corrosion. At the same time, an understanding of the basic mechanisms involved in these phenomena has been sought. Our particular investigation has dealt with potentiostatic pitting of aluminum in chloride solutions (Ref. 2) with the hope of ferreting out the experimental facts needed to identify mechanisms.

The scanning electron microscope (SEM) was used to study localized or pitting corrosion in aluminum. The experimental procedure employed the following steps: (a) anodizing the aluminum surface, thus providing an oxide passivation layer of known thickness; (b) pitting the specimen in a chloride solution with a modest applied potential (e.g., a few hundred millivolts); and (c) examining the pits formed in step (b) in the SEM. The examination included both topographical and compositional aspects.

Figure 1 presents a stereo pair* of micrographs of a set of three pits that apparently started independently but joined as they grew. In these micrographs, a portion of the oxide cover of the uppermost pit was removed with a microprobe in order to see the pit bottom more clearly. The part of the pit left unmarred by the microprobe shows the crystallographic attack that was taking place in the pit. The oxide layer is viewed unmistakably detached above the pit, having withstood the corrosive attack that removed a considerable amount of aluminum below. Although not shown clearly in Fig. 1, near the center of the oxide over each pit is a small hole only a small fraction of the size of the pit itself. These holes were associated with a surface defect and apparently provided entry to and exit from the pit.

---

*The pits can be viewed in stereo by placing an opaque sheet of material perpendicular to the page along the line dividing the two micrographs and allowing the eyes to merge the two images. With some luck the sheet is not necessary. However, a stereoscopic viewer is best if available.

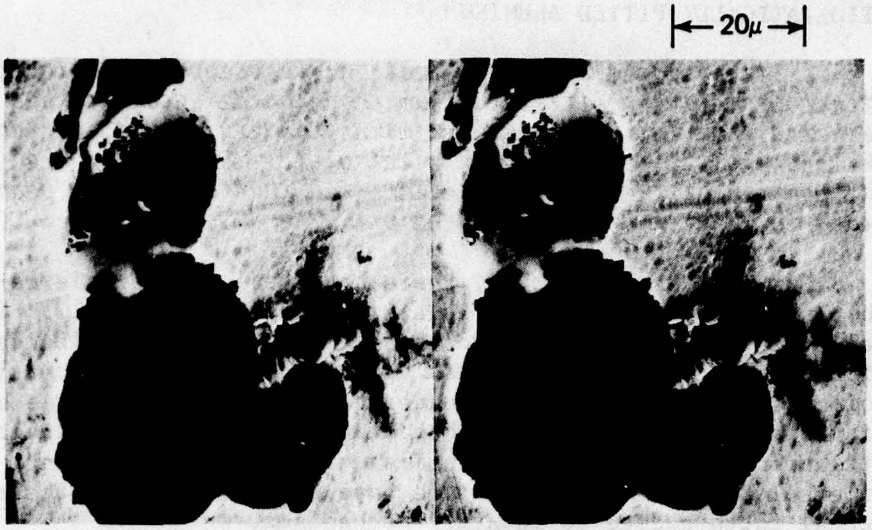

Fig. 1 A Stereo Pair of Micrographs of Three Pits after Using a Microprobe to Remove Part of the Oxide Film of the Uppermost Pit. The beam voltage was 30 kV.

Using the energy dispersive X-ray analysis system attached to the SEM, the chemical composition of various materials associated with the pits was determined. Of particular interest was a chloride containing a corrosion product whose X-ray spectrum indicated a [Cl] to [Al] concentration ratio significantly less than unity. This suggests a hydroxychloride aluminum complex.

The following conclusions were drawn from the experimental evidence:

1. The oxide layer remains intact, except for small breaks near the center, occluding the pit proper from the bulk electrolyte;

2. The undermining of the oxide layer is very extensive. Comparatively large amounts of matter are removed from the pit through small breaks;

3. The chloride corrosion product in its state of preservation is probably a hydroxychloride aluminum complex; and

4. Breaks in the oxide near the pit center were commonly observed to be associated with a surface defect.

Principal Investigators: C. B. Bargeron and R. B. Givens. Dr. Bargeron is a senior physicist and Mr. Givens is an engineering assistant in the Electronic Physics Group of the Research Center.

References

1. See, for example, Localized Corrosion, B. F. Brown, J. Kruger, and R. W. Staehle (eds.), NACE, Houston, TX, 1974.

2. C. B. Bargeron and R. B. Givens, "Stereoscopic Investigation of Potentiostatically Pitted Aluminum" (to be submitted to the J. Electrochem. Soc.).

STRUCTURE OF THE GROUND STATES OF THE NOBLE GAS-HALOGEN MOLECULES KrF AND XeF USING A SPIN-CORRELATED VALENCE BOND THEORY

A semiempirical valence bond (VB) wave function that includes electron correlation has been found to successfully account for the electron nuclear hyperfine structure (hfs) interactions in the inert-gas monohalide molecules KrF and XeF. Comparison of theoretical and experimental hfs constants yields estimates of the interatomic distance and electron charge distribution in the ground states of these unusual molecules.

Interest in the chemical bonding and structure of the inert gas compounds, which is generally high because these compounds violate the classical principle of inertness of closed shell atoms, has been further stimulated by the possibility of constructing powerful, partially tunable ultraviolet (UV) lasers based on emission from excited states of the inert-gas-monohalide diatomic molecules. Also of great theoretical interest and possibly of practical importance in calculating optical transition frequencies and transition intensities in these molecules is the fact that fairly elaborate molecular orbital (MO) calculations carried out at other laboratories predict that all the inert gas monohalides have nonbonding ground states (Ref. 1), whereas experiments at other laboratories have indicated that XeF and KrF are chemically bound (Ref. 2). Most recently, work at APL described elsewhere in this report has demonstrated that XeCl is also chemically bound (Ref. 3).

We have initiated a VB study of the inert gas monohalides, the advantage of the VB over the molecular orbital method being that it is considerably easier to include electron correlation in the VB wave function. The utility of such a VB wave function has

been demonstrated previously in studies of optical transition intensities (Ref. 4) and hfs interactions (Ref. 5) in the halogen-molecule anions, $(XM)^-$, which are isoelectronic to the inert gas monohalides.

The studies to date, which are still in a preliminary stage, use the VB wave function,

$$\Psi = N[\varepsilon\Phi(A\text{---}X) + \sqrt{1-\varepsilon^2}\ \Phi(A^+\text{---}X^-)] ,$$

to elucidate the structure of these molecules, where ε weighs the neutral (A---X) and ionic $(A^+\text{---}X^-)$ structures. For the ground state, ε is close to one, whereas ε is much smaller than one in the excited state responsible for UV emission to the ground state. N is a normalization constant. $\Phi(A\text{---}X)$ is an antisymmeterized product of Hartree-Fock self-consistent-field (SCF) atomic functions for the rare gas species A and halogen species X centered on their respective nuclei separated by a distance R, the internuclear distance. $\Phi(A^+\text{---}X^-)$ is a similar function only involving the ionic SCF wave functions. In this way intra-atomic correlation is built into the wave function. It should be noted that this is a wave function for a diatomic molecule that is one electron short of the completely filled shell structure $(A\text{---}X^-)$ and depicts the missing electron or "hole" as being shared between the two atoms.

To compute the isotropic hyperfine constant with this function it is important to include interatomic correlation. For example, in the structure (A---X) where the hole is on the halogen X, interatomic correlation is included by considering the van der Waals polarization of the halogen orbitals by the rate gas atom A, which contributes significantly to the halogen isotropic hyperfine constant. On the other hand for the ionic structure $(A^+\text{---}X^-)$ where the hole resides on the rare gas atom, the polarization of the ionic orbitals on A^+ by the negative charge on X^- is necessary to compute adequately the rare gas isotropic hyperfine constant. A key point in the calculation, which is too lengthy to be described in detail here, is that the polarization of A^+ by X^- in $\Phi(A^+\text{---}X^-)$ admixes various excited states of A^+ into the ground state, and most of these states involve excitation of a valence s electron into the almost filled p shell of A^+. The spin of the excited s electron must be opposite to the net spin of the almost filled p shell; thus this excitation leads to an unpaired electron spin density in the valence s shell. We have a similar situation in the neutral structure (A---X) involving the hole on X where the polarization mechanism is the van der Waals interaction.

Values of R and ε are determined on the basis of the best fit between the calculated and experimental isotrpic hyperfine constants A_0. These values are used to compute the anisotropic constant B, which is compared to the experimental anisotropic constant. The anisotropic part of the hfs is determined largely by the unpaired electron density in the valence p orbitals and hence is not as sensitive to electron correlation as the isotropic constant. The results for XeF are tabulated in Table 1. From the table it is seen that the results are in good agreement with experiment. The two internuclear distances correspond to using the experimental isotropic constant A_0 of Xe to determine R and ε or to using the experimental A_0 of F to evaluate these quantities. The closeness of the internuclear distances can also be used as a gauge on the success of the theory. The agreement between the theoretical and experimental values for the anisotropic coupling constant B is excellent, particularly for F, where near coincidence of these quantities is more than we would expect from the semiempirical theory. Computations are in progress for KrF and XeCl.

This theory suggests that since the isotropic hyperfine constant A_0, which is a measure of the quality of an electronic wave function, can be calculated using a VB wave function, a correlated wave function should be used to calculate the electronic structure of these molecules in order to assess if the failure of the MO theory to predict bounding in some of these molecules is due to shortcomings of the theory or the fact that the molecules are bound in a matrix but not in the free state.

Table 1

COMPARISON OF EXPERIMENTAL AND THEORETICAL HYPERFINE COUPLING CONSTANTS FOR XeF

Electron Spin Resonance Nucleus	Exp A_0 (MHz)	R(mn)	ε	Exp B(MHz)	Theory B(MHz)
Xe^{129}	1367	0.241	0.8	1108	1214
F^{19}	517	0.248	0.8	2126	2125

<u>Principal Investigators</u>: F. J. Adrian and A. N. Jette. Dr. Adrian is Supervisor of the Microwave Physics Group, and Dr. Jette is a senior physicist in the Electronic Physics Group of the Research Center.

References

1. D. H. Liskow, H. F. Schaefer, III, P. S. Bagus, and B. Liu, "Probable Nonexistence of Xenon Monofluoride as a Chemically Bound Species in the Gas Phase," J. Am. Chem. Soc., Vol. 95, 1973, p. 4056.

2. J. R. Morton and W. E. Falconer, "Electron Spin Resonance Spectrum in XeF in gamma-Irradiated Xenon Tetrafluoride," J. Chem. Phys., Vol. 39, 1963, p. 427.

3. F. J. Adrian and V. A. Bowers, "ESR Spectrum of XeCl in Argon at 4.2K," J. Chem. Phys. (in press).

4. F. J. Adrian and A. N. Jette, "Theoretical Investigation of the Polarization and Band Intensities of the Optical Transitions of the V_k Center using a Valence-Bond Wave Function for the Halogen-Molecule Anions," Phys. Rev., Vol. B9, 1974, p. 3587.

5. A. N. Jette and F. J. Adrian, "Theoretical Investigation of the Hyperfine-Structure Constants of the V_k and (XY) Centers Using a Valence-Bond Wave Function for the Halogen-Molecule Anions," Phys. Rev. B. (in press).

MEASUREMENT OF MECHANICAL PROPERTIES OF VISCOELASTIC MATERIALS

A high-sensitivity technique for measuring the tensile modulus of viscoelastic materials, such as solid propellants, has been developed. Because the tests involve small deformations and are, therefore, nondestructive, the same sample can be repeatedly tested over a long period of time to provide information on aging effects on mechanical properties, without the uncertainties due to sample variability when the usual destructive tests are employed.

Considerable difficulty has long been encountered in attempts to measure accurately the tensile modulus of viscoelastic materials, such as filled elastomers and solid propellants. Changes in the network structure of the polymeric binder with time and temperature as revealed by changes in the tensile modulus are important for assessing the effects of chemical aging and may be useful in predicting propellant service life. In two recent review articles (Refs. 1 and 2) the need for improved tensile modulus measurements was emphasized. One of the greatest difficulties in this work has been the scatter in the data, which often has been so large as to obscure the changes due to chemical aging. The lack of reproducibility of results in previous work is probably due to two factors: sample variability and inaccuracy in the measurement technique.

We have evolved a nondestructive small-deformation technique in which a low-frequency dynamic stress is applied to the sample by a force transducer (driver), and the displacements of the sample are sensed by small ceramic phonograph cartridge pickups coupled into special FET high-impedance amplifiers. The small-deformation approach avoids permanent damage to the material and, by permitting the same sample to be tested repeatedly, avoids any scatter in the measurements due to sample-to-sample variations. Because of the relatively low tensile modulus of these viscoelastic materials, the most commonly used transducer for strain measurement, the resistance strain gauge, is unsuitable in our application, since its compliance is comparable to the material being tested and would require large corrections to the measurements. The phonograph cartridge pickups, on the other hand, require only very small tracking forces and faithfully follow the motions of the medium. In addition, the pickups can be positioned to provide high spatial resolution and could be used to observe anisotropic behavior in the mechanical properties of the sample.

A simplified schematic diagram of the apparatus is shown in Fig. 1. The driver unit is a vibration generator with a maximum force capability of 1 lb in the frequency range 0 to 10 kHz. A series of phonograph cartridges is mounted on the sample, as indicated, to measure relative displacements. By using a low-frequency AC dynamic stress, drifts in position, including those due to creep, are eliminated, and only the coherent displacement produced by the driver is measured. A traveling stage microscope is used to calibrate the system by unclamping the sample from the base plate and vibrating the sample as a rigid unit. The system has exceptional sensitivity. Early experiments demonstrated that a displacement of 1×10^{-6} cm or 1/50th the wavelength of visible light could be easily resolved. Therefore, the inherent sensitivity of the technique is about two orders of magnitude higher than that theoretically attainable by a diffraction-limited optical microscope.

Experiments have been carried out on propellant samples covering the frequency range from 40 Hz down to the order of 0.01 Hz. Figure 2 shows a typical set of small-deformation dynamic modulus data obtained on a 1/2 in. × 1/2 in. × 5 in. rectangular prism propellant sample at 74°F. The driving force was 0.18 lb and produced strains in the range of 1 to 5×10^{-4} in./in. The measurements exhibit small scatter and suggest that the technique may provide very useful information on the properties of viscoelastic materials. The dynamic modulus curve shown in Fig. 2 has the general shape that is expected for a polymeric viscoelastic material. Analysis of curves of this type can be used to characterize the mechanical properties of these materials.

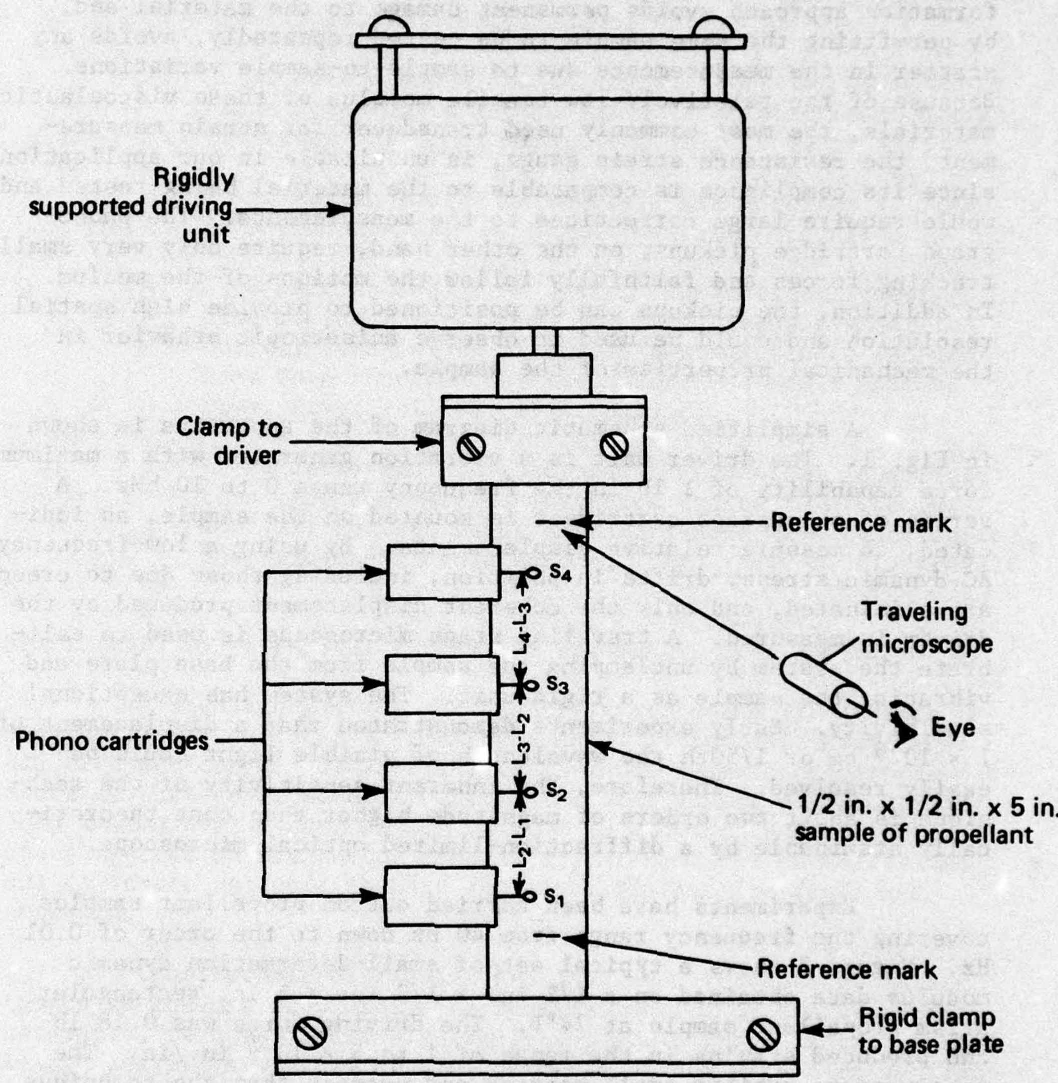

Fig. 1 Experimental Arrangement for Tensile Modulus Measurements

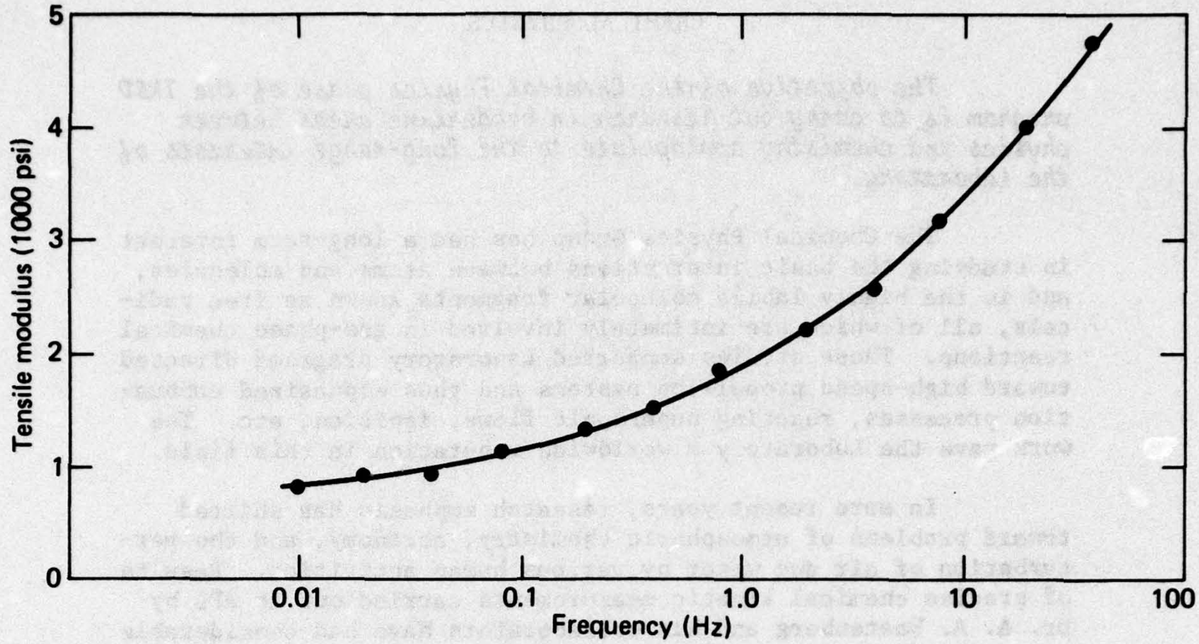

Fig. 2 Small-Deformation Dynamic Modulus Measurements on a Solid Propellant

Principal Investigators: S. N. Foner and B. H. Nall. Dr. Foner is Supervisor of the Electronic Physics Group of the Research Center, and Mr. Nall is a senior engineer in the Electronic Physics Group.

References

1. P. L. Nichols, "The Use of Elevated Temperature Aging to Predict Propellant Service Life," CPIA Publication 264, May 1975, pp. 19-61.

2. F. R. Mayo, "The Chemistry of Aging of Hydrocarbon Binders in Solid Propellants," CPIA Publication 262, February 1975.

CHEMICAL PHYSICS

The objective of the Chemical Physics phase of the IR&D program is to carry out research in borderline areas between physics and chemistry appropriate to the long-range interests of the Laboratory.

The Chemical Physics Group has had a long-term interest in studying the basic interactions between atoms and molecules, and in the highly labile molecular fragments known as free radicals, all of which are intimately involved in gas-phase chemical reactions. These studies supported Laboratory programs directed toward high-speed propulsion systems and thus emphasized combustion processes, reacting supersonic flows, ignition, etc. The work gave the Laboratory a worldwide reputation in this field.

In more recent years, research emphasis has shifted toward problems of atmospheric chemistry, aeronomy, and the perturbation of air and water by various human activities. Results of precise chemical kinetic measurements carried out at APL by Dr. A. A. Westenberg and his collaborators have had considerable impact on our knowledge of atmospheric behavior and its prediction. A continuing program in acoustic leak detection for gas distribution systems, funded by an outside nonprofit agency, was a direct outgrowth of fundamental research in the mechanism of intermolecular energy transfer initiated by Dr. J. G. Parker. During the past year, another aspect of this general field, i.e., the investigation of the effects of laser-excited oxygen molecules on biological organisms in water, has attracted wide attention and interest. It is also significant that the stature of Dr. L. Monchick was recognized by his appointment as William S. Parsons Visiting Professor in the Chemistry Department of The Johns Hopkins University during the year 1975-76.

Current emphasis is on areas of atmospheric, laser, and pollution chemistry. Projects include the measurement of reaction rates between atoms, free radicals, and molecules, rates of molecular energy transfer, and studies of molecular collision processes. All of these processes are fundamentally involved in various problems connected with stratospheric flight, laser technology, sound propagation, and biological systems of significance to the Department of Defense. Results are described in detail in five papers that are presently being prepared or have been accepted for publication.

KINETICS OF GAS-PHASE REACTIONS

A new flash photolysis-resonance fluorescence apparatus for atom-molecule reaction rate measurements has been built and tested.

The chemical kinetics research program emphasizes the study of elementary reaction rates involving atoms and free radicals under precisely controlled experimental conditions. Such reactions are basic to all technologically important chemical changes occurring in gases.

As part of the continuing effort to maintain a position at the forefront of activity in this field, the experimental techniques employed at the Laboratory for such studies underwent a pronounced change during the past year. Perhaps the most sensitive method now available for measuring the concentration of atoms (and a few diatomic radicals) is that of resonance fluorescence. In this method, the atoms are caused to undergo a transition to an excited state by resonance radiation from an external lamp containing atoms of the same kind. Subsequent fluorescence (in the vacuum ultraviolet) of these excited atoms is measured at right angles to the lamp by a suitable photomultiplier. The sensitivity of the approach comes from the modern ability to monitor single photons by digital counting techniques. This ability to measure very low atom concentrations (down to 10^{10} per cm^3) has the important consequence that experimental conditions may be arranged to eliminate the complication of secondary reactions.

In one of its powerful applications, the resonance fluorescence detection technique is coupled with flash photolysis as an essentially instantaneous atom source. A trace of a suitable parent molecule highly diluted with an inert gas is partially dissociated by an intense light (UV) flash (20 to 200 joules) to give an initial pulse of atoms in a collimated beam along the flash path. Another reactant species is also present at a concentration much larger than the atoms so that pseudo-first-order reaction of the atoms takes place. The reacting atoms are illuminated by a suitable resonance lamp at right angles to the flash column, and the fluorescing atoms are then monitored from a third mutually perpendicular direction by a photomultiplier as the atoms decay. The real-time decay of the reacting atoms is measured by a multichannel photon-counting system, and from this the reaction rate constant may be determined.

Activity during the past year has concentrated heavily on assembling and setting up the necessary apparatus to perform experiments of the type described above. This involved the design and construction of a reaction chamber with suitable windows, resonance lamps of the flowing gas-microwave excitation type, a flash lamp, and triggering device, as well as the acquisition of the necessary electronic equipment and the means of interfacing directly to a computer for rapid data analysis. The setup and testing work has largely been accomplished.

Preliminary trials with the apparatus are being carried out on the O + C_2H_2 reaction, an example that has been thoroughly studied in this laboratory (Ref. 1) and elsewhere by several independent techniques so that it constitutes a good "known" test case. In connection with the trials on this reaction, an interesting UV chemiluminescence was discovered as a minor reaction channel. Proper interpretation of the main reaction will require inclusion of this chemiluminescent channel, and work along this line is proceeding. After this initial shakedown phase, it is planned to study a number of reactions of interest to atmospheric and polymer combustion chemistry.

<u>Principal Investigators</u>: A. A. Westenberg and N. deHaas. Dr. Westenberg is Supervisor of the Chemical Physics Group of the Research Center, and Mr. deHaas is a senior physicist.

<u>Reference</u>

1. A. A. Westenberg and N. deHaas, "Absolute Measurements of the O + C_2H_2 Rate Coefficient," <u>J. Phys. Chem.</u>, Vol. 73, 1969, pp. 1181-1186.

MOLECULAR ENERGY TRANSFER

Research is directed toward an understanding of the mechanism of molecular energy transfer in collisions of gas molecules. Types of energy involved include rotational, vibrational, and electronic. Possible transfer modes consist of vibration → translation (V-T), inter- and intra-molecular vibration → vibration (V-V), vibration → rotation → translation (V-R-T), electronic → translation (E-T), and electronic → vibration (E-V). A new area of research that has emerged involves the transfer of molecular electronic energy to microbiological systems.

Effort over the past year has been mainly in two areas: analysis and interpretation of data obtained previously on the effect of laser-excited dissolved oxygen on coliform counts of natural water samples, and an investigation of fluorescence of laser-excited gaseous oxygen at wavelengths in the neighborhood of 1.27 μ.

The main conclusions obtained from this analysis are that: (a) substantial reduction in coliform levels may be induced, the magnitude of which exhibits a fundamental dependence on dissolved oxygen concentration, laser intensity, and irradiation time; (b) reduction of coliform levels by oxygen pressure alone is observed but the effect is, on the average, small compared to that

observed when the sample is simultaneously irradiated; (c) thermal effects accompanying irradiation are negligible; (d) the inactivation rate is inhibited for oxygen pressure in excess of 10 atm; and (e) protein and nucleic acid levels determined from ultraviolet absorption measurements for a water sample subjected to combined irradiation and oxygen pressurization are considerably greater than corresponding values obtained for an unprocessed sample, indicating the mode of inactivation of coliform to be cell wall destruction.

Consideration of results (a) to (c) in conjunction with the established experimental fact that bacteria are unaffected by radiation alone for wavelengths large compared to 260 nm (where nucleic acids absorb strongly and genetic damage occurs) implies strongly that laser-excited singlet molecular oxygen $O_2(^1\Delta_g)$ is the single cause of bacterial destruction, the role of the laser being solely to produce selective excitation of oxygen from the ground electronic state.

A theoretical treatment of the effect of singlet molecular oxygen on microorganisms has been presented in Ref. 1 in which the process has been modeled as a diffusion-controlled reaction. From this study it is evident that one of the key factors in determining the efficacy of $O_2(^1\Delta_g)$ in killing bacteria is the collisional deactivation time. Experimental investigation (Ref. 2) has shown that this collisional lifetime depends strongly on the solvent, varying from 2 μs for distilled water to several hundred microseconds for the freons. Calculations of the kill probability carried out in Ref. 1 were for distilled water, thus ignoring quenching due to dissolved impurities. In most cases, the effect of impurities would be expected to be small since water is a relatively efficient quencher, although on an absolute basis quenching still involves something like 10^8 collisions of $O_2(^1\Delta_g)$ with water. However, it is an experimental fact that certain compounds in small concentration can produce a rather large effect. A particular case is that of the aromatic hydrocarbons for which it has been found (Ref. 3) that the most efficient quenchers, interestingly enough, are also high in carcinogenic activity. Measurement of the collisional lifetime of dissolved oxygen for natural water samples would thus give an indication of the presence of trace amounts of efficient quenchers, the exact nature of which would subsequently be determined from a chemical analysis.

Consideration of the fundamental factors involved indicates that lifetimes of singlet molecular oxygen may be determined by monitoring the fluorescence at 1.27 μ subsequent to excitation at 1.064 μ by means of a Q-switched Nd:YAG laser. This irradiation excites the oxygen to the first vibrational level of the $^1\Delta_g$ state, i.e., $O_2(^1\Delta_g)(v' = 1)$. Since water is known to be a very efficient

of vibration in oxygen (Ref. 4), vibrational deactivation rapidly ensues, i.e.,

$$O_2(^1\Delta_g)(v' = 1) \rightarrow O_2(^1\Delta_g)(v' = 0) + \text{energy}. \qquad (1)$$

The most probable following transition is a collisional deactivation,

$$O_2(^1\Delta_g)(v' = 0) \rightarrow O_2(^3\Sigma_g^-)(v = 0) + \text{energy} , \qquad (2)$$

corresponding to a transition to the ground electronic state $O_2(^3\Sigma_g^-)$. In addition to the transition 2, a radiative deactivation

$$O_2(^1\Delta_g)(v' = 0) \rightarrow O_2(^3\Sigma_g^-) + h\upsilon \qquad (3)$$

may also occur at a wavelength $\lambda = 1.27\ \mu$. This fluorescence is thus spectrally separated from the exciting wavelength, permitting isolation by means of appropriate optical filtering.

To provide an understanding of the fundamental processes involved in the collisional deactivation of $O_2(^1\Delta_g)$, experimental measurements of the fluorescent decay in high-pressure gaseous oxygen have been carried out at pressures in the range of 35 to 96 atm. These measurements indicate the onset of the fluorescence to be immediate, appearing within 10 μs after irradiation (pulse duration is 20 ns). An explanation of this result requires that either the radiative transition

$$O_2(^1\Delta_g)(v' = 1) \rightarrow O_2(^3\Sigma_g^-)(v = 1) + h\nu_1 \quad (\lambda_1 = 1.28\ \mu) \qquad (4)$$

takes place with the same probability as

$$O_2(^1\Delta_g)(v' = 0) \rightarrow O_2(^3\Sigma_g^-)(v = 0) + h\nu_0 \quad (\lambda_0 = 1.27\ \mu) , \qquad (5)$$

which is reasonable since the Franck-Condon factors for the two processes are essentially equal, or that the vibrational deactivation

$$O_2(^1\Delta_g)(v' = 1) \rightarrow O_2(^1\Delta_g)(v' = 0) \qquad (6)$$

is much more rapid than would be expected for the vibration → translation (V-T) process. Alternative paths for vibrational deactivation are presented by the nearly resonant exchange processes

$$O_2(^1\Delta_g)(v' = 1) + O_2(^3\Sigma_g^-)(v = 0) \rightarrow O_2(^1\Delta_g)(v' = 0) + O_2(^3\Sigma_g^-)(v = 1) \; , \qquad (7)$$

i.e., a vibrational exchange, or

$$O_2(^1\Delta_g)(v' = 1) + O_2(^3\Sigma_g^-)(v = 0) \rightarrow O_2(^3\Sigma_g^-)(v = 1) + O_2(^1\Delta_g)(v' = 0) \; , \qquad (8)$$

an electronic exchange. Experimental measurements (Ref. 5) indicate that for $O_2(^1\Delta_g)$ molecules in the v' = 0 level, resonant electronic exchange is an extremely rapid process requiring on the order of 10 collisions. Whether or not this is true for vibrationally excited species is not clear.

Experimental values of the time constant obtained from analysis of the time rate of fluorescence decay agree well with those obtained by other means, indicating the deactivation process to be controlled by binary collisions. A further point of interest is the fact that the magnitude of the level to which the fluorescent signal rises initially has been found to depend on the cube of the pressure. The implication of this is that the rate of spontaneous emission varies linearly with pressure in agreement with results reported by Badger et al. (Ref. 6).

<u>Principal Investigator</u>: Dr. J. G. Parker is a senior physicist in the Chemical Physics Group.

References

1. J. G. Parker, "Effect of Laser Radiation at 1.064μ on Total Coliform Counts of Oxygenated Potomac River Water Samples" (submitted for publication).

2. P. B. Merkel and D. R. Kearns, "Radiationless Decay of Singlet Molecular Oxygen in Solution. An Experimental and Theoretical Study of Electronic-to-Vibrational Transfer," J. Am. Chem. Soc., Vol. 94, 1972, pp. 7744-7753.

3. R. Benson and N. Geacintov, "Quenching of Excited Triplets of Aromatic Hydrocarbons by Molecular Oxygen," J. Chem. Phys., Vol. 59, 1973, pp. 4429-4434.

4. K. H. Becker, W. Groth, and W. Schurath, "The Quenching of Metastable $O_2(^1\Delta_g)$ and $O_2(^1\Sigma_g^+)$ Molecules," Chem. Phys. Lett., Vol. 8, 1971, pp. 259-262.

5. I. T. N. Jones and K. D. Bayes, "Electronic Energy Transfer from $^{32}O_2(^1\Delta_g)$ to $^{36}O_2(^3\Sigma_g^-)$," J. Chem. Phys., Vol. 57, 1972, pp. 1003-1004.

6. R. M. Badger, A. C. Wright, and R. F. Whitlock, "Absolute Intensities of the Discrete and Continuous Absorption Bands of Oxygen Gas at 1.26 and 1.065μ and the Radiative Lifetime of the $^1\Delta_g$ State of Oxygen," J. Chem. Phys., Vol. 43, 1965, pp. 4345-4350.

KINETIC AND COLLISION THEORY

Significant new results have been obtained in the methodology of calculating scattering cross sections, in the kinetic theory of diffusion of excited states, and in the correlation of ion transport with molecular parameters.

The studies (Refs. 1 and 2) previously completed on the differential and gas transport properties of He collisions with CO and HCl have now been extended to the examination of two new popular approximate methods. In the first, the equivalent potential (EP) method, the real anisotropic potential is replaced by a weighted average of the potential with the same transition selection rules as the real potential; in the second, the angular momentum of the CO or HCl about the axis connecting the center of mass to the He center is constrained to be a constant of motion. The second approximation (Ref. 3), the coupled states or CS model,

works very well in contrast to the EP method, which seems to have thrown away too much information. Therefore, the CS method is likely to be very useful in collision studies. The usefulness of these methods for spectral pressure broadening is also being studied by Drs. Monchick, Green, and Kouri. Their results are being prepared for publication.

In preparation for a continuation of these studies to collisions of two diatomic molecules, it became apparent that no broad theory describing self-diffusion or the relative diffusion of similar molecules in different quantum states had ever been developed. The troubled history of the theory of spin diffusion showed, indeed, that it was not a trivial exercise. L. W. Hunter and L. Monchick have set up a general theory that takes account of exchange symmetry and embraces a set of phenomena as varied as electronic, vibration, or rotation energy diffusion, charge migration, and nuclear spin diffusion. Phenomenological transfer equations may be set up, and one may define diffusion coefficients that in certain cases take on the form of the diffusion coefficients usually found in kinetic theory. This work is being prepared for publication.

Ion mobility is also a diffusion phenomenon. The particular case of H^+, H_2^+, and H_3^+ diffusing through helium was investigated, and a previous anomaly found in H^+-He ion mobility studies was traced to an unexpectedly strong attraction due to a resonance with the (H^+He)-H state. In fact, consideration of the potentials inferred from ion mobility data indicates that the type of interaction changes uniformly from covalent to the van der Waals type as the collision partner of helium changes from H^+ to H_2^+ to H_3^+. This work is described in Ref. 4.

Principal Investigators: L. Monchick, S. Green, E. A. Mason, D. J. Kouri, and L. W. Hunter. Dr. Monchick is a senior chemist in the Chemical Physics Group of the Research Center and was Parsons Professor in the Chemistry Department of The Johns Hopkins University from 1 September 1975 to 1 June 1976. Dr. Green is a Senior Postdoctoral Fellow at Columbia University and the NASA Institute for Space Studies, Dr. Mason is at Brown University, and Dr. Kouri is at the University of Houston; none of them was funded by this project. Dr. Hunter, of the Fire Problems Group, also was not funded by the IR&D program.

References

1. L. Monchick and S. Green, "Validity of Central Field Approximations in Molecular Scattering: Low Energy CO - He Collisions," J. Chem. Phys., Vol. 63, No. 5, 1 September 1975, pp. 2000-2009.

2. S. Green and L. Monchick, "Validity of Approximate Methods in Molecular Scattering: Thermal HCl - He Collisions," J. Chem. Phys., Vol. 63, No. 10, pp. 4198-4205.

3. L. Monchick and S. Green, "Validity of Approximate Methods in Molecular Scattering: III. Effective Potential and Coupled States Approximations for Differential and Gas Kinetic Cross Sections," presented at Gordon Research Conference, Summer 1976 (manuscript in preparation).

4. L. H. Viehland, E. A. Mason, T. H. Stevens, and L. Monchick, "Test of the H_2^+ - He Interaction Potential. Comparison of the Interactions of the He with H^+, H_2^+, and H_3^+" (accepted by Chem. Phys. Lett.).

MICROWAVE PHYSICS

The program of the Microwave Physics Group is directed toward improved understanding of fundamental relationships between the structure of matter and its interactions with electromagnetic radiation, which will guide future innovation in the generation and utilization of electromagnetic radiation. The work also provides experimental and theoretical expertise in a number of areas of spectroscopy, which are used in joint projects with other groups.

Current work emphasizes three areas of study. The first comprises studies of highly conjugated organic molecules whose interesting optical, semiconductive, and photochemical properties are currently used in dye lasers, and which may be the basis for future solid state devices. Nature employs these molecules, especially the porphyrins, for energy transfer and conversion in biological systems, and part of our work on porphyrins has been supported by a grant from the National Institutes of Health.

Work has recently begun on photoacoustic spectroscopy, a new and rapidly developing field of research, which detects electromagnetic radiation by the resultant heating of the sample and subsequent development of a pressure wave in a gas in contact with the sample. The technique is uniquely suited to spectroscopy of highly absorbing, poorly reflecting samples and, furthermore, it can determine the fraction of absorbed electromagnetic radiation that is degraded to heat. It is believed that the technique will be very useful in the investigation of a variety of problems of importance in defense technology including semiconductors, especially in thin films, amorphous catalysts, and surface corrosion.

Studies of the structure and reaction mechanisms of free radicals are carried out in collaboration with the Electron and Atomic Physics Group. These studies have made the Laboratory internationally recognized in this field, which includes such important areas as development of high-energy fuels, synthesis of unique materials and, most recently, development of a class of high-energy ultraviolet lasers based on emission from the inert gas monohalides. A by-product of the work has been major contributions to the theory of chemically induced magnetic polarization, a recent development of great importance to the study of free radicals and photochemical reaction mechanisms. The relevance of the field is recognized by a NATO Advanced Study Institute on Chemically Induced Magnetic Polarization scheduled for April 1977. Dr. F. J. Adrian, head of the Research Center's Microwave Physics Group, is to be one of the invited lecturers at this meeting.

These studies are described in more detail in the seven publications and three abstracts authored or co-authored by group members which either appeared in print or were accepted for publication during FY 76 and in three additional articles recently submitted for publication. Results also were described in ten addresses at scientific meetings and academic symposiums. The work was carried out by the five senior scientists and one associate engineer of the Microwave Physics Group of the Research Center.

PHOTOEXCITED TRIPLET MECHANISM OF CHEMICALLY INDUCED NUCLEAR SPIN POLARIZATION

A new mechanism of chemically induced nuclear spin polarization (CIDNP) has been proposed, and strong experimental evidence advanced for its occurrence in some photolytic reaction of quinones. The mechanism begins with electron-spin-selective singlet-triplet intersystem crossing of a photoexcited molecule and subsequent reaction of the triplet to yield a pair of electron-spin-polarized radicals. The electron polarization of these radicals is subsequently transferred to the nuclear spins by electron-nuclear cross relaxation.

Theoretical research in chemically induced magnetic polarization continues at APL, in collaboration with experimental research by Dr. H. M. Vyas and Prof. J. K. S. Wan at Queen's University, Kingston, Ontario, Canada. The experimental work is not funded by the IR&D program.

Detailed knowledge of photochemical reaction mechanisms is important for such problems as detection of radiation, utilization of solar energy, photochemical degradation of materials, and a number of other problems. However, the complexity and rapidity of the elementary reactions that lead from the initial absorption of a light photon to the final product(s) makes the acquisition of such knowledge quite difficult. A promising technique for studying photochemical reactions uses the recently observed phenomenon of chemically induced magnetic polarization. This is the generic name for a number of processes whereby free radical reactions in liquids yield abnormal populations of the nuclear spin states of the diamagnetic products and reactants, and abnormal populations of the electron spin states of the free radical intermediates. The importance of the phenomenon is that these nuclear and electron spin polarizations are sufficiently long lived to be easily observed by conventional nuclear magnetic resonance (NMR) and electron spin resonance (ESR) techniques, yet they result from, and thus give information about, very rapid individual steps in the overall reaction mechanism that are difficult to study directly.

A very important source of chemically induced magnetic polarization is the interplay between electron-spin-dependent chemical bonding interactions between two radicals and the nuclear-spin-dependent magnetic interactions in the individual radicals (radical pair mechanism). For some time, this was believed to be the only polarization mechanism. However, it was shown recently that another mechanism known as the photoexcited triplet mechanism was the source of the electron spin polarization observed during photolytic reactions of many carbonyl compounds (Ref. 1). In this mechanism, a photoexcited molecule undergoes a spin-selective intersystem crossing to an electron-spin-polarized triplet state, which then reacts to yield a pair of electron-spin-polarized radicals. Although the mechanism appears to operate only in photolytic reactions of carbonyl compounds, these compounds, especially the ketones and quinones, play a very important role in synthetic and mechanistic photochemistry.

The question was raised of whether nuclear spin polarization could be produced by this triplet mechanism combined with transfer of the electron spin polarization of the radicals to the nuclei by the magnetic interactions between electrons and nuclei (cross relaxation or Overhauser effect) (Ref. 2). The mechanism is depicted in Fig. 1, where the electron polarization process is denoted by different quantum efficiencies (Q+ and Q-) for production of radicals in e+ and e- electron spin states, and the electron polarization is transferred to the nuclei by the cross-relaxation transitions W_0 and W_2. Finally, the radicals react to form nuclear-spin-polarized diamagnetic products, a critical step

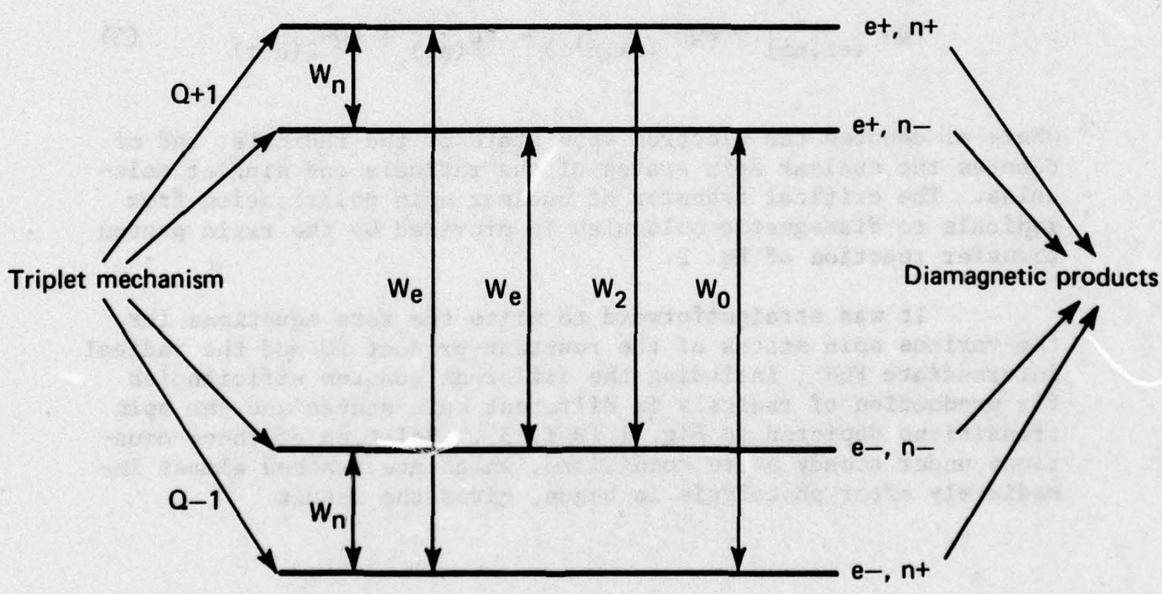

Fig. 1 Steps in the Photoexcited Triplet Mechanism of Chemically Induced Nuclear Spin Polarization

because it must occur rapidly (within approximately 10^{-5} to 10^{-7} s) before the pure electron spin transitions, W_e, and pure nuclear spin transitions, W_n, destroy all polarizations.

A class of reactions deemed very likely to yield CIDNP by the photoexcited triplet mechanism is the cyclic photoreduction of quinones by hydroquinones or other hydrogen donors to yield semiquinone radicals that ultimately react to regenerate the original quinone. The process is important in various photochemical processes, and a closely related reaction is believed to be involved in photosynthesis. The reaction mechanism is illustrated below for the CIDNP-producing photochemical reaction of tetrafluoro 1, 4 benzoquinone ($O = C_6H_4 = O$ or FQ, for short) with the corresponding hydroquinone ($HO\text{-}C_6H_4\text{-}OH$ or FQH_2):

$$FQ_{(n\pm)} \xrightarrow{h\nu} {}^3FQ^*_{(e+,n\pm)} \xrightarrow{FQH_2} 2FQH\cdot_{(e+,n\pm)}$$
$$FQ_{(n\pm)} \xrightarrow{h\nu} {}^3FQ^*_{(e-,n\pm)} \xrightarrow{FQH_2} 2FQH\cdot_{(e-,n\pm)} \qquad (1)$$

$$FQH\cdot_{(e\pm,n\pm)} + FQ_{(n\mp)} \rightleftarrows FQ_{(n\pm)} + FQH\cdot_{(e\pm,n\mp)} \qquad (2)$$

$$FQH\cdot_{(e\pm,n\pm)} + FQH\cdot_{(e\mp,n'\pm)} \rightarrow FQ_{(n\pm)} + FQH_{2(n'\pm)} \qquad (3)$$

where e± denotes the electron spin state of the radicals, and n± denotes the nuclear spin states of the radicals and singlet molecules. The critical transfer of nuclear spin polarization from radicals to diamagnetic molecules is provided by the rapid proton transfer reaction of Eq. 2.

It was straightforward to write the rate equations for the various spin states of the reactant-product FQ and the radical intermediate FQH·, including the different quantum efficiencies for production of radicals in different spin states and the spin transitions depicted in Fig. 1 (Ref. 3). Solution of these equations under steady state conditions, which are reached almost immediately after photolysis is begun, gives the result

$$\rho_N = ([FQ_{n+}] - [FQ_{n-}])/[FQ] = -\frac{1}{8} \quad I(Q_+ + Q_-[FQ]k_2 \quad \frac{2(Q_+ - Q_-)}{Q_+ + Q_-} \xi \qquad (4)$$

where

$$\xi = \frac{(W_2 - W_0)}{(W_n + W_e + 2W_2)(W_n + W_e + 2W_0) - (W_n - W_e)^2} . \qquad (5)$$

Here I is the light intensity, k_2 is the rate of the reaction of Eq. 3, [FQ] is the total fluoroquinone concentration, and $[FQ_{n+}]$ and $[FQ_{n-}]$ are its concentrations in the two nuclear spin states.

The foregoing equations show that the polarization depends on the relative magnitudes of the spin transitions W_2 and W_0. In the present system, $W_2 = 6W_0$ (Ref. 2); thus it is predicted that the polarization will be negative or emissive in agreement with the observed polarization. Since the magnetic field dependencies of $(Q_+-Q_-)/(Q_++Q_-)$ (Ref. 1) and the spin transition rates are known, it is possible to compute the field dependence of the polarization by this mechanism. As shown in Fig. 2, the predicted field dependence agrees well with the experiment; whereas the predicted field dependence of CIDNP by the radical pair mechanism for this system, also shown in Fig. 2, disagrees with experiment at low fields (Ref. 3).

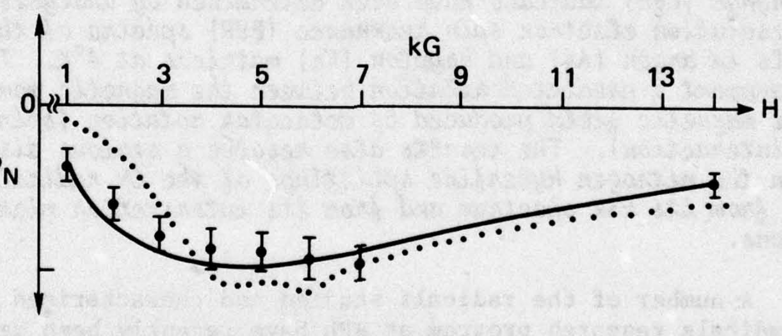

Fig. 2 Field Dependent ^{19}F CIDNP Intensity (ρ_N) of Tetrafluoro, 1,4-Benzoquinone for Photolysis of FQ in FQH_2, Benzene Solution. Irradiation was performed in an auxiliary magnet in field H except for the point at 14 kG where the sample was irradiated in the spectrometer. ●: Experimental points. ———: CIDNP calculated from the photoexcited triplet mechanism. ••••••: CIDNP calculated from the radical pair mechanism.

Principal Investigators: F. J. Adrian, H. M. Vyas, and J. K. S. Wan. Dr. Adrian is Supervisor of the Microwave Physics Group. Dr. Vyas and Professor Wan are at Queens University, Kingston, Ontario, Canada, and are not funded by the program.

References

1. F. J. Adrian, "A Possible Test of the Photoexcited Triplet Mechanism of Chemically Induced Electron Spin Polarization: Dependence of the Spin Polarization on Polarized Light Orientation," J. Chem. Phys., Vol. 61, 1 December 1974, pp. 4875-4879.

2. F. J. Adrian, "A Possible Overhauser Mechanism for ^{19}F Nuclear Spin Polarization in the Reaction of Fluorobenzyl Halides with Sodium Naphthalene," Chem. Phys. Lett., Vol. 26, 1 June 1974, pp. 437-439.

3. F. J. Adrian, H. M. Vyas, and J. K. S. Wan, "Magnetic Field and Concentration Dependence of CIDNP in some Quinone Photolyses: Further Evidence for an Overhauser Mechanism," J. Chem. Phys., Vol. 65, 15 August 1976, pp. 1454-1461.

g-TENSOR AND SPIN DOUBLING CONSTANT IN THE $^2\Sigma$ RADICALS CN AND C_2H

The electron magnetic moment tensors of the cyanogen (CN) and ethynyl (C_2H) radicals have been determined by analysis of high-resolution electron spin resonance (ESR) spectra of these radicals in argon (Ar) and krypton (Kr) matrices at 4°K. The results support a predicted relation between the magnetic moment and the magnetic field produced by molecular rotation (spin doubling interaction). The results also resolve a serious discrepancy between the nitrogen hyperfine splittings of the CN radical obtained from its ESR spectrum and from its interstellar microwave emissions.

A number of the radicals studied and characterized by the free radicals research program at APL have recently been detected in interstellar space by radio astronomers at other laboratories. Two especially interesting examples are the CN and C_2H radicals. These species are so reactive that, prior to the interstellar observations (Refs. 1 and 2), the only information about their magnetic fine and hyperfine structure came from ESR studies (at APL) of these radicals trapped in inert gas matrixes at 4°K (Refs. 3 and 4). Our matrix ESR data were useful in establishing the identify of these radicals from their interstellar emissions, which correspond to

transitions from the first excited rotational state to the ground state. However, there also were some apparent severe discrepancies between the results of these highly dissimilar experiments, particularly in regard to a predicted relation between the electron magnetic moments of these radicals and an interaction known as the spin-doubling interaction.

The magnetic moment of an electron in a radical usually differs slightly from the free spin value because perturbation of the orbital motion of the electrons within the molecule by the external magnetic field results in only a small orbital contribution to the net moment. Similarly, the perturbation of the orbital motion of these electrons by molecular rotation creates a magnetic field whose interaction with the electronic magnetic moment is known as the spin-doubling interaction because it splits each rotational line into a doublet. These two effects are related by Larmor's theorem, which states that under certain fairly general conditions the effect of an external magnetic field, H, on a magnetic moment, μ, may be represented by a rotating coordinate system, or, physically, a rotating molecule, at the rotation frequency $\omega = \mu H$. If the electron magnetic moment is written as $\mu = g\beta S$, where S is the electron spin, then this relation is (Ref. 5)

$$\gamma = -2B_o(g_\perp - g_e) , \qquad (1)$$

where γ and B_o are the spin-doubling and rotational constants; $g_\perp$ is the electron g factor in a direction perpendicular to the molecular axis (direction of the rotation axis); and $g_e = 2.00232$ and is the free spin g value.

The electron magnetic moment values obtained from the initial ESR measurements at APL (Refs. 3 and 4) and elsewhere indicated an apparent failure of Eq. 1 for CN and C_2H. A breakdown of Eq. 1 for these molecules was a definite possibility because the approximations in deriving Eq. 1 via the Larmor theorem are most likely to fail in molecules such as CN and C_2H where the center of mass, about which the molecule rotates, is substantially displaced from the nuclei about which the electrons rotate. However, it was recognized that, before any definite conclusions could be reached, it would be necessary to remeasure the g values with very high precision. Also the possibility must be considered that the measured g values are not the isolated radical values, but are changed by interactions between the radical and the host matrix and/or averaging of the isolated radical values over some rotational motion of the radicals in the matrix. These measurements

and their analysis, presented in the remainder of this report, show that Eq. 1 is valid for CN and C_2H. This is fortunate because Eq. 1 is likely to be useful for estimating the spin-doubling constants of other interstellar molecules from terrestial ESR measurements.

In order to maximize measurement accuracy, several improvements were made in the automatic frequency control loop that stabilizes the microwave frequency of the ESR spectrometer. Also, the proton magnetometer, which measures the magnetic field strength, was calibrated using the precisely known g factor of the hydrogen atom in Ar and Kr matrices.

Possible effects of matrix interactions on the g factors were studied by using both Ar and Kr matrices. The CN and C_2H radicals were produced by depositing at 4°K the desired rare gas containing 1% of HCN or C_2H_2, respectively, and photolyzing with vacuum ultraviolet light from an H_2 discharge lamp.

It was found that matrix perturbations did affect the g values of C_2H but not those of CN. The observed differences between the C_2H g values in Ar and Kr, combined with the theory of matrix shifts of g, indicated that the Ar value, $g_\perp = 2.00288$, should be close to but slightly less than the isolated radical value. Use of this value in Eq. 1 gave $\gamma = -48.9$ MHz, in satisfactory agreement with the observed value of -62.3 MHz (Ref. 2). Estimates of the matrix shift of $g_\perp$ for C_2H using the observed difference in $g_\perp$ for the Ar and Kr matrices and the observed matrix shifts of the H atom gave even better agreement: $g_\perp = 2.00309$ and $\gamma = -67.3$ MHz.

The CN case was more complex, even though there were no matrix shifts of g, because the ESR spectrum of this radical in Ar at 4°K was inconsistent with the spectrum of an axially symmetric radical. In this spectrum, shown in Fig. 1, let us momentarily ignore the outer lines of the triplet shown in Fig. 1a, which are due to the nitrogen hyperfine splitting, and concentrate on the expanded trace of the center line shown in Fig. 1b. The line has a complex shape containing two distinct peaks at the outer limits of the line and an interior shoulder, which features are denoted as g_1, g_3, and g_2, respectively. In a polycrystalline matrix the line represents a superposition of spectra for all possible orientations of the radical with respect to the external magnetic field, and the distinct features correspond to those radicals that are so oriented that the magnetic field is parallel to a principal axis of the electron magnetic moment or g factor tensor. Since there are three, rather than two, distinct features, CN in Ar cannot be an axially symmetric system, but has the three distinct g values: $g_1 = 2.00165$, $g_2 = 2.00067$, and $g_3 = 2.00036$.

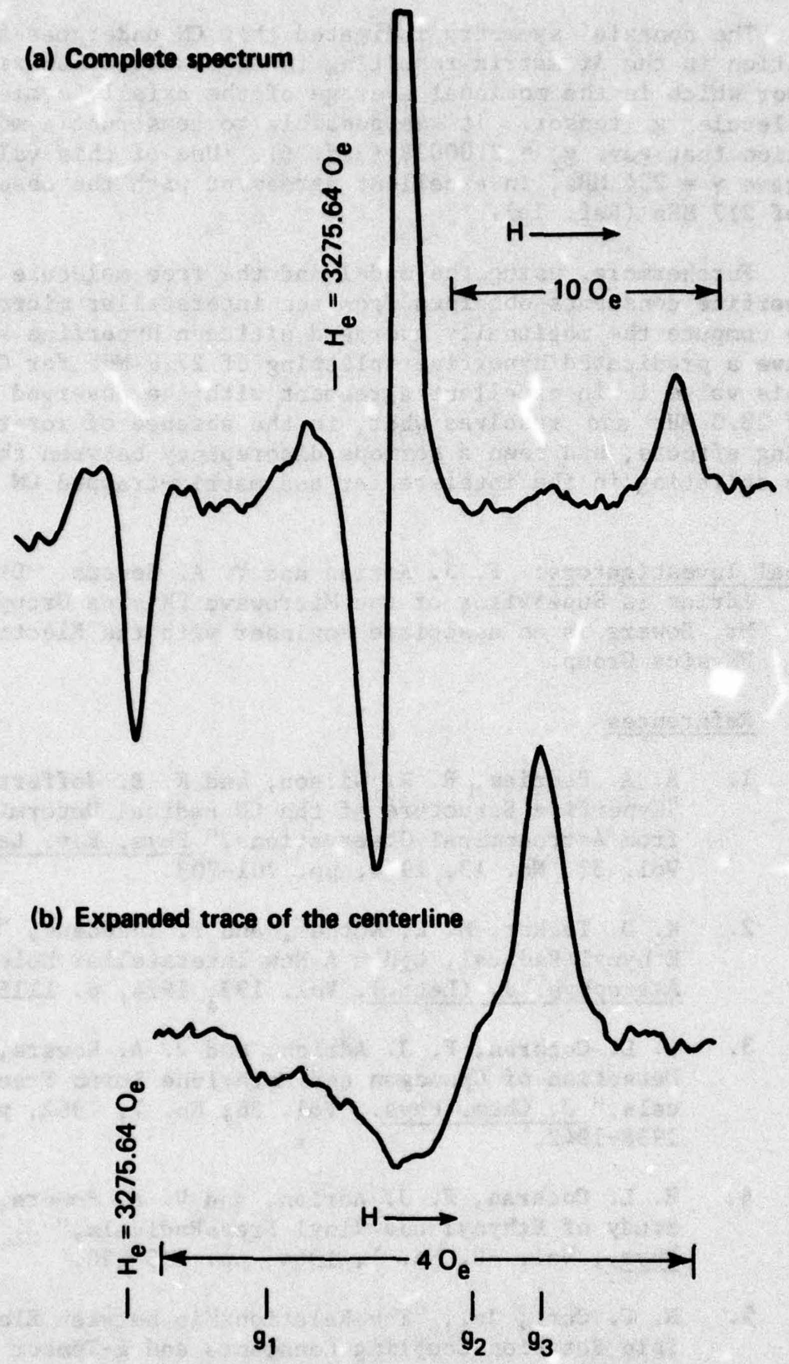

Fig. 1 ESR Spectrum of CN in an Ar Matrix at 4° K. H_e denotes the resonant field of a free electron spin.

The nonaxial symmetry indicated that CN undergoes a complex motion in the Ar matrix resulting in an observed nonaxial g tensor which is the motional average of the axially symmetric free molecule g tensor. It was possible to construct a model of the motion that gave $g_{\perp} = 2.00028$ (Ref. 6). Use of this value in Eq. 1 gave $\gamma = 234$ MHz, in excellent agreement with the observed value of 217 MHz (Ref. 1a).

Furthermore, using the model and the free molecule nitrogen hyperfine constants obtained from the interstellar microwave data to compute the motionally averaged nitrogen hyperfine splitting gave a predicated hyperfine splitting of 27.9 MHz for CN in Ar. This value is in excellent agreement with the observed splitting of 28.0 MHz and resolves what, in the absence of rotational averaging effects, had been a serious discrepancy between the hyperfine splitting in the interstellar and matrix-trapped CN radicals.

Principal Investigators: F. J. Adrian and V. A. Bowers. Dr. Adrian is Supervisor of the Microwave Physics Group. Mr. Bowers is an associate engineer with the Electron Physics Group.

References

1. A. A. Penzias, R. W. Wilson, and K. B. Jefferts, "Hyperfine Structure of the CN Radical Determined from Astronomical Observations," Phys. Rev. Lett., Vol. 32, No. 13, 1974, pp. 701-703.

2. K. D. Tucker, M. L. Kutner, and P. Thaddeus, "The Ethynyl Radical, C_2H — A New Interstellar Molecule," Astrophys. J. (Lett.), Vol. 193, 1974, p. L115.

3. E. L. Cochran, F. J. Adrian, and V. A. Bowers, "ESR Detection of Cyanogen and Methylene Imino Free Radicals," J. Chem. Phys., Vol. 36, No. 7, 1962, pp. 1938-1942.

4. E. L. Cochran, F. J. Adrian, and V. A. Bowers, "ESR Study of Ethynyl and Vinyl Free Radicals," J. Chem. Phys., Vol. 40, No. 1, 1964, pp. 213-220.

5. R. F. Curl, Jr., "The Relationship between Electron Spin Rotation Coupling Constants and g-Tensor Components," Mol. Phys., Vol. 9, 1965, pp. 585-597.

6. F. J. Adrian and V. A. Bowers, "g-Tensor and Spin Doubling Constant in the $^2\Sigma$ Molecules CN and C_2H," Chem. Phys. Lett., Vol. 41, August 1976, pp. 517-520.

ESR IDENTIFICATION OF CHEMICALLY BOUND XENON MONOCHLORIDE

Electron spin resonance spectroscopy has shown that, contrary to theoretical predictions, chemically bound XeCl is formed when Cl_2 is photodissociated in an argon matrix containing 1% of xenon.

Interest in the electronic structure and chemical bonding of the rare gas monohalides, which is generally high because they violate the principle that closed shell atoms do not form compounds, has been further stimulated by the discovery that emission from the excited states of these molecules can yield high-energy ultraviolet laser action. In work done at other laboratories, theory predicts that all these molecules have nonbonding ground states, whereas experiments, most notably electron spin resonance (ESR) studies, have indicated that XeF and KrF have bound ground states. Estimates of the bond length and charge distribution of XeF obtained by comparison of the observed magnetic constants of XeF with those calculated from a semiempirical wave function (details are given in the Atomic Molecular and Electron Physics Group's contribution to this report) are supportive of chemical bonding in this molecule.

It was also suggested by the study that XeCl might be bound, although very weakly. We prepared XeCl by matrix isolation methods and observed by ESR (Ref. 1), in agreement with this hypothesis. The preparation followed the method of Ault and Andrews (Ref. 2) for XeF and KrF (deposition of an $Ar:Xe:Cl_2 = 98:1:1$ sample on a sapphire rod at 4°K and photolyzing with ultraviolet light either during or after deposition). Except for the weak sharp lines around 3274 G that are due to traces of radicals such as ClOO, the resulting ESR spectrum, shown in Fig. 1, is consistent with expectations for the species XeCl. That is, it is typical of a radical with an axially symmetric but highly anisotropic electron magnetic moment randomly oriented in a polycrystalline matrix. The regions denoted as $g_{\parallel}$ and $g_{\perp}$ correspond to radicals oriented parallel and perpendicular to the magnetic field. The g values are $g_{\parallel} = 1.962$ and $g_{\perp} = 2.303$, where $\mu_B \underset{\sim}{g} \cdot \underset{\sim}{S}$ is the electronic magnetic moment tensor. The g shifts, i.e., $\Delta \underset{\sim}{g} = \underset{\sim}{g} - g_e$, where $g_e = 2.0023$ is the free spin g value, are similar to but larger than those of XeF. This is the expected effect of the increased halogen spin-orbit interaction or the decreased chemical bonding on going from XeF to XeCl.

As indicated in Fig. 1a, the parallel region has resolved hyperfine structure (hfs). The four strongest lines, associated with the 53% abundant, $I = 0$, Xe isotopes (^{132}Xe, ^{134}Xe, etc.), are

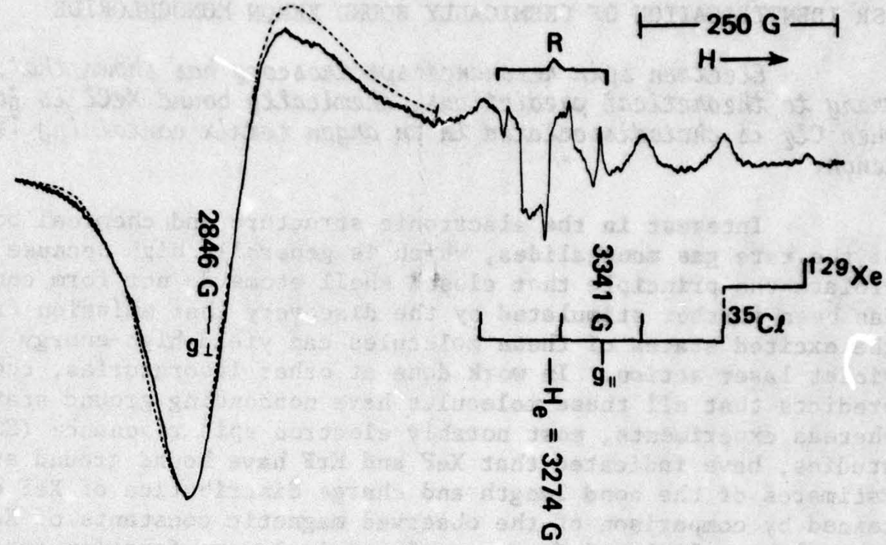

Fig. 1a ESR Spectrum of the Photolysis Products of an AR:Xe:Cl_2 = 98:1:1.Sample at 4.2° K:———. The sharp weak lines in the region denoted by R are traces of radical impurities. H_e denotes the resonant field of a free electron spin. Computer spectrum in the perpendicular region for the parameters given in the text: -------.

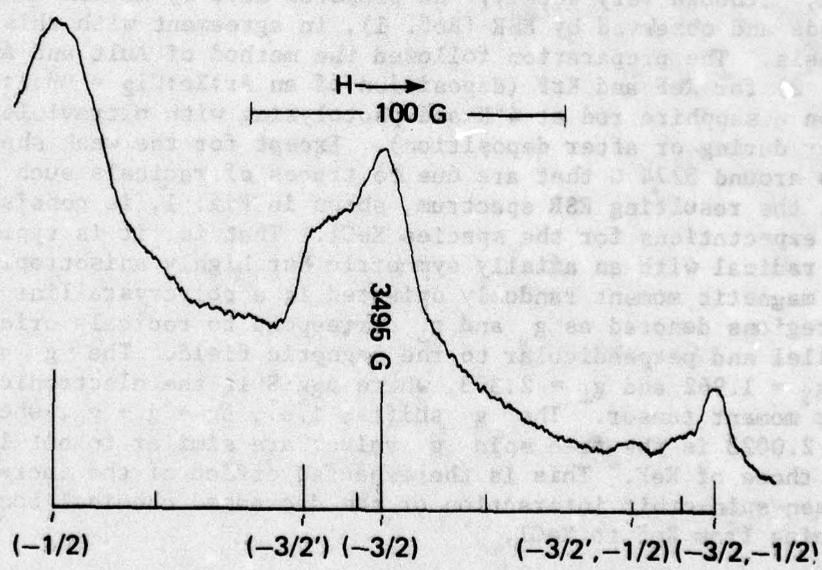

Fig. 1b Expanded Trace of the Three Highest Field Lines of the Complete Spectrum in Fig. 1a. The stick spectrum at the bottom is computed from the ^{35}Cl and ^{129}Xe hfs constants given in the text, where the numbers in parentheses indicate the magnetic quantum numbers of the strong hfs lines. The first number is M_{Cl}, with the ^{37}Cl isotope indicated by a prime, and the second number, if present, is M_{Xe} of ^{129}Xe. The weak lines, not denoted by numbers, are ^{131}Xe hfs lines.

a Cl hfs quartet [$|A_{\parallel}(^{35}Cl)/h|$ = 288 MHz]. The weak highest field line is due to hfs splitting of the high field member of the Cl quartet by the 26% abundant, I = 1/2, ^{129}Xe isotope [$|A_{\parallel}(^{129}Xe)/h|$ = 582 MHz]. This assignment is substantiated by an expanded trace of the three highest field lines, shown in Fig. 1b. The two highest field lines in Fig. 1b have structure caused by hfs splittings from both the 75% abundant ^{35}Cl and 25% abundant ^{37}Cl which proves both these lines are $|M_{Cl}|$ = 3/2 hfs lines, and the relative intensities of these lines are consistent with assignment of the highest field line as part of a ^{129}Xe doublet.

No structure is discernible in the perpendicular region of the spectrum; however, trial and error comparison of observed and computed line shapes in this region have the following estimates of the perpendicular hfs constants: $A_{\perp}(^{35}Cl)/h \simeq 0$; $|A_{\perp}(^{129}Xe/h)| \simeq 280$ MHz; and a Lorentzian intrinsic line shape having a width of 32 G between maximum and minimum slope points. As shown in Fig. 1b, this assignment gave good agreement between the observed and computed lines; nonetheless, these values are very approximate because they are strongly dependent on the intrinsic line shape, which cannot be accurately determined without detailed knowledge of the broadening mechanism.

The Xe hfs splittings are much smaller in XeCl than in XeF (Ref. 1). This is consistent with the expected weaker bonding and a correspondingly smaller transfer of unpaired electron density from the halogen to Xe in XeCl as compared with XeF.

The method of preparation combined with the hfs data proves the observed species is XeCl. The Xe hfs argues strongly for chemical bonding in XeCl, which bonding may be defined roughly as nonzero ε in the XeCl wave function: $\psi_{XeCl} = N[\ 1 = \varepsilon^2 \psi(Xe...Cl) + \varepsilon\psi(Xe^{+}...Cl^{-})]$. For $\varepsilon = 0$, the Xe hfs is due solely to orthogonality-dictated admixture of Xe, 5s, and 5pz orbitals into the Cl 3pz unpaired electron orbital. Calculation shows that even at separation R = 0.32 nm, which is considerably less than R = 0.42 nm estimated from the nearest true van der Waals molecule ArXe, simple orthogonalization cannot account for the observed Xe hfs. A more detailed argument (Ref. 1) shows that the observed perpendicular g shift ($\Delta g_{\perp}$) also requires chemical bonding in XeCl.

Principal Investigators: F. J. Adrian and V. A. Bowers. Dr. Adrian is Supervisor of the Microwave Physics Group. Mr. Bowers is an engineering associate in the Electron Physics Group.

References

1. F. J. Adrian and V. A. Bowers, "ESR Spectrum of XeCl in Argon at 4.2 K," J. Chem. Phys., Vol. 65, No. 10, 15 November 1976, pp. 4316-4318.

2. B. S. Ault and L. Andrews, "Absorption and Emission Spectra of Argon Matrix-Isolated XeF and KrF," J. Chem. Phys., Vol. 64, 1 April 1976, pp. 3075-3076.

SPECTROSCOPIC STUDIES OF ELECTRON DONOR-ACCEPTOR MOLECULES

Electron spin resonance (ESR) of polycrystalline and single crystal samples of triphenylene doped with copper porphin have been obtained. It is shown that the copper porphin molecules occupy substitutional sites in this host. The information should be useful in the interpretation of the polarization characteristics of the optical spectra of this and similar materials.

Extensive studies have been made of highly conjugated organic molecules because of their optical, semiconductive, photoconductive, and photochemical properties. Work at APL has centered around the class of porphyrin molecules. These are good model compounds for studying the relationship between structure and function of such compounds, and are also important components of biological energy conversion and transport systems. Many of the techniques being used to study these molecules are also applicable to other organics such as dye laser molecules and the more recently synthesized TCNQ complexes.

High-resolution sharp-line optical spectra of free base and various metal complexes of porphin, the parent compound of all porphyrins, have been recently obtained at APL (Refs. 1 and 2). The spectra were obtained by incorporating small amounts of the porphin molecules into the organic single crystal host, triphenylene. The use of a periodic lattice greatly reduces inhomogeneous line broadening mechanisms, and working at liquid helium temperature (4.2°K) reduces thermal broadening. The technique not only gives much better resolution, but also allows for obtaining polarized optical spectra. However, proper interpretation of the optical spectra depends on the number of crystallographic sites occupied by the porphin molecules and the orientation of the molecules within these sites. ESR spectroscopy can yield this and other detailed information about the local environment of paramagnetic substituents in crystals. Therefore it was applied to the crystallographic site problem for triphenylene doped with copper porphin, a system that should be representative of the porphin-doped triphenylenes.

The ESR spectra of Cu^{2+} can be characterized by a g-factor or electron magnetic moment and by the magnetic interaction between the electron and the copper nucleus, described by the hyperfine coupling constant A. The result was a splitting of the ESR line into four hyperfine lines. There is also an interaction, A_N, between the electron and the nuclei of the four nearest neighbor nitrogen atoms surrounding the Cu^{2+} ion. Since the magnetic electron is mainly localized on the Cu ion, the interaction is called a superhyperfine (shf) interaction. If all the nitrogens are equivalent, one would expect each of the four Cu hyperfine lines to be split into nine shf components. Triphenylene has four molecules per unit cell, and ESR spectra from CuP in each nonequivalent site will be observed. One sees that, in general, the spectrum will be extremely complex. At the expense of the orientational information, the multiple site problem can be eliminated by crushing single crystals and obtaining a so-called powder ESR spectrum. The principal components of the g, A, and A_N tensors can be determined from one powder spectrum. Once these values are known, the number of porphin sites and the orientation of the molecules in these sites can be determined from the dependence of the single crystal spectra on magnetic field orientation. An ESR powder spectrum obtained at 16.449 GHz is shown in Fig. 1. Three parallel components are resolved with the fourth just masked by the perpendicular spectrum. Each parallel hyperfine line is further split by the shf interaction into lines separated by 14.2 G. In addition, there are lines that are approximately one-half as intense between these shf lines. These are either due to a magnetically inequivalent site or to the resolution of lines from the ^{65}Cu isotope. On the basis of their expected intensity ratio of approximately two to one and the fact that the weaker lines appear half-way between the stronger ones at two different microwave frequencies, these weaker lines are assigned to ^{65}Cu.

The perpendicular portion of the powder spectrum is more complex, caused not only by the shf structure but also by the fact that there is a large anisotropy in the nuclear hyperfine interaction. Although the isotope splittings in the perpendicular region were not observed at room temperature, spectra taken at low temperatures did resolve structure attributed to ^{65}Cu.

Analyses of the data showed the tensors to be axially symmetric. The resulting principal components are

$$g_{\parallel} = 2.190 \qquad A_{\parallel}(Cu) = 196\ G \qquad A_{\parallel}(N) = 19.8\ G$$

$$g_{\perp} = 2.043 \qquad A_{\perp}(Cu) = 33\ G \qquad A_{\perp}(N) = 14.2\ G$$

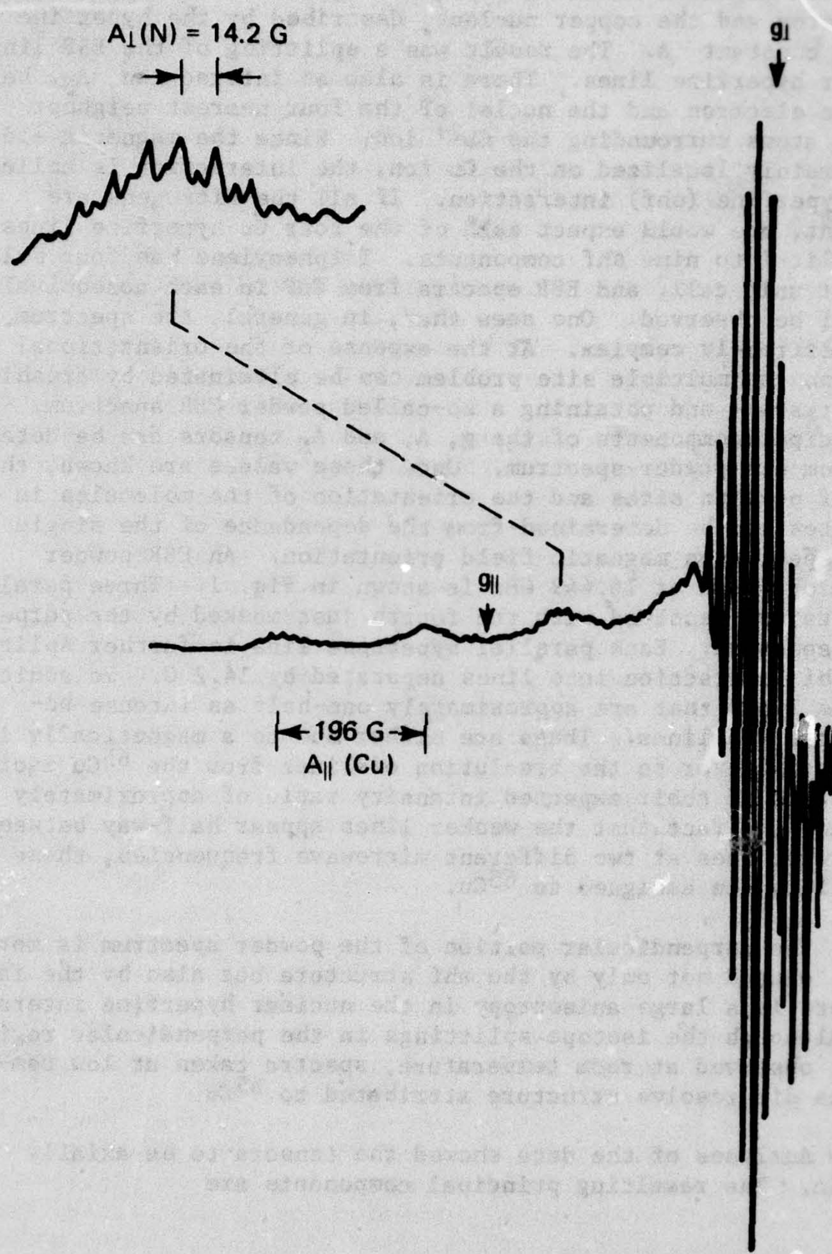

Fig. 1 ESR Powder Spectrum of CuP in Triphenylene at 16.449 GHz. The magnetic field is increasing to the right.

A rotational study of the single crystal samples showed that the normals to the four porphin planes make equal angles of 51° with the c-axis. With the magnetic field along one of these normals, one obtains $g_{\parallel}$, $A_{\parallel}$(Cu), and $A_{\perp}$(N). Weaker lines attributed to ^{65}Cu were also observed in this orientation.

There are several orientations of the crystal for which the magnetic field is perpendicular to at least one of the normals to the porphin planes. It was not possible to isolate completely the perpendicular spectrum of one site from overlapping lines caused by other sites. Further, when $A_{\parallel}(N) \neq A_{\perp}(N)$, there is an orientation dependence of the shf splitting and more than nine lines for each Cu hf line may be observed. These considerations made the analysis of the perpendicular spectrum difficult but the spin-Hamiltonian parameters obtained were in good agreement with the powder data. The single crystal data are consistent with CuP molecules in substitutional triphenylene sites.

Results of this work were reported at a recent American Physical Society meeting (Ref. 3) and submitted for publication. Reports of single site optical spectra of zinc porphin have also been given (Refs. 4 and 5).

<u>Principal Investigators</u>: J. Bohandy and B. F. Kim. Drs. Bohandy and Kim are senior physicists of the Microwave Physics Group of the Research Center.

<u>References</u>

1. B. F. Kim and J. Bohandy, "Low Temperature Optical Spectra of Zn Porphin in Triphenylene," J. Chem. Phys., Vol. 59, 1973, p. 213.

2. J. Bohandy and B. F. Kim, "Optical Spectra of Ni Porphin, Pd Porphin, and Free Base Porphin in Single Crystal Triphenylene," Spectrochimica Acta, Vol. 32A, 1976, p. 1083.

3. J. Bohandy and B. F. Kim, "ESR of Copper Porphin," Bull. Am. Phys. Soc., Vol. 21, 1976, p. 272.

4. B. F. Kim and J. Bohandy, "Site Selective Spectra of Zn Porphin in Triphenylene," Optics News, 1975.

5. B. F. Kim and J. Bohandy, "Single Site Optical Spectra of Zn Porphin in Triphenylene," 31st Symposium on Molecular Structure and Spectroscopy, Ohio State University, June 1976.

PHOTOACOUSTIC SPECTROSCOPY OF LUMINESCENT MATERIALS

Photoacoustic Spectroscopy (PAS) of solids has been used to determine the nonradiative transition rate, net energy loss during excitation, and lifetime of a metastable level in an optically pumped phosphor. PAS is unique in that the measurement does not require the metastable level itself to be radiative. Hence measurements on trap lifetime and energy depth of a trap in many primary photochemical systems, including photosynthetic systems, are possible in principle.

Optical absorption spectroscopy remains an important tool for determining the energy level structure and population dynamics in solids and liquids. This knowledge has provided the basis for many of the recent developments in the science and technology of materials. Recently, PAS has emerged as a new form of optical absorption spectroscopy that offers certain unique advantages over current methods, especially in extending the range of samples that can be studied optically. Using PAS methods, absorption spectra may be obtained from opaque or scattering samples such as metals, polycrystalline aggregates, gels, and biomaterials. This aspect of PAS spectroscopy is unique and stems from the fact that S_{PAS}, the photoacoustic signal, is associated with the heat produced in the sample by the absorbed light, and not the light transmitted through the sample. Hence we have

$$S_{PAS}(\lambda) = I(\lambda)\ A(\lambda)\ H(\lambda) \tag{1}$$

where $I(\lambda)$ is the intensity of the incident light, $A(\lambda)$ is the optical absorbence, and $H(\lambda)$ is the fraction of the absorbed light converted to heat in the sample. The use of Eq. 1 has been justified by detailed consideration of the physical and instrumental aspects of PAS spectroscopy, including the optical and thermal properties of the sample and the properties of the PAS cell (Ref. 1). Using Eq. 1, we see that, if $H(\lambda)$ = constant, $S_{PAS}(\lambda)/I(\lambda)$ = constant × $A(\lambda)$, and the PAS spectrum is equivalent to the optical absorption spectrum.

Most prior applications of PAS spectroscopy have assumed $H(\lambda)$ = constant. Recently (Ref. 2), however, it was pointed out that many solids have metastable excited states that may be populated by light absorbed in specific transitions in the solid. In these cases, absorbed light energy is trapped as electronic energy in excited states of the absorbing solid and may be reemitted as fluorescent or phosphorescent radiation rather than appearing as

photoacoustically detectable heat. For these cases, $H(\lambda) \neq$ constant. The correspondence between the PAS spectrum and the optical absorption spectrum then breaks down and the PAS spectrum depends upon both the optical absorption in the solid and the energy level position, and the radiative and nonradiative lifetimes of the metastable level (Ref. 3).

PAS signal generation in these luminescent materials may be understood by using the energy level diagram, Fig. 1. The diagram is appropriate for the ground and low-lying excited states of many aromatic organic compounds, organic dyes, and rare earth and transition metal phosphors. In Fig. 1, for any pair of levels, i, j, $k_{ij} = \rho_{ij} + \nu_{ij}$ is the total transition rate and is composed of a radiative part ρ_{ij} and a nonradiative part ν_{ij}. Also, f_{ij} are the pumping rates associated with optical absorption. Since S_{PAS} is associated with heating of the sample, large PAS signals are

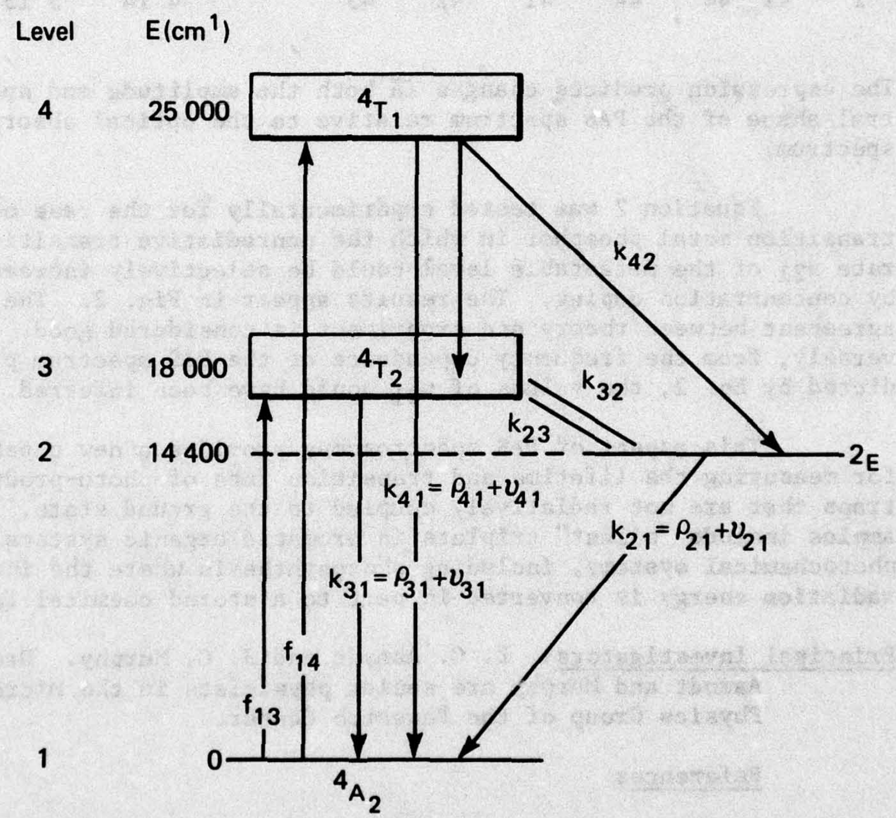

Fig. 1 Simplified Energy Level Diagram of Cr^{3+}. k, ρ, and υ represent the total, radiative, and nonradiative transition rates, respectively. f is the optical pumping rate.

associated with large nonradiative rates ν_{ij}. The expression for S_{PAS} obtained from analysis of this diagram is

$$S_{PAS}(\lambda)/I(\lambda) = H_4 + H_{23} \tag{2}$$

where

$$H_4 = \alpha f_{14}\left[E_4\nu_{41} + (E_4 - E_2)k_{42} + (E_4 - E_3)k_{43}\right]\Big/k_{44}$$

$$H_{23} = \alpha\Big[(E_3 - E_2)(f_{13} + b_2 f_{14}) + (E_2\nu_{21}/k_{21})(f_{13} + [b_2 + b_3]f_{14}) \,/\, (1 - j\omega/k_{21})\Big]$$

and

$$b_i = k_{4i}/k_{44}; \quad k_{44} = k_{41} + k_{42} + k_{43}; \quad \alpha = 1/(E_4 f_{14} + E_3 f_{13}).$$

The expression predicts changes in both the amplitude and spectral shape of the PAS spectrum relative to the optical absorption spectrum.

Equation 2 was tested experimentally for the case of a *transition metal phosphor in which the nonradiative transition* rate ν_{21} of the metastable level could be selectively increased by concentration doping. The results appear in Fig. 2. The agreement between theory and experiment is considered good. Conversely, from the frequency dependence of the PAS spectrum predicted by Eq. 2, the values of ν_{21} could have been inferred.

This aspect of PAS spectroscopy provides a new capability for measuring the lifetime and transition rate of photo-produced traps that are not radiatively coupled to the ground state. Examples include "silent" triplets in aromatic organic systems and photochemical systems, including photosynthesis where the incident radiation energy is converted in part to a stored chemical form.

Principal Investigators: L. C. Aamodt and J. C. Murphy. Drs. Aamodt and Murphy are senior physicists in the Microwave Physics Group of the Research Center.

References

1. L. C. Aamodt, J. C. Murphy, and J. G. Parker, "Size Considerations in the Design of Cells for PAS Spectroscopy" (submitted to the J. of Appl. Phys.).

2. L. C. Aamodt and J. C. Murphy, "Photoacoustic Spectroscopy of Ruby Powders," Bull. Am. Phys. Soc., Vol. 21, 1976, p. 423.

3. J. C. Murphy and L. C. Aamodt, "Photoacoustic Spectroscopy of Luminescent Solids: Ruby" (to be submitted).

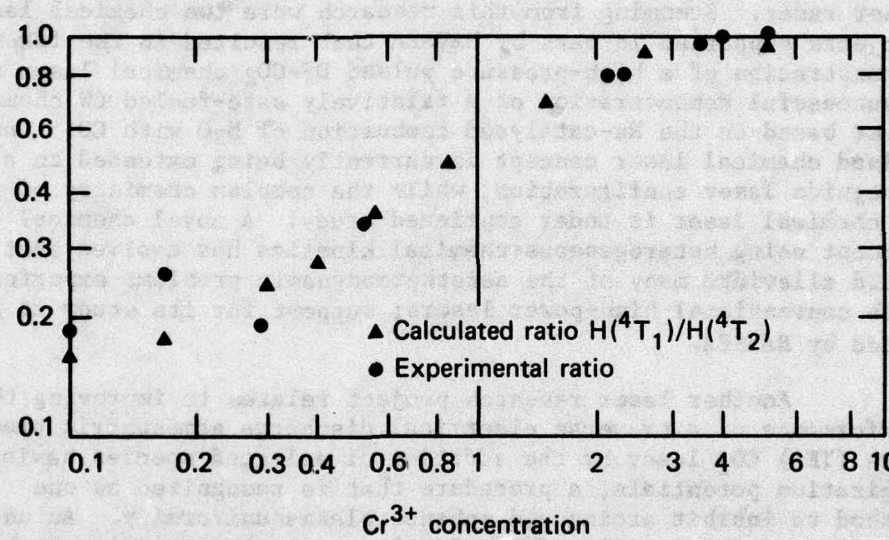

Fig. 2 Ratio of PAS Cr^{3+} Band Intensities in Ruby versus Ion Concentration

QUANTUM ELECTRONICS AND EXCITATION MECHANISMS

Few scientific discoveries have excited the scientific community and opened new vistas for research and development as has the laser. Laser, electro-optics, and quantum electronics in general, comprise an expanding technology demanding an alert awareness to assess its impact fully. The APL Research Center is quite active in this field with interests spanning from basic research to military and civilian applications.

Immediately following the discovery of the laser, the Research Center at APL became active in laser physics research and in exploring potential laser applications in the military and medical fields. A representative example was the development of one of the first argon laser retinal photocoagulators for clinical use at the Johns Hopkins Medical Institutes. In recent years an active interest has developed in infrared lasers because of their unique applications in plasma physics, communications, and high-resolution laser radar. Stemming from this research were two chemical laser projects supported in part by NAVSEA that resulted in the first demonstration of a high-pressure pulsed DF-CO_2 chemical laser and a successful demonstration of a relatively safe-fueled CW chemical laser based on the Na-catalyzed combustion of N_2O with CO. The pulsed chemical laser concept is currently being extended to a waveguide laser configuration, while the complex chemistry of the CW chemical laser is under continued study. A novel chemical laser concept using heterogeneous chemical kinetics has evolved that could alleviate many of the aerothermodynamic problems experienced with conventional high-power lasers; support for its study is provided by NAVSEA.

Another laser research project relates to improving the performance of a traverse electrical discharge atmospheric pressure (TEA) CO_2 laser by the addition of selected species having low ionization potentials, a procedure that is recognized as one method to inhibit arcing and enhance plasma uniformity. An understanding of the details of the CO_2 laser plasma chemistry both with and without such additives becomes important in this problem, and several diagnostic approaches are being used in its resolution. This research is also supported in part by NAVSEA.

In addition to the laser studies, research in organic conductors and photo-assisted electrolysis is in progress. The organic conductor research is a continuing effort in conjunction with The Johns Hopkins University. It has concentrated on the synthesis of new organic compounds, measurements of their physics properties, and interpretation of the measurements with the ultimate goal of yielding an understanding of these unique materials.

Research on photo-assisted electrolysis is a new endeavor. It is an alternate approach to solar cells as a means of utilizing solar energy and is based on photo-effects at a semiconductor/electrolyte interface. Experiments have been completed with a pair of TiO_2-Pt electrodes immersed in various electrolytes to determine the effects of illumination on current-voltage characteristics and gas evolution. A program has been initiated to prepare and evaluate other semiconductor materials.

Each of these projects is reported briefly herein. Greater detail appears in five publications that appeared this year and two additional reports that have been submitted for publication. The research is being conducted by the Quantum Electronics and Excitation Mechanisms Groups with a staff of six senior scientists, one associate scientist, and two technicians.

CHEMICAL LASERS: HIGH-PRESSURE PULSED DF AND DF-CO_2 CHEMICAL LASERS

The exothermic chain reactions between deuterium and fluorine have been used to generate laser emission in DF and DF-CO_2 chemical waveguide lasers. Lasing occurs at 10 μm in stable D_2-F_2-CO_2-He mixtures at pressures as high as 1 atm with peak power of 5 kW for pulses with a duration of 20 μs. Spectral studies show CO_2 emission from both R-branch lines near 10.2 μm and P-branch lines centered at 10.6 μm, in contrast to the commonly observed 10.6 μm emission from most pulsed and CW CO_2 lasers. However, the general features observed from spectral studies of both DF and DF-CO_2 systems indicate that the pumping of the laser transitions by excited DF is identical to that previously observed in chemical lasers of large volume.*

Chemical lasers are particularly attractive candidates for high-powered laser systems since the principal energy source is a chemical reaction. The DF-CO_2 and DF chemical lasers are attractive for military applications because the laser outputs correspond to atmospheric windows. Supported in part by NAVSEA, the Research Center has conducted a continuing experimental study in high-pressure pulsed DF and DF-CO_2 chemical lasers. The initial study of a flash-photolysis-initiated DF-CO_2 chemical-transfer laser operated at pressures to 1 atm has led to subsequent studies directed toward the more efficient initiation and utilization of the pump reaction. Electrical initiation of the $D_2 + F_2$ reaction was found to require less input energy for initiation than flashlamp initiated systems, but laser output energy is also diminished (Ref. 1). During the past year, our spectral studies have identified some of DF vibrationally-excited states from which

energy is transferred to CO_2, supporting the theory that the high rate of transfer of energy to CO_2 involves $\Delta J \geqq 2$ in DF (Ref. 2).

In all preceding work, only a fraction of chemical energy available in the reaction is used since the active laser volume established by the optical resonator is substantially less than the reactor volume. A possible technique to circumvent the problem is by using a hollow dielectric waveguide resonator to confine the reacting mixture. In our previous work, a 3-mm-dia quartz laser tube with a volume of 4 cm^3 was used with the chemical reactions initiated by an external flashtube. It yielded laser output power of 2.5 kW at 10 μm pulses of 20 μs duration from stable D_2-F_2-CO-He mixtures (Ref. 3). Our more recent studies with a coaxial flashtube-lasertube system have yielded a power output more than double any previously observed. This represents a laser energy density of more than 25 J/liter atm; by comparison, the larger chemical laser generated 19 J/liter atm based on total gas volume and 50 J/liter atm based on the stable-resonator laser mode volume.

Spectral studies show that lasing from CO_2 begins with emission on the P(18), P(20), and P(22) lines at about equal intensity. We have now shown that, within a few microseconds, lasing on the P(18) and P(22) lines sharply diminishes and the P(20) at 10.59 μm becomes dominant (Ref. 4). The concentration in one line is presumably indicative of rotational equilibrium being attained with a maximum population in the J = 19 rotational state corresponding to a rotational temperature of 400°K. Additional strong lines at 10.247, 10.2335, and 10.26 μm are observed with 10.26 being the strongest. These are apparently the R(20), R(22), and R(18) lines of the 00°1 to 10°0 vibrational-rotational transition. These lines are associated with the same energy levels as the P branch lines observed, but with $\Delta J \geqq -1$ in emission. Observation of the R-branch lines in a laser that does not contain a wavelength selective element (such as a diffraction grating) as part of the resonator has not previously been reported since the gain for the R branch is usually less than that for the P branch for most values of the population ratio of the upper and lower states. However, as this ratio increases, the gains for the two branches are almost equalized. It is possible that an abnormal rotational population distribution of the 100-vibrational state is responsible for the unusually high relative gain of the R-branch lines, or the cause may be selective refraction or absorption effects in the reactor tube.

In spectral studies of lasing from DF with its large rotational constant, rotational equilibrium is not obtained, and a large number of vibrational-rotational transitions are observed. Strong lines observed in the DF chemical waveguide laser are

listed in Table 1. These spectral lines closely correspond to those observed in large-volume DF systems, as contrasted to the atypical observations in the DF-CO_2 spectra. Time resolved spectra show steady J shifting to higher P values as the laser emission progresses corresponding to an increase in rotational temperature from 300°K (P(4)) to 400°K (P(9)) and finally to 600°K (P(11)).

Table 1

DF CHEMICAL WAVEGUIDE LASER TRANSITIONS (μm)

v	1-0	2-1	3-2	4-3
P(4)		3.6665	3.7878	3.913
P(5)		3.6983	3.8206	3.9487
P(6)	3.6128	3.7310	3.8547	
P(7)	3.6456	3.7651	3.8903	
P(8)	3.680	3.8007	3.9272	
P(9)	3.716	3.8375		
P(10)	3.752	3.8757		
P(11)		3.9155		

Principal Investigators: T. O. Poehler and R. Turner. Dr. Poehler is Group Supervisor and Mr. Turner is a senior physicist of the Quantum Mechanics Group of the Research Center.

References

1. T. O. Poehler and R. E. Walker, "Transverse Discharge Pulsed CO_2 Chemical Transfer Laser," Appl. Phys. Lett., Vol. 22, March 1973.

2. R. Turner and T. O. Poehler, "Electrically Initiated Pulsed Chemical DF-CO_2 and DF Lasers," J. Appl. Phys., Vol. 47, July 1976, p. 3038.

3. T. O. Poehler, R. E. Walker, and J. W. Leight, "High Pressure Chemical Waveguide Laser," Appl. Phys. Lett., Vol. 26, May 1975, p. 560.

4. T. O. Poehler and J. W. Leight, "DF-CO_2 and DF Chemical Waveguide Laser" (to be published).

CHEMICAL LASERS: CHEMILUMINESCENCE IN THE NA + N_2O AND NA-CATALYZED N_2O + CO REACTIONS

Chemiluminescence measurements of chemical reactions provide information on energy deposition into excited states of atoms and molecules. The sodium chemiluminescence has been studied in low-pressure diffusion flames involving Na-N_2O and Na-N_2O + CO in a helium diluent in order to assess the role of electronically excited sodium in the pumping mechanism of the N_2O-CO chemical laser. The results indicate that the direct production of excited sodium followed by quenching is not sufficient to provide the observed vibrational inversion in the chemical laser.

The Na-catalyzed N_2O + CO chemical laser developed at APL (Refs. 1 and 2) uses the principal reactions:

$$Na + N_2O \rightarrow NaO + N_2 + 21.0 \text{ kcal/mole} \quad (1)$$

$$NaO + CO \rightarrow CO_2 + Na + 66.2 \text{ kcal/mole} \quad (2)$$

Lasing occurs at 10.8 μm with N_2O as the optically active species. The laser pumping mechanism is believed to involve reaction 2, by forming either vibrationally excited CO_2 directly or electronically excited Na(Na^*). Since the vibration-to-vibration and vibration-to-electronic energy transfer rates are rapid between the various species, any species that is formed in an excited state will rapidly transfer energy and equilibrate with the others. The photon yield from Na^* was measured in reactions 1 and 2 in order to assess the role of Na^* in the pumping mechanism of the chemical laser.

Chemiluminescence measurements were made with a conventional low-pressure diffusion flame. The reaction of N_2O with Na produced a well-defined, spherically symmetric diffusion flame. The emission spectrum was scanned from 400 to 900 nm, but for the relatively low reactant concentrations used in this work, only the Na(3p → 3s) emission at 589 nm was observed. (In previous measurements at higher reactant concentrations in a fast-flow chemical laser reactor, a broad emission was detected at 600 to 680 nm from excited Na_2 in addition to the strong Na(3p → 3s) emission, but no other Na transitions were observed.) The Na(3p → 3s) emission was measured at conditions where quenching of Na^* by N_2O and self-absorption of the emission was negligible compared to the spontaneous emission rate. The photon yield of the Na-N_2O system was found to be $\sim 3 \times 10^{-4}$.

Although this yield is rather low, it is surprising that any emission was observed since reaction 1 is not sufficiently exothermic to provide the excitation to the 3p level of Na (48 kcal/mole). Thus, additional reactions are definitely occurring and two excitation mechanisms were previously proposed to explain the production of Na* (Refs. 3 and 4).

When CO was added to the N_2O-Na system, the chemiluminescence increased a hundred-fold. The emission was measured as a function of the sodium concentration and the CO/N_2O ratio. Taking into account the combustion efficiency and the chain-length, the photon yield was determined at conditions where self-absorption was minimal and the rate of emission was faster than the rate of quenching. The photon yield was found to be $\sim$0.02 without a strong dependence on either the sodium concentration or the CO/N_2O ratio.

The Na* photon yield required for Na* production followed by quenching to be the dominant laser pumping mechanism can be estimated from the known energy deposition into the N_2O upper laser level (Ref. 2). If one assumes that all of the energy in Na* is transferred to the upper laser level of N_2O (most favorable case), the minimum photon yield necessary to account for laser pumping is 0.25 ± 0.04. Since the measured photon yield is only 0.02, the proposed pumping mechanism involving Na* cannot solely be responsible for the vibrational inversion in the chemical laser. This implies that either direct production of vibrationally excited CO_2 is favored, which then produces excited N_2O via rapid vibration-to-vibration energy transfer, or that another (unknown) reaction is involved in the pumping mechanism. Definitive experiments on the chemical kinetics are necessary to determine the processes that are occurring in this chemical laser.

Details on the chemiluminescence measurements have been documented and submitted for publication (Ref. 5).

Principal Investigators: R. C. Benson. Dr. Benson is a Senior Chemist in the Excitation Mechanisms Group.

References

1. D. J. Benard, R. C. Benson, and R. E. Walker, "N_2O Pure Chemical CW Flame Laser," Appl. Phys. Lett., Vol. 23, No. 2, 15 July 1973, pp. 82-84.

2. R. C. Benson, C. B. Bargeron, and R. E. Walker, "Gain Measurements in a Transverse-Flowing Na-N_2O + CO Chemical Laser," Chem. Phys. Lett., Vol. 35, No. 2, 1 September 1975, pp. 161-166.

3. R. E. Walker and J. E. Creeden, "The Reaction Between Na Vapor and N_2O at Room Temperature," Combust. Flame, Vol. 21, 1973, pp. 39-43.

4. R. C. Benson, C. B. Bargeron, and R. E. Walker, "Parametric Investigation of the Na-N_2O + CO Chemical Laser," APL/JHU TG 1266, October 1974.

5. R. C. Benson, "Sodium Chemiluminescence in the Na-N_2O and Na-Catalyzed N_2O + CO Reactions," submitted to J. Chem. Phys.

INFRARED LASERS: ADDITIVES TO IMPROVE CO_2 LASER EFFICIENCY

The addition of low ionization-potential gases to carbon dioxide lasers provides a means of increasing the electron density and hopefully the efficiency of the laser. Xenon, which has an ionization potential (12.17 eV) lower than the dissociation potential of CO_2 (13 eV), and has a metastable state at 8.6 eV, is being studied as an additive in a small high-pressure CO_2 laser. Xenon has the advantage over the more commonly used additives, such as tripdopylamine, that it does not contaminate the discharge. There are two feasible mechanisms by which xenon can be used to increase the electron density: one, photoionization by visible light of metastable atoms that are produced in an electrical discharge; and second, ionization of xenon by the collision of two metastable atoms.

An important requirement in high-flow transverse electrical discharge atmospheric pressure (TEA) CO_2 lasers is the production of a high electron-ion pair density by methods that do not disturb the optical quality of the laser medium. Creation of a plasma of proper electron density allows electron heating by the main discharge at an energy level where an efficient transfer of electron energy to the appropriate excited molecular states can occur. Prior work has been reported on the enhancement of TEA laser plasma density by the use of low-ionization-threshold organic impurities ionized generally by spark discharge radiation. Problems have been found with the limited photon mean free paths in the laser medium, as well as acoustic disturbances in the laser cavity. A program has recently been initiated, with partial support by NAVSEA, to study alternative low-ionization species that can be ionized by more conventional means to improve plasma properties of the laser.

The experiment is performed in a transverse discharge between Rogovsky shaped electrodes (2.2-cm wide, 43-cm long, with a

1.3-cm gap) excited by a preionization discharge preceding the main discharge, an arrangement that permits a variety of excitation conditions. The discharge tube is located within an optical cavity so that laser emission may be studied as a function of additive and excitation conditions. The experiment is also instrumented to permit the measurement of: (a) xenon metastable density using resonant optical absorption along the discharge axis at 823.1 nm; (b) electron density, n_e, and electron collision frequency, ν_{ea}, using two frequency microwave probes at typically 29 and 39 GHz; and (c) preionization and excitation currents. The discharge is nominally operated with helium at 300 Torr to which 2% xenon is added either separately or in conjunction with 10% CO_2. Two different excitation currents have been used, a (slow) 180 ns wide pulse (FWHA) and a (fast) 50 ns wide pulse.

With slow excitation, the maximum xenon metastable population is 4×10^{12} cm^{-3} and occurs 4.5 μs after the excitation current. This is later than the time at which the CO_2 10.6 μm emission normally occurs and so would require special handling or excitation of the xenon to be useful. However, a more serious problem is the effect of CO_2 and N_2 on the quenching of the xenon metastable population. If quenching rates are too large, the xenon metastable population will be destroyed before it can make a significant contribution to the electron density. Preliminary results indicate that the quenching cross section is 20×10^{-16} cm^2 for CO_2 and much less for N_2. The CO_2 quenching cross section is large enough to prevent the metastable reaction from providing a significant number of electrons at the CO_2 pressures normally associated with laser operation. The effect of fast excitation on the xenon metastable population has not been measured.

Because of the high electron-to-neutral collision frequency, ν_{ea}, typical of high-pressure discharges, microwave transmission and interferometer measurements must be interpreted using a more exact model than is the case when the collision frequency can be neglected. In the present experiment, the signal transmitted through the plasma and the interferometer output have been derived from an exact calculation of the propagation constant as a function of collision frequency, assuming that refractive and internal reflection effects are negligible. The experimental results, at 29 and 39 GHz, have been fitted to the calculated values to obtain a single value of collision frequency from which the electron density can be derived from both transmission and interferometer measurements. These agree well in most cases. The collision frequency can also be derived from simultaneous transmission measurements at two microwave frequencies.

The microwave data are best fitted with a collision frequency of 1.2 to 1.5×10^{11} s^{-1}. The electron density profiles as

AD-A048 852 JOHNS HOPKINS UNIV LAUREL MD APPLIED PHYSICS LAB F/G 20/12
INDIRECTLY FUNDED RESEARCH AND EXPLORATORY DEVELOPMENT AT THE A--ETC(U)
JUL 77 R W HART N00017-72-C-4401
UNCLASSIFIED APL/JHU/SR-77-2 NL

2 OF 3
AD
A048852

a function of time for fast and slow excitation with 30 Torr of CO_2 and 300 Torr of helium, alone, and with 6 Torr of xenon added are shown on Fig. 1. In the case of the slow discharge, the addition of xenon increases the electron density 3 to 4 times by collisions between metastable Xe^* ions as in

$$Xe^* + Xe^* \rightarrow Xe^+ + Xe + e.$$

The fast discharge results in a tenfold increase in maximum density over that obtained with the slow discharge. In this case the addition of xenon results in a reduction in electron density at the time of laser emission. The decay of electron density in all cases is exponential, indicating that an electron attachment process is involved. The rate constants for the slow discharge are: $K(CO_2) = 3.7 \times 10^6\ s^{-1}$ and $K(CO_2)\text{-}Xe) = 1.4 \times 10^6\ s^{-1}$; for the fast discharge they are: $K(CO_2) = 2.9 \times 10^6\ s^{-1}$ and $K(CO_2\text{-}Xe) = 5.6 \times 10^6\ s^{-1}$. Measurements of these and other rate constants for deexcitation of Xe^* by important laser gases such as N_2 and CO_2 are the first measurements of some of these parameters under laser discharge conditions.

In all cases, the addition of xenon decreases the electrical energy that can be deposited in the gas because of the formation of arcs, with the result that the output power at 10.6 μm is reduced below that obtainable without xenon. Increasing the speed of the current excitation pulse results in a much more significant increase in electron density. However, the electron loss rate is also greater so that at the time of laser emission (≈ 1.5 μs after the start of the excitation current) the electron densities are comparable. This agrees with the fact that the CO_2 laser outputs are comparable for the two excitation currents.

Complementary to the xenon additive investigations is a basic study of infrared emission and lasing action in pure helium. This is a continuing research project with earlier studies concentrating on low-pressure linear discharges in helium that generate lasing action at 95 and 216 μm; the results from that research have recently been published (Ref. 1). The experiments have now been extended to high-pressure (300 Torr) transverse discharges where lasing action has been observed at 1.435, 1.369, and 1.865 μm. Only the 1.865 μm emission had been observed previously in a low-pressure discharge. The energy levels responsible for this laser emission have not yet been identified.

1.3-cm gap) excited by a preionization discharge preceding the main discharge, an arrangement that permits a variety of excitation conditions. The discharge tube is located within an optical cavity so that laser emission may be studied as a function of additive and excitation conditions. The experiment is also instrumented to permit the measurement of: (a) xenon metastable density using resonant optical absorption along the discharge axis at 823.1 nm; (b) electron density, n_e, and electron collision frequency, ν_{ea}, using two frequency microwave probes at typically 29 and 39 GHz; and (c) preionization and excitation currents. The discharge is nominally operated with helium at 300 Torr to which 2% xenon is added either separately or in conjunction with 10% CO_2. Two different excitation currents have been used, a (slow) 180 ns wide pulse (FWHA) and a (fast) 50 ns wide pulse.

With slow excitation, the maximum xenon metastable population is 4×10^{12} cm^{-3} and occurs 4.5 μs after the excitation current. This is later than the time at which the CO_2 10.6 μm emission normally occurs and so would require special handling or excitation of the xenon to be useful. However, a more serious problem is the effect of CO_2 and N_2 on the quenching of the xenon metastable population. If quenching rates are too large, the xenon metastable population will be destroyed before it can make a significant contribution to the electron density. Preliminary results indicate that the quenching cross section is 20×10^{-16} cm^2 for CO_2 and much less for N_2. The CO_2 quenching cross section is large enough to prevent the metastable reaction from providing a significant number of electrons at the CO_2 pressures normally associated with laser operation. The effect of fast excitation on the xenon metastable population has not been measured.

Because of the high electron-to-neutral collision frequency, ν_{ea}, typical of high-pressure discharges, microwave transmission and interferometer measurements must be interpreted using a more exact model than is the case when the collision frequency can be neglected. In the present experiment, the signal transmitted through the plasma and the interferometer output have been derived from an exact calculation of the propagation constant as a function of collision frequency, assuming that refractive and internal reflection effects are negligible. The experimental results, at 29 and 39 GHz, have been fitted to the calculated values to obtain a single value of collision frequency from which the electron density can be derived from both transmission and interferometer measurements. These agree well in most cases. The collision frequency can also be derived from simultaneous transmission measurements at two microwave frequencies.

The microwave data are best fitted with a collision frequency of 1.2 to 1.5×10^{11} s^{-1}. The electron density profiles as

a function of time for fast and slow excitation with 30 Torr of CO_2 and 300 Torr of helium, alone, and with 6 Torr of xenon added are shown on Fig. 1. In the case of the slow discharge, the addition of xenon increases the electron density 3 to 4 times by collisions between metastable Xe^* ions as in

$$Xe^* + Xe^* \rightarrow Xe^+ + Xe + e.$$

The fast discharge results in a tenfold increase in maximum density over that obtained with the slow discharge. In this case the addition of xenon results in a reduction in electron density at the time of laser emission. The decay of electron density in all cases is exponential, indicating that an electron attachment process is involved. The rate constants for the slow discharge are: $K(CO_2) - 3.7 \times 10^6\ s^{-1}$ and $K(CO_2)-Xe) - 1.4 \times 10^6\ s^{-1}$; for the fast discharge they are: $K(CO_2) - 2.9 \times 10^6\ s^{-1}$ and $K(CO_2-Xe) - 5.6 \times 10^6\ s^{-1}$. Measurements of these and other rate constants for deexcitation of Xe^* by important laser gases such as N_2 and CO_2 are the first measurements of some of these parameters under laser discharge conditions.

In all cases, the addition of xenon decreases the electrical energy that can be deposited in the gas because of the formation of arcs, with the result that the output power at 10.6 μm is reduced below that obtainable without xenon. Increasing the speed of the current excitation pulse results in a much more significant increase in electron density. However, the electron loss rate is also greater so that at the time of laser emission (≈ 1.5 μs after the start of the excitation current) the electron densities are comparable. This agrees with the fact that the CO_2 laser outputs are comparable for the two excitation currents.

Complementary to the xenon additive investigations is a basic study of infrared emission and lasing action in pure helium. This is a continuing research project with earlier studies concentrating on low-pressure linear discharges in helium that generate lasing action at 95 and 216 μm; the results from that research have recently been published (Ref. 1). The experiments have now been extended to high-pressure (300 Torr) transverse discharges where lasing action has been observed at 1.435, 1.369, and 1.865 μm. Only the 1.865 μm emission had been observed previously in a low-pressure discharge. The energy levels responsible for this laser emission have not yet been identified.

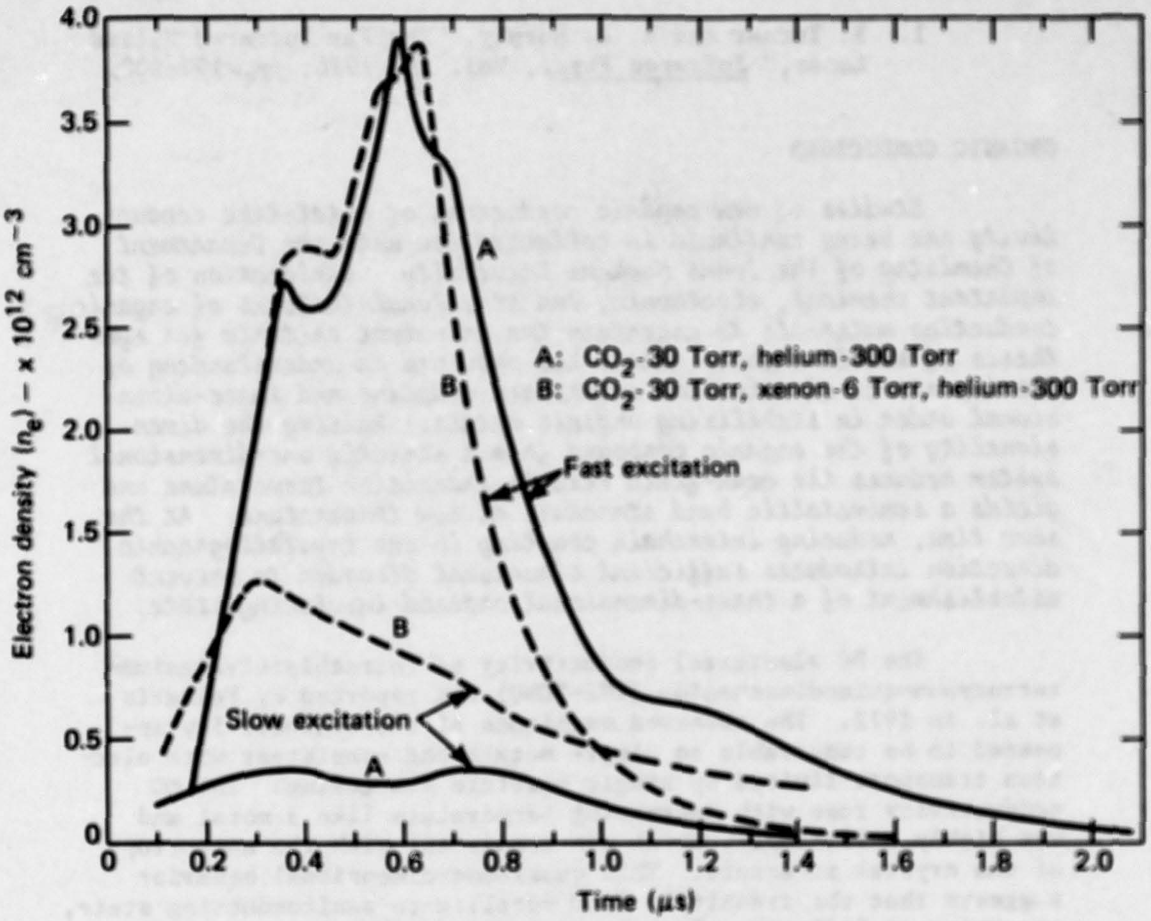

Fig. 1 Electron Density versus Time for Two Excitation Currents. Slow excitation-180ns (FWHA); fast excitation-50ns (FWHA)

Principal Investigator: R. Turner. Mr. Turner is a senior physicist with the Quantum Electronics Group of the Research Center.

Reference

1. R. Turner and R. A. Murphy, "The Far Infrared Helium Laser," Infrared Phys., Vol. 16, 1976, pp. 197-200.

ORGANIC CONDUCTORS

Studies of new organic conductors of metal-like conductivity are being continued in collaboration with the Department of Chemistry of The Johns Hopkins University. Exploration of the important chemical, electronic, and structural features of organic conducting materials to ascertain the principal criteria for synthesis of stable organic metals has provided an understanding of the importance of molecular interchain coupling and three-dimensional order in stabilizing organic metals. Raising the dimensionality of the organic compound from a strictly one-dimensional system reduces the mean-field Peierls transition temperature and yields a semimetallic band structure at low temperature. At the same time, reducing interchain coupling in one crystallographic direction introduces sufficient structural disorder to prevent establishment of a three-dimensional ordered insulating state.

The DC electrical conductivity of tetrathiafulvalenium-tetracyano-quinodimethanide (TTF-TCNQ) was reported by Ferraris et al. in 1972. The observed magnitude of the conductivity appeared to be comparable to simple metals and consistent with electron transport limited by single particle scattering. The DC conductivity rose with decreasing temperature like a metal and was highly anisotropic, which was consistent with the anisotropy of the crystal structure. This quasi-one-dimensional behavior suggests that the transition from metallic-to-semiconducting state, occurring at 54°K, is a Peierls distortion, that is, a periodic distortion of the lattice driven by the conduction electrons. Subsequently, a report was made by other investigators of extraordinary DC conductivities said to be indicative of the onset of a superconducting state at 60°K in TTF-TCNQ crystals of exceptional purity and crystalline perfection. At APL, an extensive study of the importance of chemical purity and crystal perfection was performed using very rigorous sample preparation and purification procedures (Ref. 1). Only extremely dirty samples were found to have any significant change in electrical conductivity.

In a recent survey of electrical conductivity in 600 TTF-TCNQ specimens studied at 18 laboratories using either four-probe DC measurements, microwave cavity perturbation techniques (Ref. 2), or coaxial resonance, we show that the conductivities of none of the specimens exceeds the limits of single particle scattering (Ref. 3). While the work does not rule out collective effects, the conductivity is never high enough to require a collective electron (superconducting) state as an explanation. The report of paraconductivity is now believed to have arisen from experimental artifacts associated with inhomogeneous current distributions in the DC specimens and misinterpretation of the microwave perturbation measurements, as discussed in a paper that we have submitted for publication (Ref. 4).

As we showed earlier (Ref. 5) and have now confirmed (Ref. 6), the compound HMTSF-TCNQ represents a qualitative departure from previous organic conductors in that the metallic state is stable. We have also found that, while the donor molecule is electronically similar to the tetramethyl analogs TMTTF (Ref. 7) and TMTSF, the larger size of the molecule causes the lattice to be of higher dimensionality than any other organic conductor in this family. This is evident from our recent crystallographic and magnetic studies of these compounds (Ref. 8). In this work, it has been demonstrated that, since the usual Elliott-Overhauser mechanism for spin-lattice relaxation in metals via the spin orbit coupling is ineffective in one dimension, the ESR linewidth is an effective index of the dimensionality of the system.

<u>Principal Investigators</u>: T. O. Poehler, D. O. Cowan, and A. N. Bloch. Dr. Poehler is Supervisor of the Quantum Electronics Group of the Research Center. Dr. Cowan is Professor of Chemistry and Dr. Bloch is Associate Professor of Chemistry at The Johns Hopkins University. Their work is not supported by the IR&D Program.

<u>References</u>

1. R. Gemmer et al., "Chemical Purity and the Electrical Conductivity of Tetrathiafulvalenium Tetracyanoquinodimethanide," <u>J. Org. Chem</u>., Vol. 40, November 1975, p. 3544.

2. A. N. Bloch, J. P. Ferraris, D. O. Cowan, and T. O. Poehler, "Microwave Conductivities of the Organic Conductors TTF-TCNQ and ATTF-TCNQ," <u>Solid State Comm</u>., Vol. 13, 1973, p. 753.

3. G. A. Thomas et al., "Electrical Conductivity of Tetrathiafulvalenium Tetracyanoquinodimethanide (TTF-TCNQ)," Phys. Rev. B, Vol. 13, June 1976, p. 5105.

4. T. O. Poehler et al., "Microwave Response of Quasi-One-Dimensional Conductors," Bull. Am. Phys. Soc., Vol. 20, 1975, p. 440.

5. A. N. Bloch et al., "Low Temperature Metallic Behavior and Resistance Minimum in a New Quasi-One-Dimensional Organic Conductor," Phys. Rev. Lett., Vol. 34, June 1974, p. 1561.

6. D. O. Cowan et al., "The Organic Metallic State," Mol. Cryst. Liq. Cryst., Vol. 32, February 1976, p. 223.

7. T. J. Kistenmacher, T. E. Phillips, D. O. Cowan, A. N. Bloch, and T. O. Poehler, "Crystal Structure and Diffuse X-Ray Scattering in the 1.3:2 Salt of 4,4',5,5'-Tetramethyl-$\Delta^{2.2'}$-bis-1,3-Dithiole (TMTTF) and 7,7,8,-Tetracyano-p-quinodimethane (TCNQ), a Non-Stoichiometric Quasi-One-Dimensional Organic Conductor," Acta Crystallog., Vol. B32, 1976, p. 539.

8. T. O. Poehler, J. Bohandy, A. N. Bloch, and D. O. Cowan, "ESR Studies of TCNQ and TNAP Salts," Bull. Am. Phys. Soc., Vol. 21, March 1976, p. 287 (to be published).

SOLAR ENERGY CONVERSION AT THE SEMICONDUCTOR-ELECTROLYTE INTERFACE

An important alternative to photovoltaic solar energy conversion using semiconductor p-n junction solar cells may be through the utilization of semiconductor-electrolyte interface devices. The semiconductor-electrolyte interfacial region has properties similar to those of a Schottky barrier junction and can generate photovoltages and photocurrents when illuminated by solar radiation. The simplicity of the interface configuration and the possibility of using polycrystalline or even thin-film electrodes may make it relatively inexpensive to produce such a device. In addition to the photovoltaic mode, the semiconductor-electrolyte system may be used in photoelectrolysis, where electrolysis proceeds in the presence of an illuminated semiconducting electrode in an aqueous cell with reduced or no electrical energy input.

Preliminary experiments have been conducted to explore the feasibility of photoelectrolysis using an n-type TiO_2 anode in an aqueous electrolyte. Photochemical cells with a Pt cathode and a TiO_2 anode immersed in a wide range of aqueous electrolytes have been used to explore the photoelectrolyte and photogalvanic properties of semiconductor-electrolyte interfaces. Studies of the relation between electrode potential and current density, differential electrode capacity, gas evolution rates, and composition have been conducted as a function of illumination intensity, electrolyte composition, and pH. Typical current-voltage characteristics of a TiO_2-Pt cell with 1 cm^2 area electrodes in an aqueous solution are shown in Fig. 1. Illumination of the semiconducting TiO_2 electrode in the band 300 to 400 nm at an intensity of approximately 30 mW cm^{-2} is seen to induce a sharp increase in the cell current. Spectral studies show that only radiation with photon energies larger than the band gap ($E_g \approx 3$ eV) are effective in inducing this increase. In a homogeneous cell with a single electrolyte, the large photocurrent is accompanied by gas evolution at the electrodes above a critical bias of about 0.3 to 0.4 V. Mass spectrometer analysis of the evolutes shows the gases observed at the cathode and anode to be H_2 and O_2, respectively.

A variety of electrolytes including NaOH, KOH, H_2SO_4, and NaCl solutions have been used successfully, with the only requirement being that the electrolyte provides a sufficiently low cell resistance; this is usually obtained by 0.1 to 1 M solutions. In experiments at a cell bias of 1 V, the H_2 evolution rates correspond to an optical conversion efficiency of approximately 5%. Two separate electrolytes can be used in a cell to furnish part of the required bias potential, further reducing the requirement for external electrical power and increasing the optical conversion efficiency to about 10%. Careful measurement of the TiO_2 electrodes show that they are not dissolved in this process. We also have used polycrystalline film TiO_2 electrodes in some experiments, with efficiency equal to the crystalline materials that were used for the majority of the studies. Additional experiments have been conducted with Ge, Si, and GaAs semiconductor electrodes whose band gaps are more closely matched to the solar spectrum. While photoelectrolytic activity is observed in these materials, they are rapidly dissolved under the photoelectrolysis conditions in any ordinary electrolyte.

Unfortunately all the semiconductors that have been successfully used without anodic dissolution can only absorb a small fraction ($\approx$ 1%) of the solar spectrum owing to their large energy band gaps ($\gtrsim$ 3.0 eV). It is essential therefore to obtain stable materials with band gaps better matched to the solar spectrum. The search for such materials would be enormously simplified if one understood the basic reasons for the nondissolution of semiconductors that have been catalytically used in aqueous electrolytes.

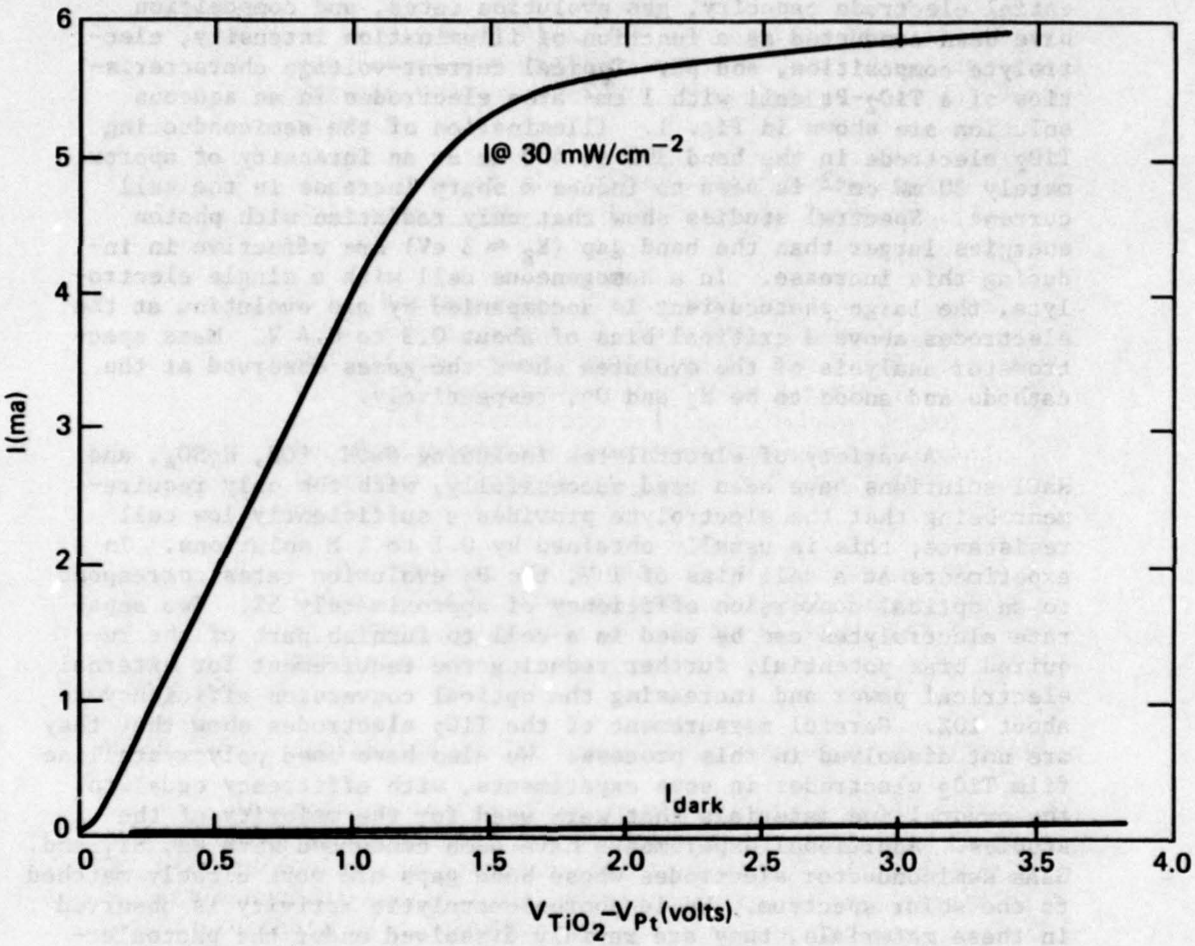

Fig. 1 Current - Voltage Characteristics for a TiO_2 Crystal Anode - Platinized Pt Cathode in 1 M NaCl Solution. The upper curve is for an illumination intensity in 300- to 400-nm band of 30 mW cm^{-2}. The lower curve is the dark current.

It is conjectured that in stable substances the constituting ions undergo reversible valence change in the presence of light and water. We are now in the process of investigating the validity of this criterion for rutile, the first electrode used in the photoelectrolysis of water. It appears desirable to experiment with hitherto unavailable mixed transition metal oxides where, by proper choice of alloy compositions, one can fabricate materials with suitable band gaps for absorbing a higher fraction of the sunlight. We have initiated a program to produce and evaluate materials that are promising candidates for this application.

Concurrently, experiments aimed at producing stable semiconductor-electrolyte systems will be conducted by choosing readily available semiconductors with band gaps around 1.0 to 1.5 eV and investigating their stability in combination with a wide range of both aqueous and nonaqueous solutions. Theoretical work on photovoltaic response of a semiconductor-electrolyte interface under appropriate boundary conditions will begin.

Whether the photogalvanic mode of operating the cell would be an improvement over the conventional solid-state photovoltaic cell is too early to evaluate; however, the possibility of using noncrystalline electrodes, the availability of a large variety of inexpensive electrolytes, and the consideration that no p-n junctions need be formed lend certain attractive features to the semiconductor-electrolyte interface.

Principal Investigators: T. O. Poehler, M. H. Friedman, and K. Moorjani. Drs. Poehler and Friedman are Group Supervisors of the Quantum Electronics and Theoretical Problems Groups, respectively, of the Research Center. Dr. Moorjani is a senior physicist in the Solid State Group of the Research Center.

SOLID-STATE PHYSICS

The Solid-State Physics group is engaged in a broad research program concerning both the fundamental and as-applied aspects of noncrystalline and polycrystalline inorganic solids. New techniques for surface and bulk analyses of solids, combined with the up-to-date thin-film technology, are being used to explore the nationally important problem of fabricating less expensive solar cells.

The primary activity of the group has been directed toward the study and applications of disordered and polycrystalline solids. Some changes and additions to the research program have been initiated in recognition of the ever-increasing role played by noncrystallinity in various branches of solid-state physics.

The work on switching in amorphous semiconductors indicated the importance of systematically investigating the impurity effects in these systems. Consequently, an effort was applied to controlled doping and quantitative determination of impurities in amorphous semiconductors. Optical and electrical measurements have been performed to delineate the behavior of impurities in disordered solids. A theoretical model of magnetic impurities in structurally disordered solids has been proposed and analyzed.

Polycrystalline semiconducting films could prove significantly useful in fabricating low-cost solar cells. The expertise of the group in vacuum deposition techniques and the knowledge acquired from the studies of amorphous semiconductors is being used to explore the possibilities. Encouraging results have already been obtained, and solar cell efficiencies of 1.5% have been achieved in polycrystalline silicon.

The members of the group continue to maintain forefront positions in the field of disordered solids. Pioneering research has been done in solar energy conversion, and members of the group have been invited to participate in a number of conferences and workshops on solar energy and to attend an international conference on Nonmetal-Metal Transitions held at Autrans, France. Seven papers were presented at conferences. The detailed activities of the group are described in eight papers that have been published and four papers that have been accepted for publication.

THIN-FILM SOLAR CELLS

Studies initiated last year on thin-film silicon solar cells have continued. Considerable progress was made in forming double-diffused p-n junctions in polycrystalline silicon films on

sapphire substrates. Crystalline films formed at substrate temperatures up to 800°C gave larger grain sizes and have better photovoltaic response than films deposited in the amorphous state and subsequently crystallized. Investigation continued on secondary ion mass spectrometry (SIMS) analysis of doping profiles and the effect of grain size on diffusion constants.

A potentially promising approach to achieving the desired goal of inexpensive solar cells is through the use of vacuum deposition techniques. Vacuum deposition is particularly useful where large areas and thin layers on smooth substrates are desired. Studies on silicon solar cells have, in fact, indicated that films with thicknesses in the range suitable for vacuum deposition (10 to 15 μm) would provide adequate efficiencies providing their grain sizes are sufficiently large and impurity levels sufficiently low. Efficiencies comparable to sliced wafers may indeed be possible, if, in addition, back fields and back reflecting surfaces could be used. While vacuum-deposited silicon films would be clearly useful, they have been generally avoided in favor of chemical-vapor-deposited layers or other materials such as Cu_2S/CdS because of their historically poor semiconducting properties. However, if the quality of the silicon films could be improved, then all the usual and standard techniques for fabricating solar cells and ensuring their stability could be used.

Samples are being formed by electron beam deposition onto substrates maintained at fixed temperatures between 500 and 800°C. The films are subsequently processed using standard integrated circuit techniques including oxidation, masking, etching, and diffusion. The investigations this year have shown that photovoltaic devices can be formed in polycrystalline vacuum-deposited silicon films on appropriate substates (Ref. 1). Junctions parallel to the substrate may be formed by diffusion. Even in films with small grain size, Fermi levels are not pinned by surface states, but can be controlled by the usual doping procedures. An interesting observation in the study was that the oxide layers grown on polycrystalline vacuum-deposited films behave in all respects similarly to those formed on single crystals. The rate of oxide growth, etching behavior, and surface protection required for oxide masked diffusion are all similar to those found in single crystal wafers. The films can thus be processed in exactly the same manner as single crystals. In the present study, solar cell efficiencies of approximately 0.02% were achieved with grain size of about 0.2 μm while efficiencies of 1.5% were achieved in samples with grain size of about 1.5 μm. Solar cell characteristic current-voltage curves are shown in Fig. 1. The improvement in the characteristics (approach to the single crystal curve) with grain size is clearly evident. The intensity of illumination used in making the measurement was equivalent to sunlight on the earth's surface.

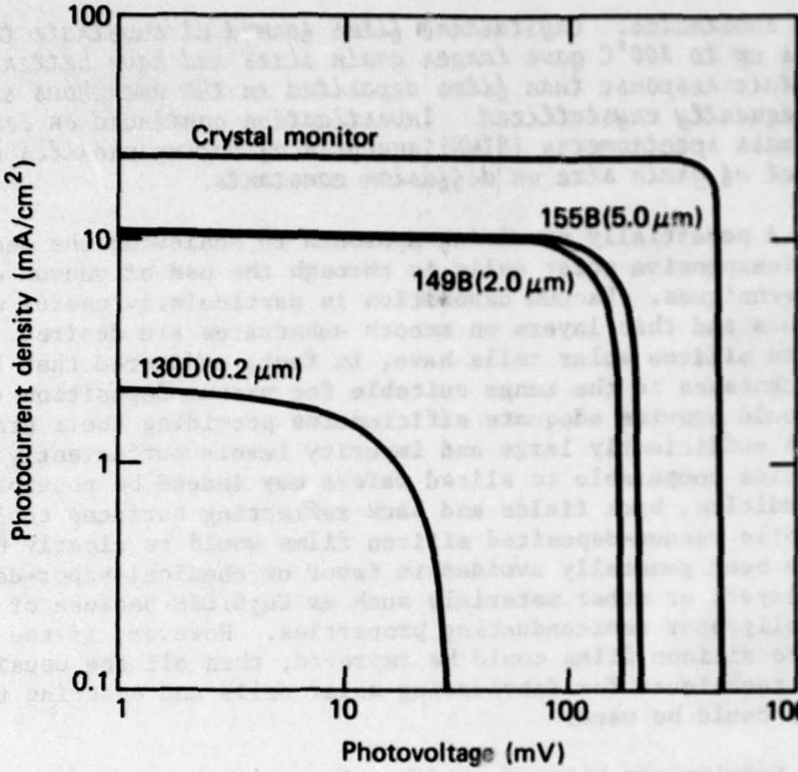

Fig. 1 Illuminated I-V Characteristics for Polycrystalline Films with Various Grain Diameters (indicated in parentheses) and a Crystal Monitor (149B)

The important work that remains is to enlarge the crystalline size while maintaining the sample purity on substrates other than sapphire. Studies on the relationship between grain size and substrate temperature are in progress. Grain size is being determined by scanning electron microscopy.

<u>Principal Investigators</u>: C. Feldman, F. G. Satkiewicz, and H. K. Charles, Jr. Dr. Feldman is Group Supervisor and Dr. Satkiewicz is senior chemist of the Solid State Group of the Research Center. Dr. Charles is a senior engineer of the Microelectronics Group of the Engineering Facilities Division of the Laboratory.

<u>Reference</u>

1. C. Feldman, F. G. Satkiewicz, and H. K. Charles, Jr., "Evaluation of Vacuum Deposited Silicon Films and Junctions for Solar Cell Applications," Proceedings of National Workshop on Low Cost Polycrystalline Silicon Solar Cells, Dallas, TX, May 1976.

SECONDARY-ION MASS SPECTROMETRY

Secondary-ion mass spectrometry (SIMS) employing a sputtering ion source has become increasingly important in the analysis of solids. The full effectiveness of this method is, however, hindered by the incomplete understanding of ion production and the inability to predict absolute ion yields. To overcome these limitations, secondary-ion energy distribution data, from broader classes of material, are needed.

Secondary-Ion Energy Distribution (SIED)

Extensive experimental SIED data are being gathered to determine whether the relatively simple dependency of the distributions on ionization potential, observed from sputtering oxides and glasses (Ref. 1), is maintained. Materials examined included several metallic elements and binary compounds such as GaAs, Cu_2S, CuS, CdS, and Si_3N_4. In attempts to reproduce some of the previous data on glasses, it was found that the secondary optics adjustments have a greater effect on the distributions than had been previously recognized. Accordingly, experiments are being conducted to obtain better understanding of the ion extraction conditions. However, the uncertainties concerning the absolute shape of these curves do not preclude the possibility of obtaining meaningful data on a relative basis, provided the critical extraction conditions are reproduced.

A SIMS Analysis of Polycrystalline Silicon Solar Cells

SIMS analysis of polycrystalline silicon thin films has provided impurity data and dopant distributions (and consequently junction depths). This information is being used to study the critical question of substrate interaction in the development of low-cost solar cells.

Calibration work was performed to provide the basis for determining the concentration profiles of the dopants (phosphorus and boron) in silicon. A number of these profiles were obtained and were compared with the corresponding profiles from a single crystal. The results show higher diffusion coefficients for the films, probably due to more rapid diffusion along grain boundaries.

One of the major problems in solar cell development is the substrate on which the thin film is deposited. A knowledge of the reaction of the substrate with the film material is necessary. SIMS is a useful technique for determining such reactivity. The instrument at APL can obtain polyatomic spectra, an ideal feature to provide an understanding of such reactions. These spectra

provide clues to the structural aspects of the material being sputtered.

The composite system Al_2O_3/Ti/B/Si has already been examined to determine the extent of reaction of Ti and B as well as the interpenetration by solution of one in the other. The results are illustrated in Figs. 1 and 2. Figure 1 shows the delineation of the phases in the as-deposited sample. The Ti profile is the least sharp because of the finite depth resolution of the sputtering beam. Figure 2 shows the distribution of species after the sample had been heated at 975°C for 2 hours. As can be seen, boron has diffused into silicon while Ti has reacted with boron. Also shown is the curve for excess boron, which is obtained by appropriate intensity decoupling and from the knowledge of relative ion yields of elemental boron and boron in TiB_2. Distribution of Al into the films was also observed, but is not shown in the figures.

Principal Investigator: F. G. Satkiewicz is senior chemist of the Solid State Group of the Research Center.

References

1. F. G. Satkiewicz, "Initial Energy Distribution of Secondary (+) Ions from the Sputtering of Non-Metallic Solids with Ar+ (3 KeV to 10 KeV)," Proceedings of the American Society for Mass Spectrometry and Allied Topics, Houston, TX, May 1975, pp. 365-367.
2. F. G. Satkiewicz and H. K. Charles, Jr., "Sputter Ion Source Mass Spectrometer Analysis of Copper Sulfide/Cadmium Sulfide Solar Cell Samples," APL/JHU TG 1284, October 1975.
3. F. G. Satkiewicz and H. K. Charles, Jr., "SIMS Analysis of Cu_2S/CdS Solar Cell Samples," Proceedings of the Twenty-Fourth Annual Conference on Mass Spectrometry and Allied Topics, San Diego, CA, May 1976.

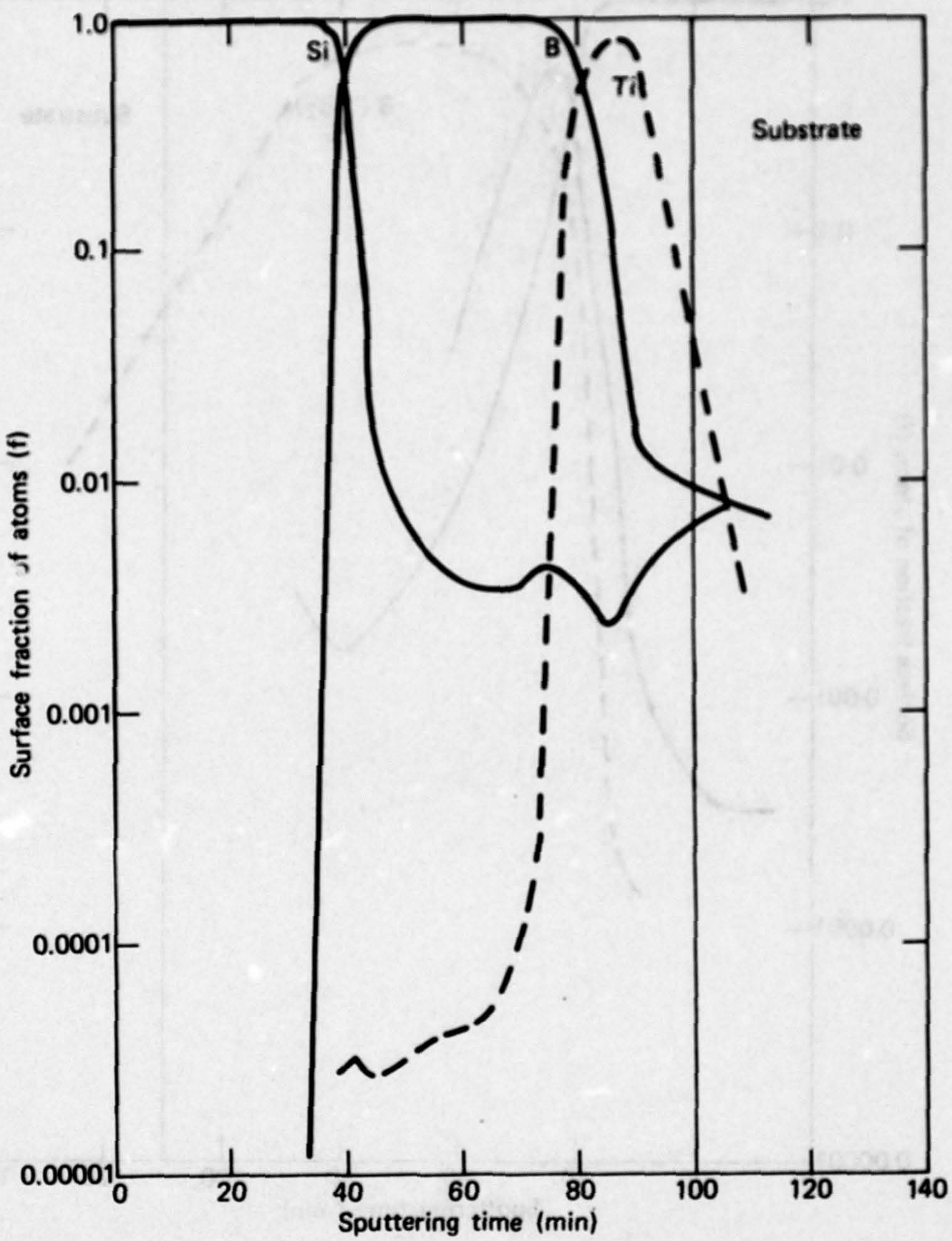

Fig. 1 SIMS Analysis of As-Deposited Composite Layer Si/B/Ti/Sapphire

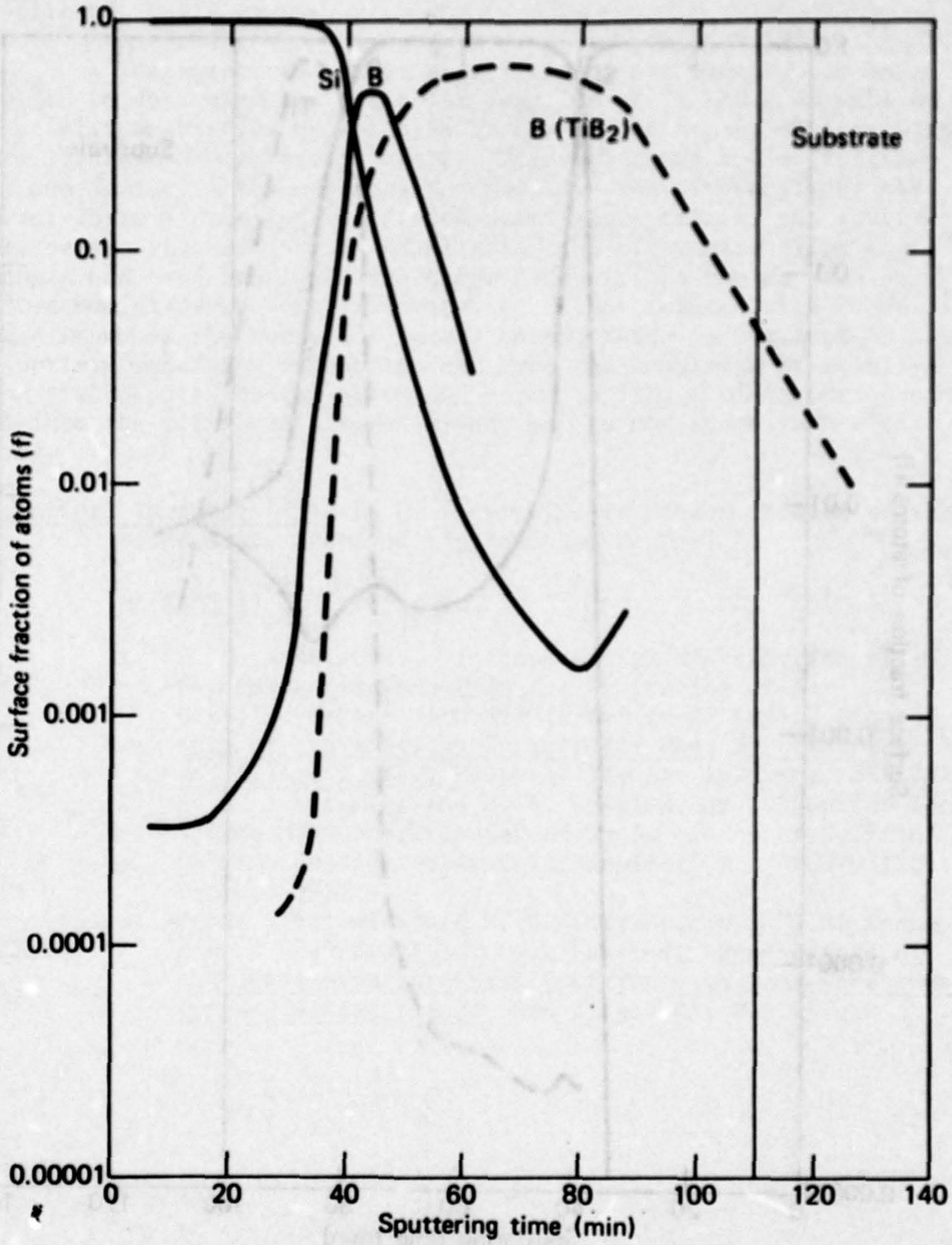

Fig. 2 SIMS Analysis of Composite Layer Si/B/Ti/Sapphire Heated for 2 Hours at 975°C

INFRARED ABSORPTION BANDS IN AMORPHOUS BORON FILMS CONTAINING CARBON AND HYDROGEN

The presence of carbon and hydrogen in amorphous boron has been shown to have a large effect on the resistivity, electron paramagnetic resonance signal, and switching characteristics of thin-film samples. Such films have potential device applications. To estimate the amount of hydrogen and carbon in these samples, a simple nondestructive method is desirable. For this purpose a technique for measuring the I-R absorption spectra of film samples has been developed that gives a semiquantitative analysis of the concentration of hydrogen and/or carbon.

Amorphous boron films containing controlled levels of carbon and/or hydrogen were examined by infrared absorption spectroscopy (I-R) in the range 700 to 4000 cm^{-1} (14 to 2.5 μm). The samples were quantitatively analyzed for hydrogen, carbon, and oxygen by secondary-ion mass spectrometry (SIMS). The purpose of this work was to identify the absorption peaks observed in the I-R spectra of the boron films and to correlate the intensities of peaks caused by hydrogen and carbon with the SIMS analysis of the samples.

Interference fringes caused by the thickness of the samples require that spectra be obtained relative to a background having the same interference pattern as the samples being investigated. For this purpose, computer-generated simulations were obtained using previously measured values of the refractive index and absorption coefficient for pure boron films. The computer simulations thus became, in effect, the 100% transmission baselines with respect to which the impurity absorption peaks can be measured. The Beer-Lambert Law, $\log T^{-1} = Ktc$, was then used to calculate the impurity concentration from the measured relative transmission in peak, T. The quantities t, c, and K are, respectively, the film thickness, the impurity concentration, and an empirical constant derived from a best fit to the SIMS analyses.

Absorption bands centered at 2560 and 1100 cm^{-1} were identified as caused by hydrogen (B-H vibrations) and carbon (B-C vibrations), respectively. Intensities of these bands were correlated with the SIMS measurements, and a reasonable quantitative agreement was achieved. The I-R measurements can thus be used to estimate the concentration of hydrogen and/or carbon in the thin-film amorphous boron samples.

Several additional absorption bands were observed that had been observed previously by others in bulk amorphous boron or in the various crystalline forms of boron. These previous identifications have been corroborated. This work represents the first time that the hydrogen band at 2560 cm^{-1} and the carbon band at 1100 cm^{-1} have been positively identified by quantitatively corre-

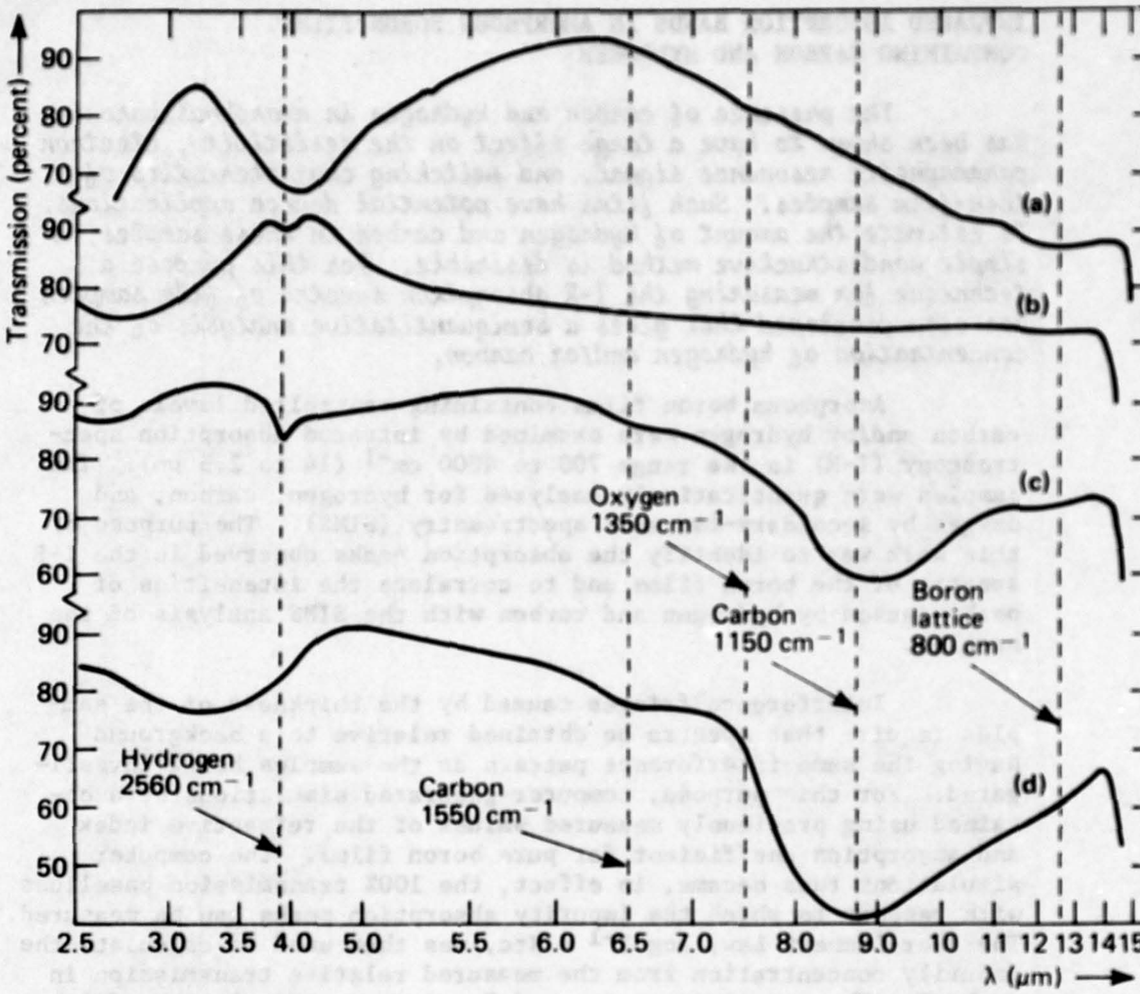

Fig. 1 Infrared Transmission Spectra of Similarly Thick Boron Films: (a) Undoped, (b) Containing Hydrogen (H_2-doped), (c) Containing Hydrogen and Carbon (C_2H_2-doped), and (d) Containing Carbon (deposited from melt containing carbon).

lating the band intensities with an independent measurement of the corresponding impurity concentration. The spectra of four films of nearly identical thickness, so as to facilitate visual comparison, are shown in Fig. 1. A report of this work is being prepared for publication.

<u>Principal Investigators</u>: C. Feldman, N. A. Blum, G. W. Turner, and F. G. Satkiewicz. Dr. Feldman is Group Supervisor, Dr. Satkiewicz is senior chemist, and Dr. Blum is a senior physicist of the Solid State Group of the Research Center. Mr. Turner is a graduate student at The Johns Hopkins University and an APL fellow.

ELECTRICAL EFFECTS OF CARBON IMPURITIES IN AMORPHOUS BORON FILMS

The influence of impurities on the electrical properties of amorphous semiconductors is of interest from a theoretical viewpoint and is important for investigating applications of these systems. At the present time, the theoretical aspects of impurity effects on electronic states in amorphous semiconducting materials and the physics of experimentally observed electrical transport characteristics are not well understood. This project has the goal of understanding the effects of carbon doping on the transport properties of amorphous boron films and of making use of these materials in practical devices.

This work has focused on the effects of carbon impurities in amorphous boron, with the ultimate goal of making thin-film function devices. Samples were formed by electron-beam deposition of boron carbide (B_4C) and by simultaneous electron-beam deposition of boron and carbon from separate sources. The deposition was made on fused silica and infrared transmitting zinc sulphide (Eastman Kodak IRTRAN) substrates with rates ranging from 50 to 200 nm/min. The resulting films varied in thickness between 0.2 and 1.5 μm. Compositional analysis of the samples was performed using secondary-ion mass and infrared spectrometry; the resistivity was measured by four-point probe and deposited-pad methods.

The resistivity versus carbon content behavior of the present samples (Fig. 1) is slightly different from the one exhibited by films obtained from deposition under a partial pressure of acetylene (Ref. 1). This may be due to the hydrogen present in the acetylene-doped films, and further experimental work is in progress to understand the difference. However, it is clear that, regardless of the method of introducing carbon, the resistivity of amorphous boron is sensitive to the amount of carbon introduced. Control of sample parameters and barrier formation in amorphous boron may thus be possible.

Principal Investigators: C. Feldman and G. W. Turner. Dr. Feldman is Group Supervisor of the Solid State Group of the Research Center and Mr. Turner is a graduate student at The Johns Hopkins University and an APL fellow.

References

1. C. Feldman, H. K. Charles, Jr., F. C. Satkiewicz, and J. Bohandy, "Electrical Properties of Carbon-Doped Amorphous Boron Films," J. Less-Common Met., Vol. 47, 1976, pp. 141-145.

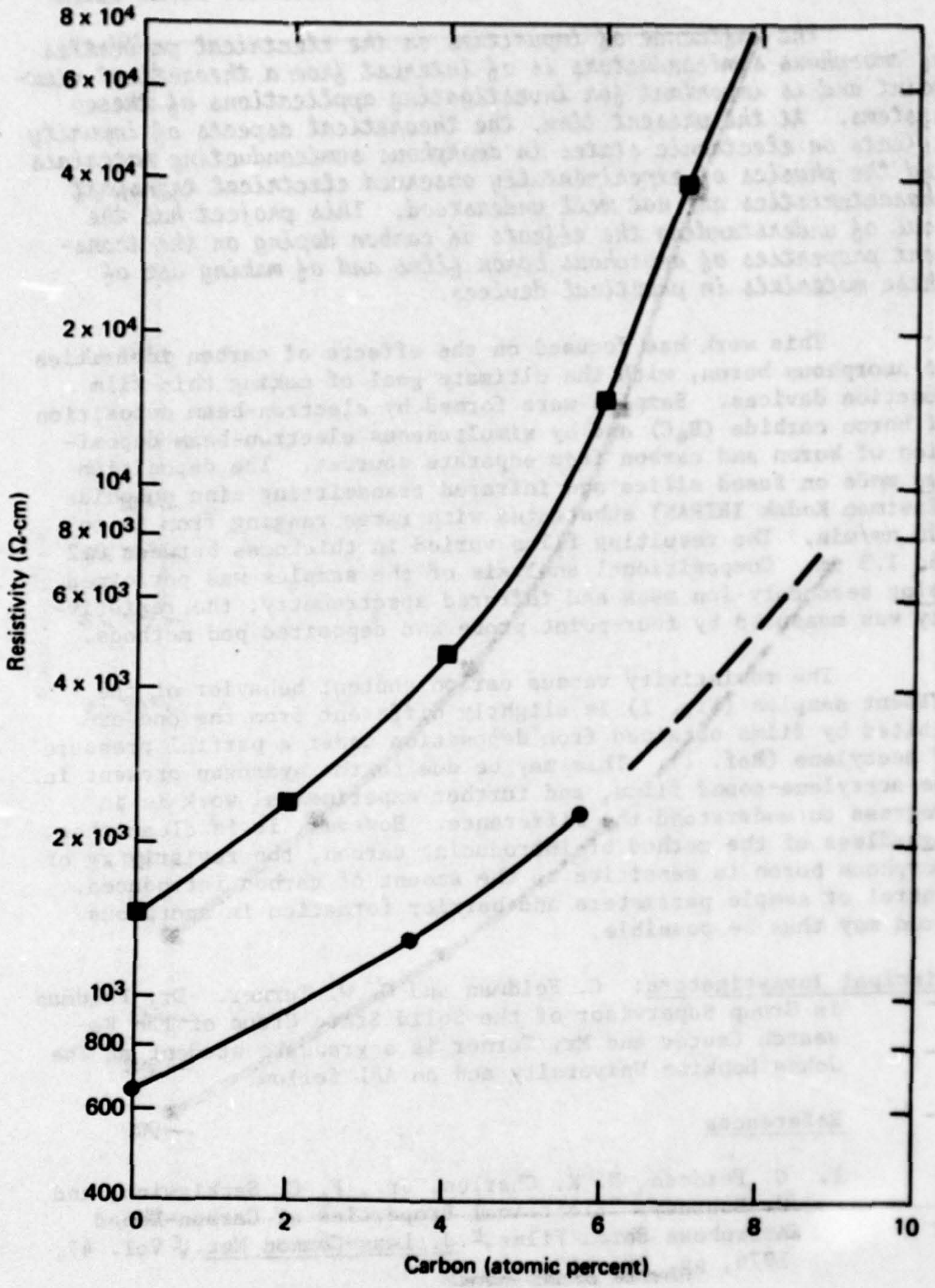

**Fig. 1 Resistivity versus Carbon Content in Amorphous Boron Films:
■ Acetylene doped, ● Carbon doped.**

2. G. W. Turner, H. K. Charles, Jr., and C. Feldman, "Switching in Amorphous Boron Films under Single-Pulse Conditions," J. Appl. Phys., Vol. 47, 1976, pp. 3618-3624.

KINETICS OF THE AMORPHOUS-TO-CRYSTALLINE TRANSFORMATION IN SILICON THIN FILMS

In order to make effective use of semiconducting amorphous films in electronic device technology, it is necessary to understand the mechanism of transformation to the crystalline state in as much detail as possible. Through this understanding there is the possibility of controlling the size and growth pattern of grains during the crystallization process. The kinetics of the amorphous-to-crystalline transformation in vacuum-deposited thin-film silicon was studied by an optical method of determining the isothermal volumetric transformation as a function of time. These results were interpreted in terms of an improved theory of transformation kinetics.

Amorphous silicon thin films were prepared by electron-beam vacuum deposition onto fused silica substrates. Each sample was heated in an inert gas tube furnace at constant temperature for a series of time increments. After each increment, the transmission of the film was measured in that part of the optical spectrum where the absorption coefficient varies most rapidly as the film transforms from the amorphous to the crystalline phase. The heating increments and optical measurements continued until the film crystallized. A plot of relative transmission versus time for two different temperatures is shown in Fig. 1. In this way, plots were obtained of the fractional volume transformed as a function of heating time. The crystallization time versus temperature is plotted in Fig. 2. Results for silicon are qualitatively similar to those obtained earlier for germanium films (Ref. 1). However, as discussed below, the kinetics of the transformation can be described by a theoretical model which is more satisfactory in several respects than the simple rate process previously described (Ref. 1).

A recent paper in the literature (Ref. 2) presents a model that includes a more realistic picture of the growth site impingement problem. This provides a method for removing nucleation sites as they are swept away in the path of the transforming regions. The theory has the advantage of distinguishing between homogeneously nucleated processes and provides specific solutions for growths in two and three dimensions. The asymptotic behavior of the solutions agrees with the form of the experimental transformation curves, whereas the earlier model gave results that broke down for large values of fractional volume transformed.

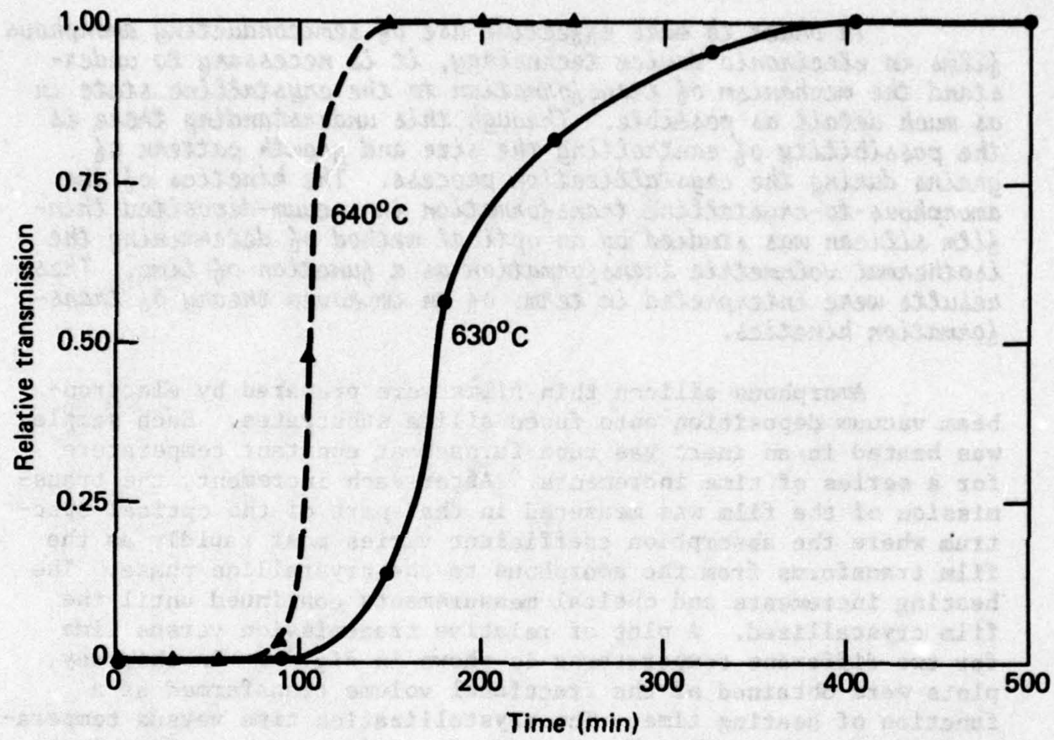

Fig. 1 Isothermal Kinetic Transformation Curves for Silicon Films at Two Different Temperatures

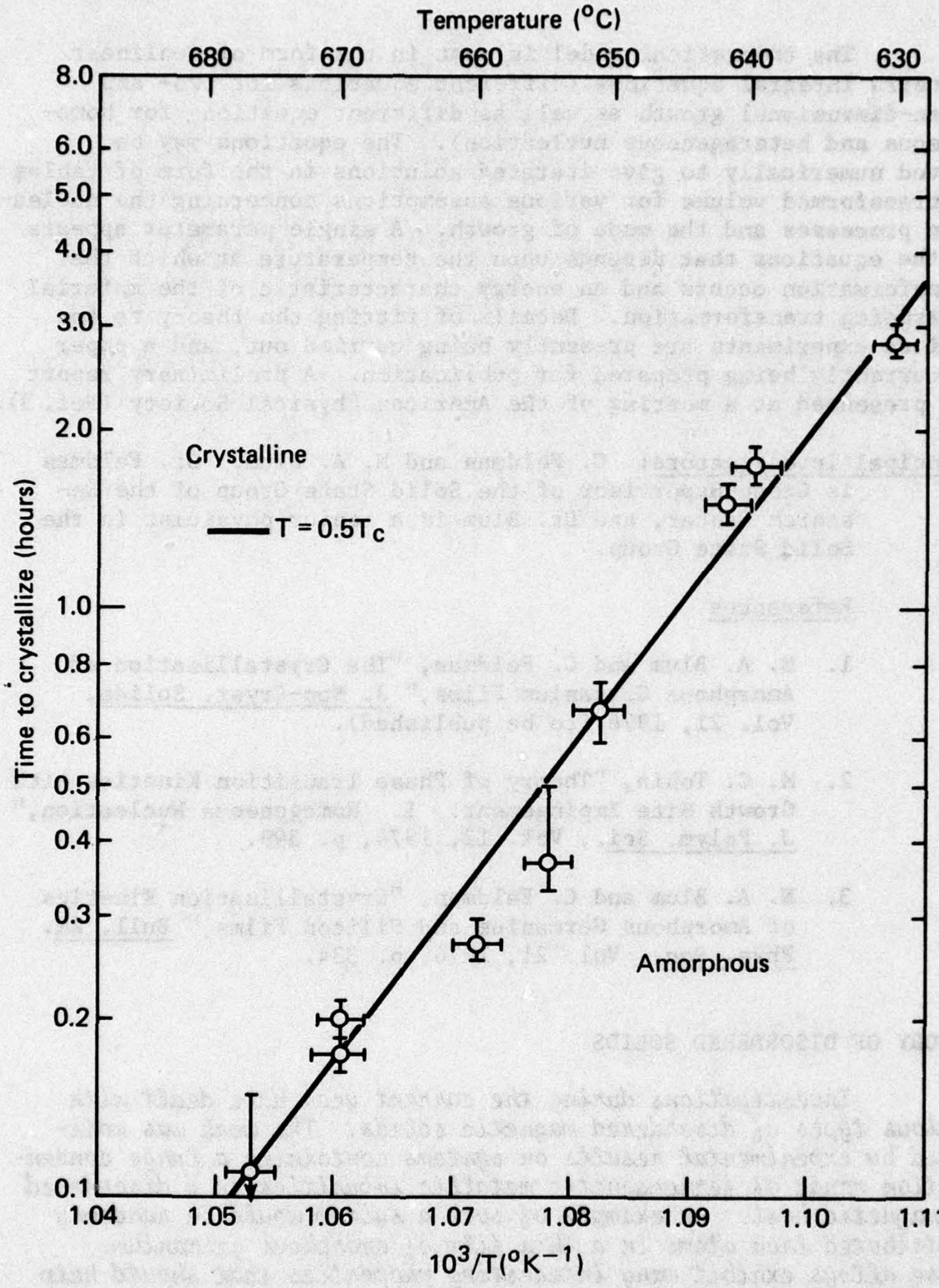

Fig. 2 Crystallization Time versus Temperature for Silicon Films. The data points and least-squares fit (solid line) correspond for each point to the time and temperature at which half the volume of the film was crystallized.

The theoretical model is cast in the form of nonlinear Volterra integral equations (different equations for two- and three-dimensional growth as well as different equations for homogeneous and heterogeneous nucleation). The equations may be solved numerically to give iterated solutions in the form of tables of transformed volume for various assumptions concerning the nucleation processes and the mode of growth. A single parameter appears in the equations that depends upon the temperature at which the transformation occurs and an energy characteristic of the material undergoing transformation. Details of fitting the theory to the silicon experiments are presently being carried out, and a paper is currently being prepared for publication. A preliminary report was presented at a meeting of the American Physical Society (Ref. 3).

Principal Investigators: C. Feldman and N. A. Blum. Dr. Feldman is Group Supervisor of the Solid State Group of the Research Center, and Dr. Blum is a senior physicist in the Solid State Group.

References

1. N. A. Blum and C. Feldman, "The Crystallization of Amorphous Germanium Films," J. Non-Cryst. Solids, Vol. 21, 1976 (to be published).

2. M. C. Tobin, "Theory of Phase Transition Kinetics with Growth Site Impingement. I. Homogeneous Nucleation," J. Polym. Sci., Vol. 12, 1974, p. 399.

3. N. A. Blum and C. Feldman, "Crystallization Kinetics of Amorphous Germanium and Silicon Films," Bull. Am. Phys. Soc., Vol. 21, 1976, p. 334.

THEORY OF DISORDERED SOLIDS

Investigations during the current year, have dealt with various types of disordered magnetic solids. The work was motivated by experimental results on systems containing a large concentration range of ferromagnetic metallic impurities in a disordered diamagnetic host. An example of such a system would be randomly distributed iron atoms in a thin film of amorphous germanium. These alloys exhibit many interesting properties that should help in understanding phenomena as varied as hopping conduction, insulator-metal transition, and magnetic interactions in disordered solids. The investigation of the last property has been emphasized in the present study.

The effect of structural and/or chemical disorder on the critical properties of a Heisenberg ferromagnet has been analyzed, and the behavior of spin glasses has been studied. The proposed models, the method used, and the results obtained are described briefly below.

A site-disordered alloy A_cB_{1-c} with concentration c of magnetic atoms A randomly distributed in a nonmagnetic lattice of B atoms with concentration (1-c) is considered. The lattice is assumed to be structurally disordered, which induces fluctuations in the ferromagnetic exchange interactions between magnetic atoms. Thus, besides the temperature and the coordination number of the lattice, the relevant parameters for the discussion of thermodynamic quantities are the concentration c of the magnetic atoms and the measure Δ of fluctuations. The crystalline ferromagnet results in the limits $c = 1$ and $\Delta = 0$, which serve as a useful check on the calculations performed.

The Hamiltonian for the above model is analyzed within the Bethe-Peierls-Weiss approximation, and the resulting free energy is averaged over all the configurations of the disordered system. A self-consistent condition on magnetization is used to yield expressions for thermodynamic quantities of interest.

It is shown that the critical concentration c_0 of magnetic atoms for the appearance of long-range magnetic order is not influenced by the presence of fluctuations (Ref. 1). The value of c_0 (= 1/3) is found to be in reasonable agreement with the experimental value (0.4 ± 0.02) recently deduced from the Curie temperature versus concentration measurements on iron atoms randomly substituted in amorphous germanium. For $c > c_0$, the fluctuations depress the values of the Curie temperature, the high temperature magnetic susceptibility (Fig. 1), and the magnetization (Fig. 2) relative to the corresponding values for the average crystal. For small values of Δ, explicit expressions for the amount of decrease in the above quantities are obtained. However, the critical indices, for magnetization as well as susceptibility, are found to be unaffected by fluctuations (Ref. 2).

The above formulation has been modified to discuss the static properties of spin glasses. These are magnetically dilute alloys that possess neither short- nor long-range magnetic order but do exhibit anomalies in their thermodynamic behavior. It is expected that a study of spin glasses will answer questions concerning the fundamental nature of exchange interactions and aid in exploring the possible uses of disordered magnetic solids in magnetic bubble memories.

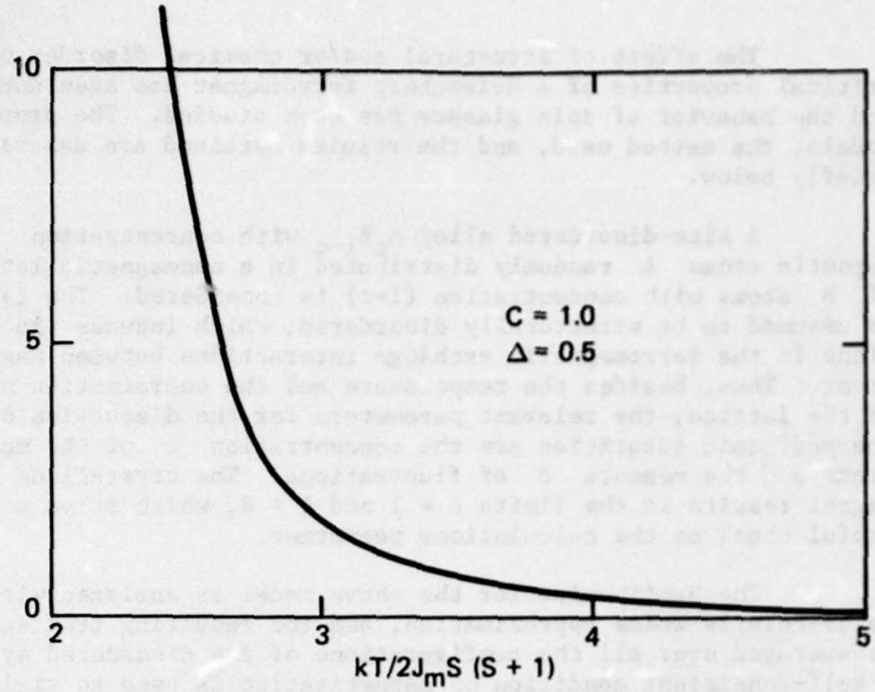

Fig. 1 Relative Susceptibility versus Reduced Temperature for a Structurally Disordered Ferromagnet. χ_m and J_m are respectively the susceptibility and the exchange constant of the mean crystal while χ_a is the susceptibility of the disordered solid.

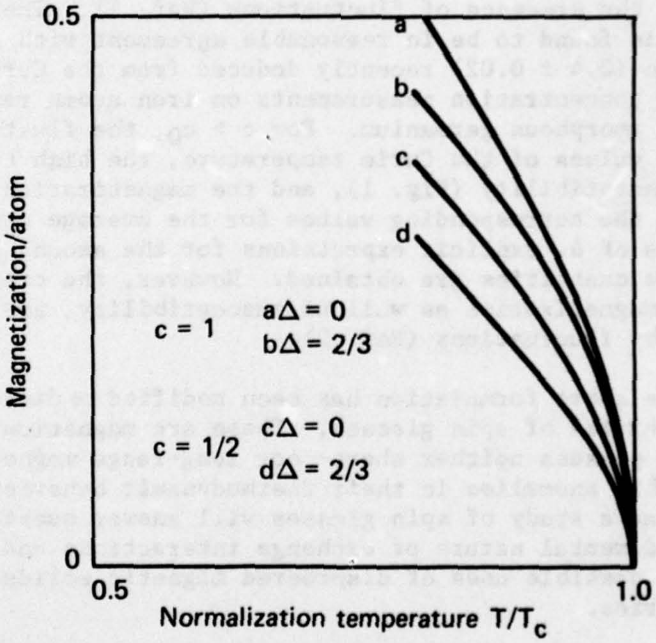

Fig. 2 Magnetization versus Normalized Temperature for Different Values of c and Δ in the Vicinity of the Curie Temperature T_c. For each case, the temperature is normalized with respect to the corresponding T_c.

In our treatment, the presence of a finite number of nearest neighbors increases the value of the spin glass transition temperature compared to the molecular field result. Furthermore, in contrast to the molecular field approximation, the magnetic susceptibility approaches the transition temperature from below with a finite positive slope in agreement with the experimental results (Ref. 3).

Principal Investigators: K. Moorjani and S. K. Ghatak. Dr. Moorjani is a senior physicist in the Solid State Group of the Research Center and Dr. Ghatak (not funded under the IR&D program) is a post-doctoral fellow at the Free University, Berlin. This work commenced during 1974-75 when both investigators were at the Phase Transition Group of the Centre National (France) de la Recherche Scientifique, Grenoble, France.

References

1. K. Moorjani and S. K. Ghatak, "Bethe-Peierls-Weiss Approximation in Disordered Ferromagnets," Magnetism and Magnetic Materials, 1975, Eds., J. J. Becker et al., AIP Conf. Proc. No. 29, AIP, NY, 1976, pp. 152-153.

2. K. Moorjani and S. K. Ghatak, "Critical Behavior of a Structurally and Chemically Disordered Ferromagnet" (to be published in J. Phys. C: Solid State Phys.).

3. S. K. Ghatak and K. Moorjani, "Spin Glasses: Beyond the Molecular Field Approximation," J. Phys. C: Solid State Phys., Vol. 9, 1976, pp. L293-L295.

4. K. Moorjani and S. K. Ghatak, "Site and Bond Disorder in a Heisenberg Ferromagnet," Bull. Am. Phys. Soc., Vol. 21, 1976, p. 386.

5. S. K. Ghatak and K. Moorjani, "Structurally Disordered Heisenberg Ferromagnet," Solid State Commun., Vol. 16, 1975, pp. 923-925.

PRECEDING PAGE BLANK - FILMED

EXPLORATORY DEVELOPMENT

INTRODUCTION

About one-fourth of the Laboratory's Indirectly Funded Research and Development (IR&D) Program is devoted to exploratory studies aimed primarily at developing new approaches in mission-related areas. The program provides for initial investigations to assess the value of promising new concepts and techniques. Where sufficiently encouraging results are obtained, direct sponsor support is generally solicited for further development.

The exploratory development program is intended to nurture the development of innovative solutions to problems in areas of importance to the Laboratory's missions. In general, projects are proposed and carried out on a part-time basis by experienced principal investigators whose primary responsibilities are to directly funded tasks. Proposals are reviewed by the Director and, if approved, are assigned a specific level of effort for a specified length of time.

The exploratory projects are relatively small, and the quality and quantity of the results that have been achieved testify to the competence, industry, and experience of the investigators and to the relevance of the work to the larger, directly funded programs with which they are primarily concerned. Many significant developments could be cited as examples. This year, it is particularly gratifying to note that the citation of the Navy Distinguished Service Medal recently awarded to Mr. Sverre Kongelbeck recognizes his work on the box launcher which was made possible by the exploratory IR&D program.

The support of national defense objectives remains the predominant activity of the Laboratory, but effort is also devoted to civilian agencies of government through work directly supported by such agencies. Accordingly, a fraction of the IR&D program is concerned with the exploration of new concepts and techniques in non-DoD areas. Major emphasis continues to be placed on topics in space science and engineering and in biomedical engineering. Projects related to navigation and air traffic control and to safety, communications, environmental impact, and energy utilization are also pursued.

A total of 30 individual projects were supported by the program during the past fiscal year, most of which are described under separate headings in the following sections. The projects that are not described in detail are very small, with a total level of effort of less than 2 man-years. Nine of these represent

the concluding and final report preparation phases of previous work and will not be discussed further. One provides for continued participation of the Laboratory in the Federal Aviation Administration (FAA) Radar Study Committee (with representatives also from the FAA, the Mitre Corporation, and the Massachusetts Institute of Technology Lincoln Laboratory).

Four new projects initiated late in the present year have not yet yielded firm conclusions. The first of these addresses a primary limitation of existing air traffic control systems, namely the unavailability of consistent and dependable aircraft height information. It is proposed that the use of a passive-receive-only height measuring antenna rotating in synchronism with, but with a slight lag with respect to, the primary 2-D radar will provide the required information. The project is designed to demonstrate the validity of this approach. Phase I, the definition of the system, is now essentially complete, and procurement of hardware is in progress.

A second small effort initiated late in the year explores a new concept for a low-cost rugged angular rate sensor. Models have been fabricated that appear adequate to serve as wing leveler inputs to an autopilot for remotely piloted vehicles; they have been tested and improvements are underway. The principle of operation involves the generation of a laminar jet of ionized air that is directed into two (or more) conductivity cells; in the presence of angular acceleration, the jet path is deflected, thereby altering the distribution of the current carried by the jet to the conductivity cells.

The third project, begun late in the year, is a small-scale effort to explore participation with government agencies in addressing the national problem of relatively low productivity growth of the United States. Agencies concerned include the National Center for Productivity and Quality of Working Life (established by Public Law 94136), the DoD Manufacturing Technology Advisory Group, and the Automation Research Council (funded by the National Science Foundation).

A fourth new project, also begun late in the year, is concerned with the feasiblity of devising a small temperature and pressure sensing and recording device that would survive passage through the condensers of power plants. The work is motivated by the need to determinate the environmental impact on organisms entrained in the cooling water. At present, no instrumentation is available for measuring the time history of the thermal stress. Preliminary considerations suggest that the APL Microwave Electronics Laboratory may be able to devise a rugged instrument package of less than 2 cm diameter that would be capable of measuring and recording on the order of 100 data points with 0.2°C temperature resolution and 30 millibar pressure resolution.

BOX LAUNCHER DEVELOPMENT

A Standard Missile Blast Test Vehicle (BTV) was fired from the APL Engineering Development Model (EDM) box launcher on 29 September 1975. All firing test objectives were accomplished. The EDM launcher was returned to APL and an analysis made of the blast effects. Shock and vibration data and films of the firing have also been analyzed. A final report of the EDM Program and the test firing is nearing completion.

APL has for several years been engaged in the development of box launcher concepts for the Navy. The work resulted in a box launcher design that was selected by the Navy in 1970 for installation on 1052-class destroyers under the Interim-Surface-to-Surface Missile Capability (ISSMC) Program. Following the ISSMC Program, APL continued design, development, and tests of improved box launcher components, structures, and mechanisms, resulting in the construction and test of the EDM box launcher.

The 1975 test firing of a BTV from the EDM box launcher was an important milestone in the APL box launcher development program. The successful test demonstrated the functional operability of the launcher and served to evaluate its new and improved mechanism designs. Important new features of the EDM box design are the unitized launch rail system with its self-contained sealed mechanisms for stowing, arming, and firing a missile and the suspension of the launch rail within the box structure by shock and vibration isolators.

The test data revealed no adverse effects on the launcher or the missile trajectory as a result of launching the missile from the elastic suspended rail, and instrumentation in the rail provided valuable data on the shock and vibration patterns generated during the firing. All of the operating mechanisms functioned as intended before, during, and after the firing, and a postfiring analysis revealed that the sealing methods used to prevent exhaust gas entry into critical areas were highly effective. The extreme aft frame of the box structure incurred some damage from the hot exhaust gases; however, this problem can be corrected by a minor change in the construction method.

During the test, the box launcher was equipped forward and aft with frangible closures of a new design. An additional forward closure was mounted in close proximity to and below the closure on the box to simulate an adjacent launcher condition, as would be encountered where several boxes might be closely grouped in a shipboard installation. Both forward and aft closures functioned as intended; however, the adjacent cell forward closure was damaged, indicating the need for further development of this component.

A complete report of the EDM development and of the results of the firing tests of this launcher is currently being prepared.

The completion of the EDM launcher firing test and the preparation of the development and test report conclude the recent indirectly funded phase of the APL Box Launcher Program. Direct Navy funding support will be pursued to establish a finalized design to meet full tactical requirements for shipboard installations. Further work required includes correction of deficiencies revealed during the test, additional shock and vibration tests with a dummy instrumented missile stowed in the launcher, adaptation of the launcher for vertical launch of the Standard Missile, temperature and humidity control design studies, and investigations of applications for specific ship types.

Principal Investigators: S. Kongelbeck and W. F. Williams. Mr. Kongelbeck is APL's Chief Engineering Consultant, and Mr. Williams is Branch Supervisor of the Mechanical Engineering Branch of the Engineering Facilities Division.

FEASIBILITY DEMONSTRATION, AUTOMATED MAINTENANCE SUPPORT TOOL

As a result of the increase in sophistication of individual components in a Combat Weapon System, readiness is frequently limited by the necessity to maintain equipment. In the case of smaller ships, the limited capability to maintain equipment with a small crew has resulted in an effective ceiling on the complexity of the components deployed. Thus, a significant increase in equipment maintainability can result in a direct increase in combat effectiveness. An Automated Maintenance Support Tool (AMST) can help to provide such a capability.

One approach to a general improvement in maintainability is the development of an AMST that can interact with and provide broad support to an operator during routine maintenance and diagnostic repair. The purpose of this IR&D project was to develop a demonstration system that would

1. Provide programmed support for routine maintenance and standard diagnostics for a given equipment set;
2. Provide nonprogrammed access to technical data, including text, drawings, waveforms, computations, etc., to support troubleshooting in situations for which no diagnosis was anticipated; and
3. Provide a mechanism by which additional programmed support can be developed for an arbitrary equipment set.

DESIGN CONCEPT

The AMST combines the technology of minicomputers with that of micrographics. The minicomputer is used to

1. Prompt the operator and, based upon the operator response, branch forward and back through a program decision tree;
2. Provide the operator with unprogrammed information retrieval access to all data in the data base;
3. Address the micrographic device and display the required graphics or text; and
4. Perform computations and analysis using parameters that have been retained, keyed in, or directly interfaced.

The micrographics device is used to

1. Automatically display graphics and text which cannot be economically retained in a computer readable format;

2. Automatically display manuals and related documents; and

3. Manually peruse micrographic materials.

The AMST data base is a replaceable automated file (e.g., magnetic tape) and a micrographic file (e.g., ultrafiche cassette). A separate data base may be used for each class of equipment to be maintained.

EQUIPMENT CONFIGURATION

The AMST equipment configuration used for the demonstration system consists of three units:

1. An Operator Unit that consists of the microform display and a keyboard computer input device. All operator inputs and outputs are made via this unit.

2. A Data Base Unit that consists of the microform and digital data bases. For the demonstration system, a single data base with several demonstration capabilities is used. The interchangeability of data bases is also demonstrated.

3. An Electronic Unit that contains a minicomputer, a magnetic tape device, a microform viewer control element, and appropriate interfacing. The demonstration system uses a permanently mounted unit; however, it can be easily demonstrated that the Electronic Unit can be packaged as a portable unit.

The demonstration system consists entirely of available, off-the-shelf equipment. The microform viewer selected is the microform Data Systems M-380. This unit allows random retrievel of any of 100 000 images within 4 s. The display unit and electronics weigh 75 lb; the cost per unit is in the $7000 range.

The minicomputer being used for the demonstration is a Computer Automation Alpha LSI-2 which is available at the Laboratory. The demonstration uses a magnetic tape but has been designed

also to use a floppy disk. While the minicomputer portion of the demonstration is not now portable, suitable off-the-shelf components, including a microprocessor, floppy disk, and keyboard, can be purchased for around $7000 and will weigh under 100 lb. Thus, the demonstration system satisfies an initial objective that an inexpensive, portable unit be produced.

DEMONSTRATION DATA BASE

A demonstration data base was prepared using the maintenance manual for the AN/SPA-25B Indicator Group. This manual was selected because it is unclassified, represents a typical shipboard electronic component, and contains a wide variety of tables, figures, block diagrams, and foldouts.

The manual is approximately 3 in. thick and contains some 550 pages plus some 30 large foldout signal-flow and schematic diagrams. The document was prepared for filming and copied onto ultrafiche. A set of operating instructions plus some material describing the AMST were also photographed. Finally, an automated index to these images was prepared.

Using this data base, the AMST demonstration system allows the user to

1. Select any one of three data bases including the maintenance manual;
2. Gain access to the Table of Contents;
3. Gain access to any page by page number;
4. Gain access to any figure or table by figure or table number;
5. Display the index to the document by alphabetic retrieval;
6. Page through the manual;
7. Scan backward and forward over a foldout figure;
8. Generate a user index to pages by user-generated mnemonics; and
9. Retrace a page selection sequence.

The demonstration system computer program has been defined as a modular system that will allow programmed tree branching as well as random retrieval. The data base developed for the demonstration system, however, makes only limited use of this capability.

CONCLUSION

The demonstration system has shown the feasibility of the AMST concept. Follow-on activities include the development of other data bases, the exploration of user interaction with the system, the packaging of a portable unit, and the expansion to support computations and test equipment interfaces. Since the initial objectives of the AMST demonstration have been met, further activities will not be funded as IR&D projects.

Principal Investigator: B. I. Blum. Mr. Blum is on the staff of the Information Processing and Display Group of the Fleet Systems Department.

KINEMATIC PERFORMANCE OF AN ADVANCED MISSILE

A small short-term exploratory effort was conducted to determine kinematic performance capabilities of an advanced surface-to-air-ramjet (ASAR) propulsion system against selected maneuvering-antiship-missile threats.

The ramjet propulsion system provides sustained thrust and speed to intercept. In addition to providing greater average and terminal speeds in many cases, this characteristic permits greater flexibility in trajectory shaping compared to shorter burning rocket missiles, within constraints imposed by guidance system considerations. The investigation employed an appropriately extended weapon simulation previously developed by the Ship Weapon Systems Group. For reasons of national security, the results of the study are classified but have been published and are available to properly authorized individuals.

Principal Investigator: R. W. Constantine. Mr. Constantine is a senior engineer in the Propulsion Group, Aeronautics Division.

SPACE RESEARCH AND TECHNOLOGY

The Laboratory has continuously participated in space science and technology since the early years of rocketry, when V-2 and Aerobee rockets first carried particle detectors above the earth's atmosphere to measure primary cosmic rays. During the present period, Space Research activities were conducted principally by scientists in the Space Physics and Instrumentation Group of the Laboratory. Support for these activities came primarily from sponsors such as NASA, National Science Foundation, Office of Naval Research, and the Air Force Geophysics Laboratory. A small but important effort supported by IR&D funds has aimed at enhancing the research effectiveness and advancing state-of-the-art knowledge in these areas.

During the current period, the Space Research and Development effort has been directed toward an understanding of the chemical and physical processes involved in the earth's atmosphere, ionosphere, and magnetosphere and in solar-terrestrial and interplanetary phenomena. The objective has been to understand the total environment of the earth and the perturbing effects from both natural and man-made sources. APL scientists collaborated with scientists from over a dozen U.S. and international learned institutions, including the University of Tokyo, the Max-Planck Institutes in Lindau and Munich, West Germany, the Norwegian Defense Research Establishment, and the Canadian Department of Energy, Mines, and Resources. The results of these researches have been published in 15 articles in scholarly journals, with 17 more articles accepted or submitted for publication, and with presentation of 29 papers at various symposia and conferences.

Significant advances have included the first high-resolution measurements of electron energy spectra resulting from the photoionization of O and N_2 in the atmosphere; the discovery of unbalanced field-aligned currents in the polar regions that reach intensities of millions of amperes; the discovery of regions in the vast plasma reservoir behind the earth that can accelerate particles to millions of electron volts; the development of radio astronomy techniques for the prediction of geomagnetic storms that can produce disturbances to terrestrial radio transmission; and the development of thin-film scintillation detectors for the measurement of elemental composition and energy spectra of cosmic radiation in interplanetary space. Some of this work is described in the following short articles; the full scope of activity is indicated by the bibliography which follows the articles.

RADIO ASTRONOMY — INTERPLANETARY SCINTILLATION

Research activities during the present period have been aimed at the prediction of solar particle events and geomagnetic activity using interplanetary scintillation (IPS) observations from the University of Iowa COCOA-Cross radio telescope (Ref. 1). Preliminary analyses of particular IPS events (which indicate disturbances in the solar wind) revealed their relationship to ionospheric absorption (Ref. 2) as well as variations in solar energetic particle fluxes (Refs. 3 and 4). A comprehensive analysis of many IPS events has now been completed (Ref. 5), making use of daily measurements of scintillation index (m) from a grid of 45 sources taken June through December 1974. These sources are grouped into ten "sky-boxes" over the northern ecliptic hemisphere and are combined for each day with the m-value of the sources in each box into an IPS activity index Q_i ($i = 1, 2, ..., 10$). This new index, which ranges from 0 for no IPS to 2.0 for large IPS, is derived from a nonparametric statistical ranking analysis that compensates for the differences in brightness distributions among the sources. An example of the Q-analysis is shown in Fig. 1. In the upper panel, the Q_i are presented in grey tone (light, $0 \le Q < 2/3$; moderate, $2/3 \le Q \le 3/4$; and dark, $4/3 < Q \le 2$). The middle panel shows $\langle Q \rangle = 0.1\ \Sigma\ Q_i$, the "all-sky" IPS activity, as well as Q-averages for the eastern, western, and high-latitude portions of the northern ecliptic. The lower panel presents solar-terrestrial data: solar wind proton density (N) and velocity (V); interplanetary magnetic field (IMF) magnitude (B_{xy}) and direction (ϕ_{xy}) in the ecliptic; and the daily index (Ap) of geomagnetic activity. A statistical analysis shows that the cross-correlation function of $\langle Q \rangle$ with Ap shows a peak at a one-day lag, i.e., Ap disturbance follows $\langle Q \rangle$ enhancement by one day.

It is apparent that IPS respond when high-density structures in the solar wind sweep over the earth. This effect, although rather obvious, has not previously been discussed in the literature. On such days of "all-sky" IPS enhancements, IPS measurements probe only the local interplanetary environment. These occasional days, which are easily identified by the Q-analysis, are therefore omitted when studying distant solar wind structures. However, they establish convincingly that the scintillation index at 34.3 MHz is responding primarily to <u>density</u> (not velocity) enhancements in the solar wind. Thus, large area single-site systems, such as COCOA-Cross, can provide a probe for distant density structures, while smaller multisite systems can provide the complementary information on velocity structures.

During the period shown in Fig. 1 (November-December 1974), the COCOA-Cross source grid of sources was relatively insensitive to

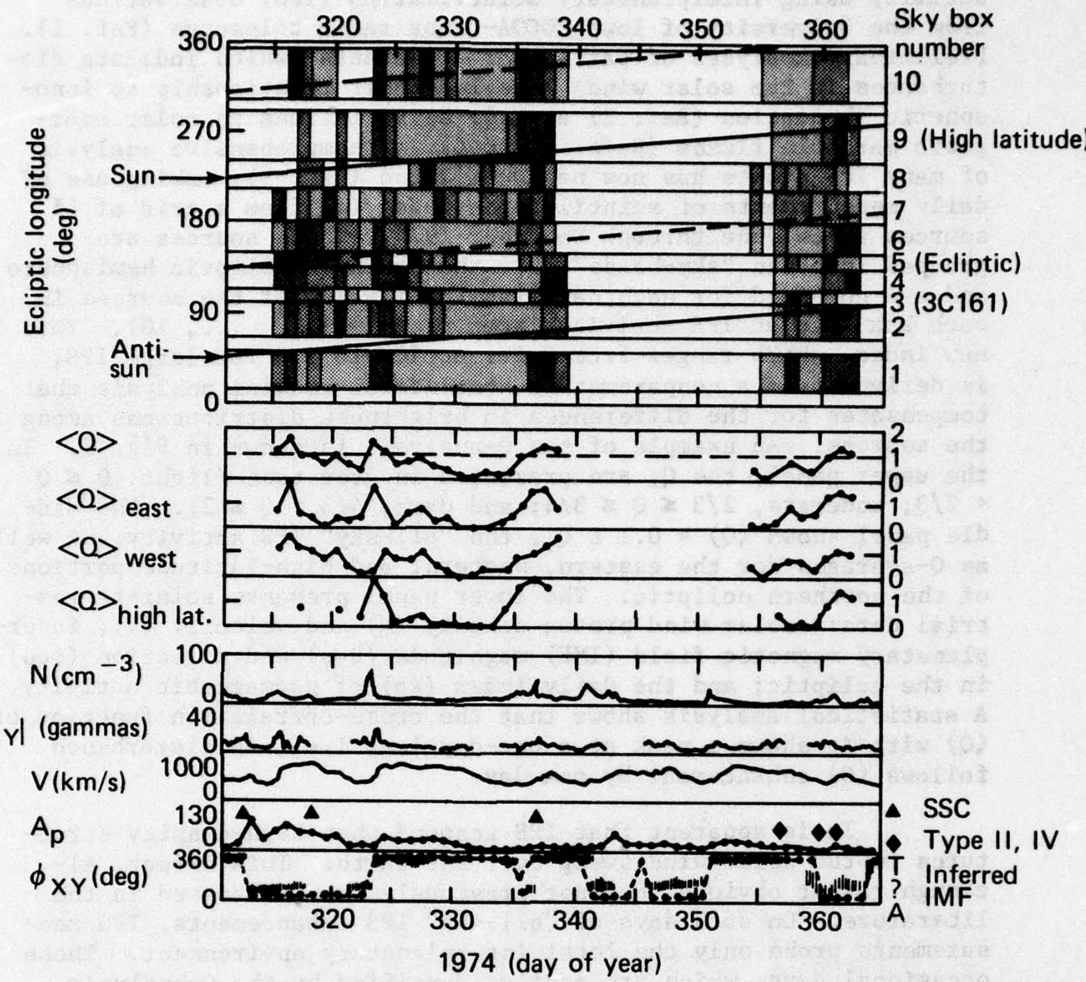

Fig. 1 Results of the Radio Source Clustering Analysis for 1974, Days 315-362

co-rotating disturbances approaching from the east, since the galactic plane (with its higher background emission) lies in this direction late in the year. Nonetheless, there is some evidence that such a disturbance was detected following the five days of very quiet interplanetary conditions preceding day 335. Moreover, it appears that plasma emission to the west of the sun was also detected.

The daily Q_1 indexes are shown in Fig. 2 for this period, as well as the locations of the ten sky-boxes. The sun is at 270° on 1 December in ecliptic coordinates where 0° is the direction of the vernal equinox. Sky-boxes 6, 7, and 8 viewing sources west of the sun all detect an IPS enhancement on days 332 and 333. At this time, the solar McMath plage region 13343 was west of central meridian and producing minor flare activity, so the IPS western activity appears to be plasma emitted from this region.

In the only sky-box (9) viewing east of the sun, there is an IPS enhancement on days 333 and 334 leading to sustained high scintillation on days 335 to 337 that drops abruptly on day 338. This sequence of activity corresponds nicely to the solar wind density structure that swept over the earth on days 335 to 337. It presumably would have been detected approaching from the east on days 333 to 334 and could no longer be viewed to the east on 338 (after passing earth). The western sources confirm this structure, since they do not fully respond until days 336 to 337. The suggested western plasma emission and eastern co-rotating density structure are sketched in Fig. 2.

Further comparison of the data will be made with geomagnetic and interplanetary measurements, both for their intrinsic content as well as to refine the analysis techniques for data available in 1975 and 1976. A basic tool for this work is the recent simplification of weak-scattering IPS theory (Ref. 6). Identification of the dominant role of solar wind density structures in IPS is an important step toward a reliable prediction technique.

References

1. W. M. Cronyn, S. D. Shawhan, F. T. Erskine, A. H. Huneke, and D. G. Mitchell, "Interplanetary scintillation observation with the COCOA-Cross radio telescope," J. Geophys. Res., Vol. 81, 1976, p. 695.

2. W. M. Cronyn, F. T. Erskine, S. D. Shawhan, B. L. Gotwols, and E. C. Roelof, "Prediction of ionospheric effects associated with solar wind disturbances using interplanetary scintillation observations at 34.3 MHz" in Effect of the Ionosphere on Space Systems and Communications, ed. J. M. Goodman, U.S. Government Printing Office, 1975, p. 223.

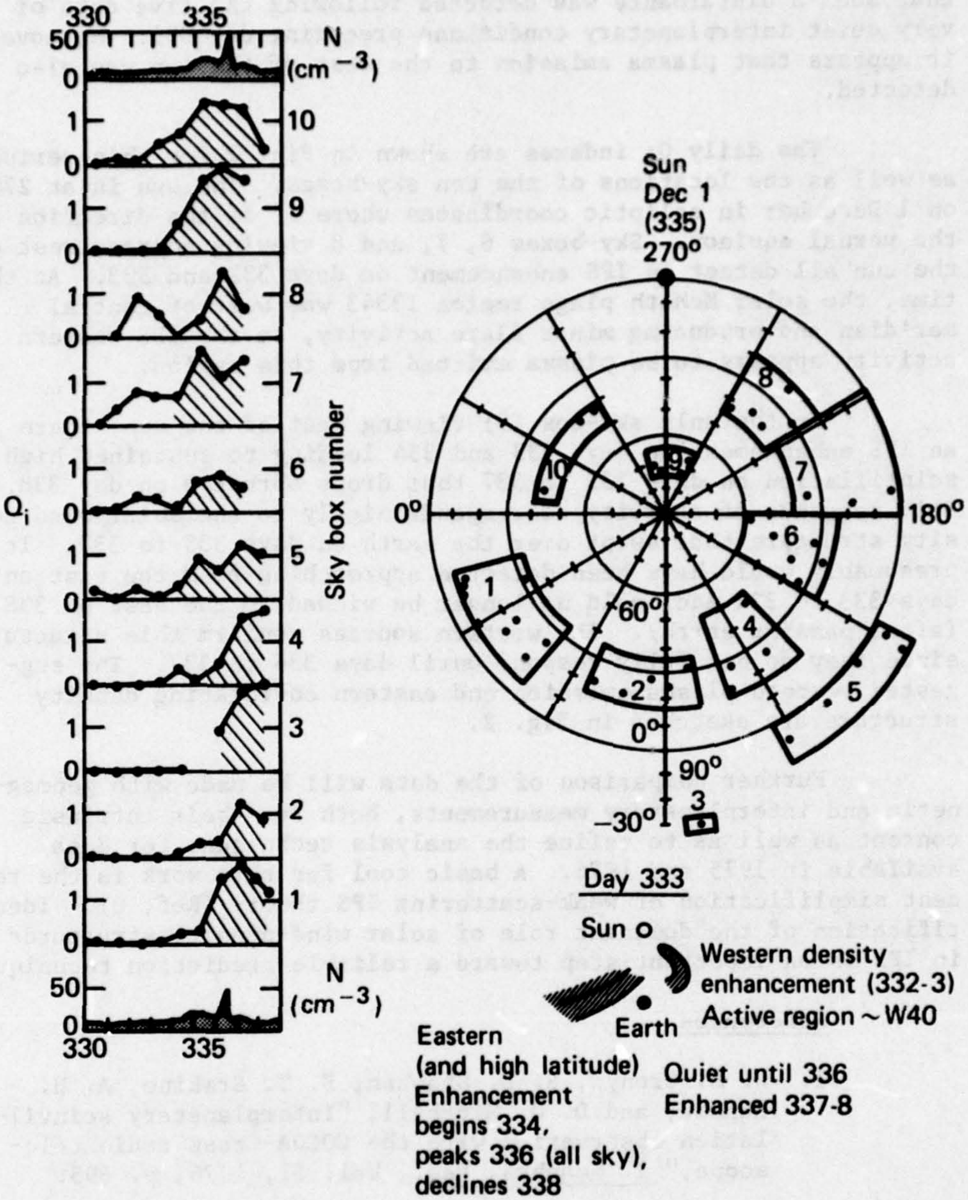

Fig. 2 IPS "Sky Box" Analysis for "Density Event" of 1974, Day 335

3. E. C. Roelof, S. M. Krimigis, W. M. Cronyn, S. D. Shawhan, and P. S. McIntosh, "Observation using interplanetary scintillation of the effect of a solar wind disturbance on a solar energetic particle event," Proc. 14th Int'l Cosmic Ray Conf. (Munich), Vol. 5, 1975, p. 1692.

4. E. C. Roelof, S. M. Krimigis, W. M. Cronyn, S. D. Shawhan, and P. S. McIntosh, "Solar wind and energetic particle events of June 20-30, 1974 analyzed using measurements of interplanetary radio scintillations at 34.3 MHz," Space Res. XVI, ed. M. J. Rycroft and R. D. Reasenberg, Akademie-Verlag (Berlin), 1976, p. 729.

5. F. T. Erskine, W. M. Cronyn, S. D. Shawhan, E. C. Roelof, and B. L. Gotwols, "Interplanetary scintillation at large elongation angles: Response to solar wind density structure," submitted to J. Geophys. Res., 1976.

6. D. G. Mitchell and E. C. Roelof, "A mathematical analysis of the theory of interplanetary scintillation in the weak-scattering approximation," J. Geophys. Res., Vol. 81 (in press), 1976.

FIELD-ALIGNED CURRENTS

Since its launch in September 1972, the Navy/APL TRIAD satellite has provided the only high-resolution vector magnetic measurements at low satellite altitudes (~ 800 km) for studies of auroral, ionospheric, and magnetospheric phenomena. The principal conclusions determined from studies of these data during this period include the following.

Large-scale field-aligned currents comprise a permanent feature in the high-latitude region and are concentrated in two principal areas encircling the geomagnetic pole, diagrammed in Fig. 1 (from Ref. 1): region 1 located near the poleward edge of the field-aligned current region and region 2 located near the equatorward part. The region 1 currents flow into the ionosphere in the morning sector and away from the ionosphere in the evening sector, whereas the region 2 currents flow in the opposite direction at any given local time. The region 1 currents appear to persist even during quiet geomagnetic conditions and dominate on the dayside, whereas the region 2 currents dominate on the nightside and are correlated with auroral electrojet intensification.

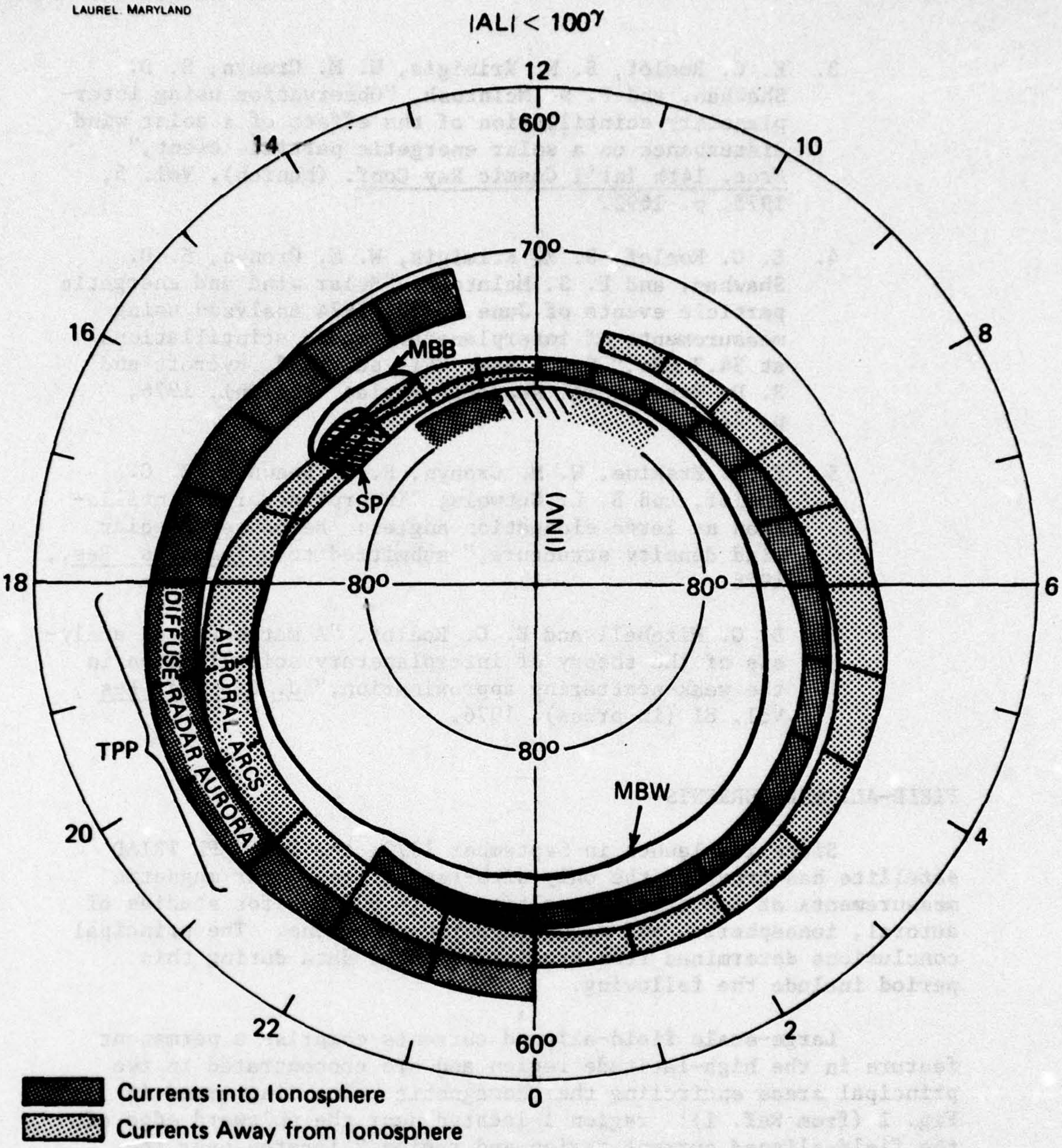

Fig. 1 Regions and Directions of Large-Scale Field-Aligned Currents Determined by Iijima and Potemra (1976 (Ref. 1 and 5)) with the Following Superimposed; (1) MBW, 35 keV Electron Background Boundary for Kp ≤ 3 from McDiarmid et al. (Ref. 3), (2) MBB Region of Peak 150 eV Electron Fluxes from McDiarmid et al. (Ref. 3), (3) SP Region of Most Probable Occurrence of Net Field-Aligned Current Directed Away from the Ionosphere from Sugiura and Potemra, and (4) TPP the Evening Region Studied with the Homer Radar and TRIAD Magnetometer Data from Tsunoda et al. (Ref. 4)

Net field-aligned currents, that is, regions where the current directed into the ionosphere is unequal to the current directed away from the ionosphere, have been discovered with the TRIAD satellite (Ref. 2). At any given magnetic local time (MLT), the current directions are the same as those determined earlier (Ref. 1), but the current intensity at the poleward edge of the auroral region (referred to as "region 1") is statistically larger than the oppositely directed current at the equatorward edge. The largest net current occurs statistically in the late afternoon near 1500 MLT. This region roughly agrees with the peak 150 eV electron intensities determined from ISIS-2 particle observations (Ref. 3).

Radar auroras observed with the 398-MHz phased-array radar located at Homer, Alaska, have been compared with field-aligned currents detected by TRIAD on an event-by-event basis in the 1800 to 2100 MLT sector (Ref. 4) (diagrammed in Fig. 1). The results of this study include

1. The downward field-aligned currents in the evening sector are closely associated with diffuse radar auroras and the eastward electrojet;

2. The upward field-aligned currents in the same time sector are associated with the visual aurora;

3. Part of the two oppositely directed field-aligned currents are connected in the ionosphere by a Pedersen current driven by a poleward-directed electric field applied across the field-aligned current region;

4. Radar auroral echoes are not observed when the field-aligned current intensity is less than ~ 0.16 amp/m, which may represent an important threshold current level for the physical process producing the auroral echoes; and

5. During periods of disturbed geomagnetic conditions an imbalance in the intensities of the field-aligned currents is noticeable in the evening sector, with the outward field-aligned current at the poleward boundary greater than the current at the equatorward boundary.

The final point supports the conclusions of Sugiura and Potemra (Ref. 2) and Iijima and Potemra (Ref. 1) concerning net field-aligned currents.

The location and directions of field-aligned currents in the cusp region are also shown in Fig. 1 (Ref. 5). The 35-keV

electron background boundary for $K_p \leq 3$ also shown in this figure (Ref. 6) has often been interpreted as the limit of closed field lines. If used in the same context here, this would imply that the large-scale field-aligned currents flow on closed field lines, whereas the cusp region field-aligned currents are associated with the magnetospheric boundary.

References

1. T. Iijima and T. A. Potemra, "The amplitude distribution of field-aligned currents at northern high latitudes observed by TRIAD," J. Geophys. Res., Vol. 81, 1976, pp. 2165-2174.

2. M. Sugiura and T. A. Potemra, "Net field-aligned currents observed by TRIAD," J. Geophys. Res., Vol. 81, 1976, pp. 2155-2164.

3. I. B. McDiarmid, J. R. Burrows, and E. E. Budzinski, "Average characteristics of magnetospheric electrons (150 eV to 200 keV) at 1400 km," J. Geophys. Res., Vol. 80, 1975, pp. 73-79.

4. R. T. Tsunoda, R. I. Presnell, and T. A. Potemra, "The spatial relationship between the evening radar aurora and field-aligned currents," J. Geophys. Res., Vol. 81, 1976, pp. 3791-3802.

5. T. Iijima and T. A. Potemra, "Field-aligned currents in the dayside cusp observed by TRIAD," J. Geophys. Res. (in press), 1976.

6. I. B. McDiarmid, J. R. Burrows, and M. D. Wilson, "Solar proton flux enhancements at auroral latitudes," J. Geophys. Res., Vol. 79, 1974, pp. 1099-1103.

NEW SATELLITE INSTRUMENTATION

A program of research is presently directed toward the detection and analysis of the energetic particle population in planetary magnetospheres and in interplanetary space. The experimental program involves measuring the elemental composition and energy spectrum of cosmic radiation using the advanced technique of three-parameter analysis (dE/dx, total energy, and time of flight). Past effort has included the development of thin-film scintillation detectors and the evolution of a three-parameter solid-state detector telescope (based on 2 μm-thick front elements) chosen for flight on

the Electrodynamics Explorer Satellite Mission. Present and future developmental efforts are increasingly based on using extremely thin foils ($\leqslant 10\ \mu g/cm^2$) as telescope front elements, with particle detection via analysis of secondary electrons emitted when incident particles penetrate the foil.

Figure 1 shows schematically an ion telescope that can measure particle fluxes above 30 keV with excellent elemental resolution over a very broad energy range. Ions incident through the collimator pass through a thin secondary emission foil ($\leqslant 10\ \mu g/cm^2$) and are detected in the *solid state detector* D2 (D3 is an anticoincidence detector that serves to reduce background count rates). Secondary emission electrons ejected from the foil are accelerated to a microchannel array plate that serves as a secondary electron detector, generating a fast timing signal coincident with the passage of the energetic ion, and both a fast timing signal (10-ns shaping time) and a slower energy signal are derived from D2. The telescope thus measures the particle's total energy and its time of flight over the 7.5-cm separation between the foil and D2. Incident ions can be uniquely characterized by these two independent parameters (energy and velocity). This instrument will be able to characterize the nucleonic component of the trapped radiation in terms of flux, energy spectra, pitch angle distribution, and elemental composition.

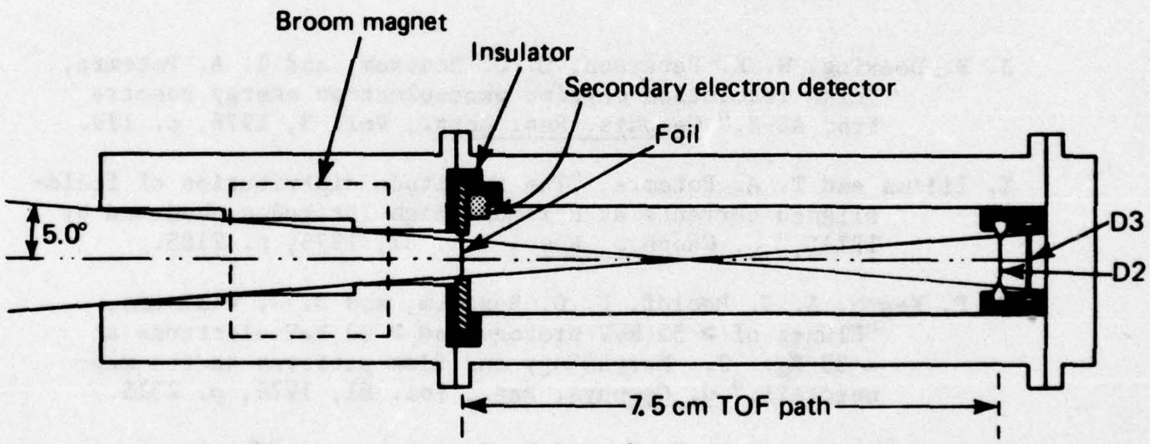

	Thickness	Area
Foil	$\leqslant 10\ \mu g/cm^2$	$15\ mm^2$
D2	$100\ \mu$	$25\ mm^2$
D3	$300\ \mu$	$50\ mm^2$

Fig. 1 Time of Flight (TOF) Ion Telescope

Principal Investigators: S. M. Krimigis, T. A. Potemra, E. C. Roelof, R. W. McEntire, B. L. Gotwols, R. E. Gold, E. P. Keath, T. Iijima, and E. T. Sarris. Dr. Krimigis is the Supervisor of the Space Physics Group and Associate Editor of the Journal of Geophysical Research; Drs. Potemra, Roelof, and McEntire and Mr. Gotwols are senior staff members. Dr. Gold is a postdoctoral research associate. Drs. Iijima and Sarris were postdoctoral fellows whose appointments expired in January and May 1976, respectively. Dr. Keath is serving as a postdoctoral associate through 1976.

PUBLICATIONS OF THE SPACE PHYSICS AND INSTRUMENTATION GROUP, 1 October 1975 to 30 September 1976

T. P. Armstrong and S. M. Krimigis, "Interplanetary acceleration of relativistic electrons observed with IMP-7," J. Geophys. Res., Vol. 81, 1976, p. 677.

W. M. Cronyn, S. D. Shawhan, F. T. Erskine, A. H. Huneke, and D. G. Mitchell, "Interplanetary scintillation observations with the COCOA-Cross radio telescope," J. Geophys. Res., Vol. 81, 1976, p. 695.

J. P. Doering, W. K. Peterson, C. O. Bostrom, and T. A. Potemra, "High resolution daytime photoelectron energy spectra from AE-E," Geophys. Res. Lett., Vol. 3, 1976, p. 129.

T. Iijima and T. A. Potemra, "The amplitude distribution of field-aligned currents at northern high latitudes observed by TRIAD," J. Geophys. Res., Vol. 81, 1976, p. 2165.

E. P. Keath, E. C. Roelof, C. O. Bostrom, and D. J. Williams, "Fluxes of $\geq$ 50 keV protons and $\geq$ 30 keV electrons at $\sim$ 35 R_e. 2. Morphology and flow patterns in the magnetotail," J. Geophys. Res., Vol. 81, 1976, p. 2315.

S. M. Krimigis, J. W. Kohl, and T. P. Armstrong, "The magnetospheric contributions to the quiet-time low energy nucleon spectrum in the vicinity of earth," Geophys. Res. Lett., Vol. 2, 1975, p. 457.

S. M. Krimigis, E. T. Sarris, and T. P. Armstrong, "Observations of Jovian electron events in the vicinity of earth," Geophys. Res. Lett., Vol. 2, 1975, p. 561.

D. G. Mitchell and E. C. Roelof, "A mathematical analysis of the theory of interplanetary scintillation in the weak-scattering approximation," J. Geophys. Res., Vol. 81, 1976, p. 5071.

E. C. Roelof, E. P. Keath, C. O. Bostrom, and D. J. Williams, "Fluxes of ≥ 50 keV protons and ≥ 30 keV electrons at ~ 35 R_e. 1. Velocity anisotropy and plasma flow in the magnetotail," J. Geophys. Res., Vol. 81, 1976, p. 2304.

E. C. Roelof, S. M. Krimigis, W. M. Cronyn, S. D. Shawhan, and P. S. McIntosh, "Solar wind and energetic particle events of June 20-30, 1974 analyzed using measurements of interplanetary radio scintillations at 34.3 MHz," Space Res. XVI, ed. M. J. Rycroft and R. D. Reasenberg, Akademie-Verlag (Berlin), 1976, p. 727.

E. T. Sarris, S. M. Krimigis, and T. P. Armstrong, "Observations of a high-energy ion shock spike in interplanetary space," Geophys. Res. Lett., Vol. 3, 1976, p. 133.

E. T. Sarris, S. M. Krimigis, and T. P. Armstrong, "Observations of magnetospheric bursts of high energy protons and electrons at ~ 35 R_e with IMP-7," J. Geophys. Res., Vol. 81, 1976, p. 2341.

E. T. Sarris, S. M. Krimigis, T. Iijima, C. O. Bostrom, and T. P. Armstrong, "Location of the source of magnetospheric energetic particle bursts by multispacecraft observations," Geophys. Res. Lett., Vol. 3, 1976, p. 437.

M. Sugiura and T. A. Potemra, "Net field-aligned currents observed by TRIAD," J. Geophys. Res., Vol. 81, 1976, p. 2155.

R. T. Tsunoda, R. I. Presnell, and T. A. Potemra, "The spatial relationship between the evening radar aurora and field-aligned currents," J. Geophys. Res., Vol. 81, 1976, p. 3791.

PAPERS ACCEPTED FOR PUBLICATION,
1 October 1975 to 30 September 1976

T. P. Armstrong, S. M. Krimigis, D. Hovestadt, B. Klecker, and G. Gloeckler, "Observations of temporal and spatial variations in the Fe/O charge composition of the solar particle event of July 4, 1974," Solar Phys., in press 1976.

J. P. Doering, T. A. Potemra, W. K. Peterson, and C. O. Bostrom. "Characteristic energy spectra of 1-500 eV electrons observed in the high latitude ionosphere from Atmosphere Explorer-C," J. Geophys. Res., in press 1976.

F. T. Erskine, W. M. Cronyn, S. D. Shawhan, E. C. Roelof, and B. L. Gotwols, "Interplanetary scintillation at large elongation angles: Response to solar wind density structure," J. Geophys. Res., submitted 1976.

R. E. Gold, B. L. Gotwols, S. M. Krimigis, and E. C. Roelof, "Propagation of relativistic Jovian electrons to Earth," J. Geophys. Res., submitted 1976.

R. E. Gold and E. C. Roelof, "Inference of the equatorial high coronal magnetic field polarity from interplanetary measurements," Solar Phys., submitted 1976.

R. E. Gold and E. C. Roelof, "Propagation of relativistic Jovian electrons to Pioneer 10 and 11 via solar wind stream-stream interaction regions," J. Geophys. Res., in press 1976.

T. Iijima and T. A. Potemra, "Field-aligned currents in the dayside cusp observed by TRIAD," J. Geophys. Res., in press 1976.

T. R. Larsen, T. A. Potemra, W. L. Imhof, and J. B. Reagan, "Energetic electron precipitation and VLF phase disturbances at mid-latitudes following the magnetic storm of 16 December 1971," J. Geophys. Res., submitted 1976.

J. T. Nolte, A. S. Krieger, E. C. Roelof, and R. E. Gold, "High coronal structure of high velocity solar wind streams," Solar Phys., in press 1976.

J. T. Nolte, A. S. Krieger, A. F. Timothy, R. E. Gold, E. C. Roelof, G. Vaiana, A. J. Lazarus, J. D. Sullivan, and P. S. McIntosh, "Coronal holes as sources of solar wind," Solar Phys., in press 1976.

J. T. Nolte and E. C. Roelof, "Statistical analysis of coronal magnetic structure during the first year of solar cycle 20," Solar Phys., in press 1976.

W. K. Peterson, J. P. Doering, T. A. Potemra, R. W. McEntire, C. O. Bostrom, R. A. Hoffman, R. W. Janetzke, and J. L. Burch," Observations of 10 eV to 25 keV electrons in steady diffuse aurora from Atmosphere Explorers C and D," J. Geophys. Res., in press 1976.

T. A. Potemra, W. K. Peterson, J. P. Doering, C. O. Bostrom, R. W. McEntire, and R. A. Hoffman, "Low energy particle observations in the quiet dayside cusp from AE-C and AE-D," J. Geophys. Res., submitted 1976.

E. C. Roelof, "Solar particle emission," Proc. of the Intern'l Symp. on Solar-Terrestrial Phys., ed. D. J. Williams, NOAA/ERL, in press 1976.

E. C. Roelof, R. E. Gold, and E. P. Keath, "Evaluation of a prediction technique for low energy solar particle events," Space Res. XVII, ed. M. J. Rycroft and R. D. Reasenberg, Akademie-Verlag (Berlin), submitted 1976.

E. C. Roelof, E. P. Keath, and T. Iijima, "Fluxes of > 30 keV electrons at $\sim 35\ R_e$. 4. Association of intense bursts of energetic particles in the magnetotail with the expansion phase of geomagnetic substorms," J. Geophys. Res., Vol. 81, in press 1976.

E. T. Sarris, S. M. Krimigis, C. O. Bostrom, and T. P. Armstrong, "Simultaneous multispacecraft observations of energetic proton bursts inside and outside the magnetosphere," J. Geophys. Res., submitted 1976.

PRESENTATIONS OF THE SPACE PHYSICS AND INSTRUMENTATION GROUP, 1 October 1975 to 30 September 1976

The following were presented at the Fall Annual Meeting of the American Geophysical Union, San Francisco, December 1975.

J. P. Doering, T. A. Potemra, W. K. Peterson, and C. O. Bostrom, "Detailed observations of low energy electrons in the north and south high latitude regions from AE-C."

B. L. Gotwols, E. C. Roelof, W. M. Cronyn, F. T. Erskine, and S. D. Shawhan, "Statistical analysis of variations in interplanetary radio scintillation indices at 34.3 MHz."

T. Iijima and T. A. Potemra, "Field-aligned currents in the dayside cusp regions observed by TRIAD."

E. P. Keath, E. C. Roelof, C. O. Bostrom, and D. J. Williams, "Correlation of ≥ 50 keV proton and ≥ 30 keV electron events in interplanetary space, the magnetosheath, and the magnetotail at 35 R_e."

D. G. Mitchell and E. C. Roelof, "Parameterization of weak scattering theory for interplanetary radio scintillations for finite angular diameter sources."

T. A. Potemra and T. Iijima, "The correlation of high-latitude field-aligned currents with the geomagnetic S_q^p field and the interplanetary magnetic field."

E. C. Roelof and E. P. Keath, "Magnetic field line merging signatures in 50 keV proton events."

The following were presented at the Spring Annual Meeting of the American Geophysical Union, Washington, DC, April 1976.

C. O. Bostrom, E. T. Sarris, S. M. Krimigis, T. Iijima, and T. P. Armstrong, "Location and characteristics of the source of magnetospheric energetic particle bursts in the vicinity of the neutral sheet by multispacecraft observations."

J. P. Doering, W. K. Peterson, C. O. Bostrom, and T. A. Potemra, "New high energy resolution measurements of the daytime photoelectron energy spectrum from Atmosphere Explorer-E."

R. E. Gold, S. M. Krimigis, and E. C. Roelof, "The predominance of spatial structures in low energy particle events 1972-1974."

B. L. Gotwols, R. E. Gold, S. M. Krimigis, and E. C. Roelof, "Association at 1.0 and 4.5 AU of Jovian electron events with solar wind streams."

T. Iijima and T. A. Potemra, "Large scale characteristics of field-aligned currents associated with substorms."

E. P. Keath, T. Iijima, and E. C. Roelof, "Association of high intensity bursts of $\sim$50 keV protons and electrons in the dusk plasmasheet near 35 R_e with substorm intensification of the westward auroral electrojet."

J. W. Kohl, S. M. Krimigis, T. P. Armstrong, and R. Lepping, "A magnetosheath burst of predominantly medium nuclei observed with Explorer 50."

S. M. Krimigis, E. T. Sarris, and T. P. Armstrong, "Evidence for closed magnetic loop structures in the interplanetary medium."

V. L. Patel, R. J. Greaves, S. A. Wahab, and T. A. Potemra, "Correlated micropulsation events in the magnetosphere and surface observations."

W. K. Peterson, J. P. Doering, T. A. Potemra, and C. O. Bostrom, "Observations of low energy (0-500 eV) electrons in the polar region from AE-D."

T. A. Potemra, C. O. Bostrom, J. P. Doering, and W. K. Peterson, "Weak acceleration processes in the auroral ionosphere inferred from AE-C low energy (0-500 eV) electron observations."

E. C. Roelof, R. E. Gold, S. M. Krimigis, and P. S. McIntosh, "Association of a nearly identical recurrent event of ~ 1 MeV He nuclei with coronal magnetic structure over 5 solar rotations."

E. T. Sarris, C. O. Bostrom, and T. Aggson, "Evidence on the acceleration of energetic protons by sporadic DC electric fields in the plasma sheet."

M. Sugiura, T. Iijima, and T. A. Potemra, "Characteristics of field-aligned currents as determined from the TRIAD magnetometer observations."

The following were presented at the International Symposium on Solar-Terrestrial Physics, Boulder, Colorado, June 1976.

R. E. Gold, S. M. Krimigis, and E. C. Roelof, "Energy, rigidity and charge-independent solar particle events 1972-1974."

R. E. Gold, B. L. Gotwols, S. M. Krimigis, and E. C. Roelof, "Relationship between Jovian electron events and solar wind streams at 1.0 and 4.5 AU."

B. L. Gotwols, R. E. Gold, D. G. Mitchell, E. C. Roelof, W. M. Cronyn, F. T. Erskine, and S. D. Shawhan, "Interplanetary radio scintillation spectra observed at 34.3 MHz and turbulence in the solar wind."

S. M. Krimigis, E. T. Sarris, and T. P. Armstrong, "Evidence for closed magnetic loop structures in the interplanetary medium."

W. K. Peterson, J. P. Doering, T. A. Potemra, and C. O. Bostrom, "Observation of low energy (0-500 eV) electrons in the polar region from AE-C and AE-D: Identification of the dayside cusp."

T. A. Potemra and T. Iijima, "Characteristics of large scale field-aligned currents: Possible source mechanisms."

E. T. Sarris, S. M. Krimigis, T. Iijima, C. O. Bostrom, and T. P. Armstrong, "Location and characteristics of the source of magnetospheric energetic particle bursts in the vicinity of the neutral sheet by multispacecraft observations."

M. Sugiura and T. A. Potemra, "Variability of the field-aligned currents deduced from the TRIAD magnetometer observations."

SATELLITE-AIDED SEARCH AND RESCUE SYSTEM

In response to an informal request from NASA Headquarters, the Space Development Department carried out a feasibility study for a satellite system to identify and locate emergency radio beacons required to be carried on aircraft and ships.

All aircraft and certain marine vessels are required to carry emergency radio beacons that are activated automatically (e.g., on impact) or manually. They radiate at 121.5 MHz and/or 243 MHz and are usually amplitude modulated with a swept tone between 300 and 1600 Hz (sweep rate ~ 2 to 4 Hz). There are upwards of 50 models of these Emergency Locater Transmitters (ELT's) on the market which vary considerably in performance and specifications. It is generally agreed that ELT's are a significant aid in search and rescue operations. The basic problem in realizing the full capability of the ELT is that of detection and location. At present, the principal listeners are commercial airline pilots (on a voluntary basis). Without direction finding equipment, they can locate an ELT only within a 300-mile radius (280 000 square mile area). A satellite-borne ELT detection system appears to offer the most cost-effective means of routine monitoring of the emergency bands over large (perhaps global) areas and can provide relatively precise position determination through Doppler navigation.

The preliminary study carried out by the Laboratory examined all aspects of a satellite-aided search and rescue program. From a systems viewpoint, improvement is needed in all areas, much of which will have to come through regulation, education, standards, and enforcement. The APL study first addressed the requirements and objectives of an operational system including orbit and constellation tradeoffs; ground station equipment and network; the use of transponders and on-board processing of data; estimates of detection times and position determination accuracy for existing and improved ELT's; and a conceptual design of an operational spacecraft including subsystem performance requirements.

Based on this operational concept, a preliminary design of a satellite was developed to demonstrate the key features of an operational system and to investigate some of the uncertainties in the system, particularly in the area of radio frequency interference and traffic on the emergency frequencies. The proposed design assumed the use of an existing Transit satellite as a "bus" which contains many of the basic subsystems, to which is added an instrument module consisting of an antenna array, a multichannel bent-pipe transponder, a demonstration onboard processor, and

other mission-unique subsystems. The design was carried out to a level of detail sufficient to make reliable weight and power estimates and to develop a preliminary schedule and cost plan.

The orbital configuration of the satellite is shown in Fig. 1, and the antenna footprints on the earth's surface are shown in Fig. 2.

The ground station was designed to be self contained and portable in order to allow study of radio frequency interference in various parts of the world and to permit operational use of the demonstration satellite following a period of testing and software development. Many detailed studies were conducted, such as the careful evaluation of two current models of ELT's. A visit to the Air Force Rescue Coordination Center (RCC) provided some appreciation of the real problems faced by this group and of the potential benefits of a satellite-aided search and rescue system.

The results of the APL study were presented to NASA representatives at Goddard Space Flight Center in May 1976. This was followed by a letter from NASA to the Navy Strategic Systems Projects Office and a subsequent meeting to explore the availability of a Transit satellite for use in this program. NASA has also looked into installing a simpler system on existing operational weather satellites, and the final program may well be international since Canada has a strong interest in this problem and has been studying it independently.

Investigators: The study was carried out by the staff of the Space Development Department. It was coordinated by C. O. Bostrom, Chief Scientist, and R. E. Fischell, Chief Engineer.

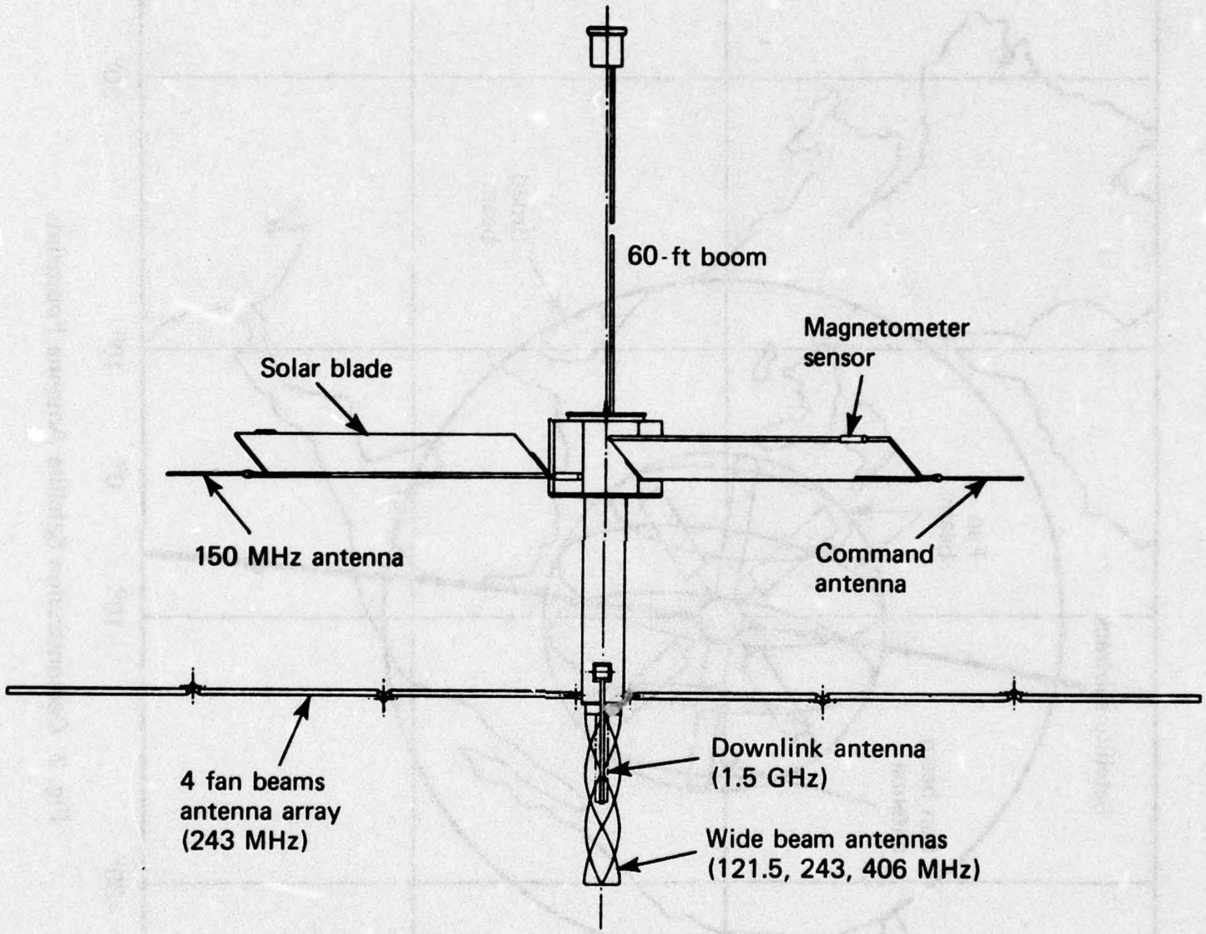

Fig 1 SOS Orbital Configuration (elevation)

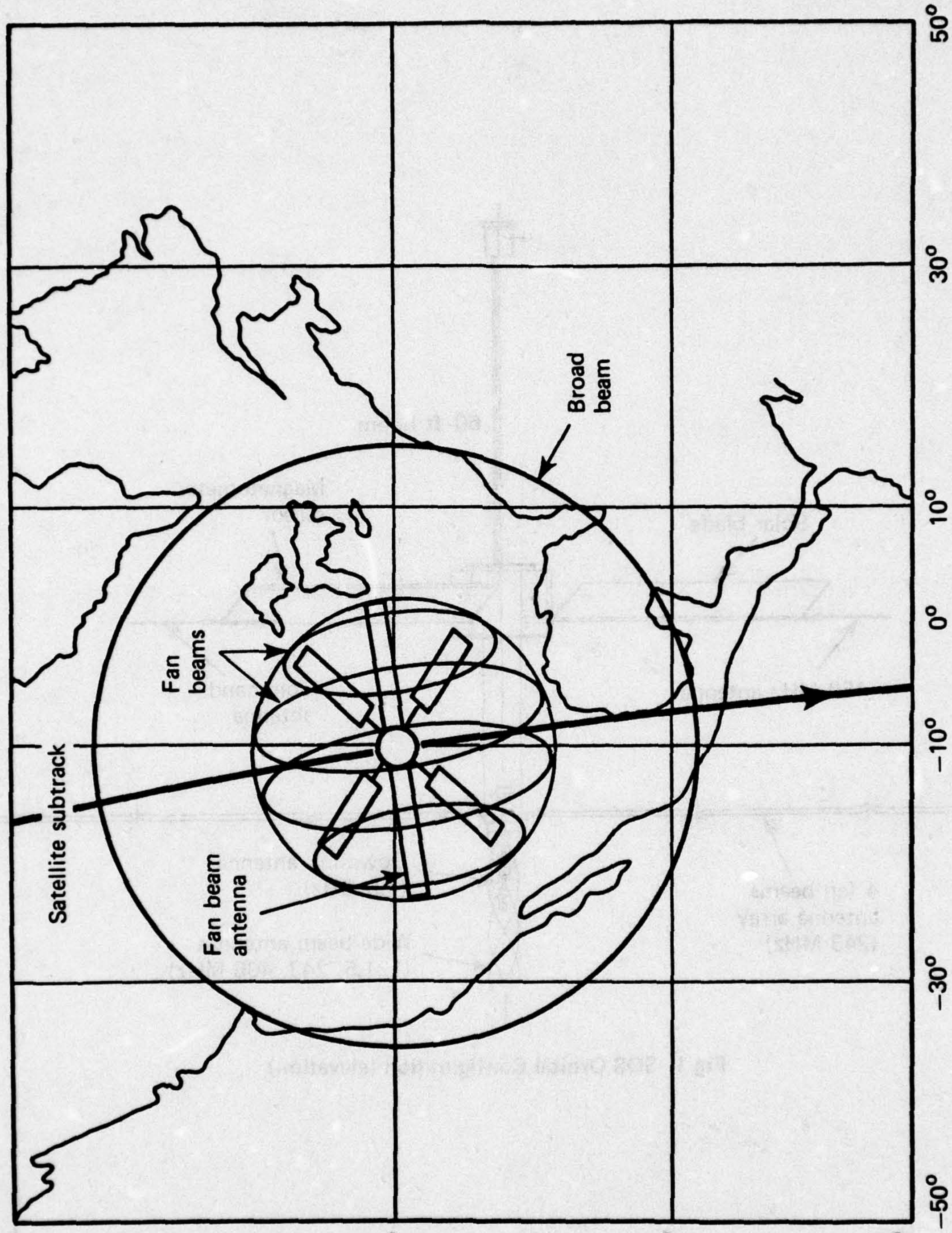

Fig. 2 Demonstration Satellite Antenna Footprints

GLOBAL POSITIONING SYSTEM PACKAGE

The Applied Physics Laboratory is developing the Global Positioning System Package (GPSPAC) for the Defense Mapping Agency (DMA) to provide real-time position fixes aboard a near-earth satellite host vehicle, using signals received from the GPS Navigation Satellite Tracking and Ranging Global Positioning System (NAVSTAR) constellation of satellites. GPSPAC will consist of a receiver/processor assembly (R/PA), being procured from Magnavox, plus a stable oscillator and an antenna/preamplifier assembly which APL will design, fabricate, and test. GPSPAC will also interface with the power, command, telemetry, thermal, and mechanical systems of the host vehicle; APL will provide support in these areas.

The GPSPAC program began with a study of the feasibility of designing a navigation set that would be flown on a host near-earth spacecraft and would use the NAVSTAR GPS signals to compute the host vehicle position and velocity. The study concluded with the issuance of a study report (Ref. 1) that established the feasibility of the concept.

Effort was then directed at determining suitable contractors, involved in other GPS-related work, who might be requested to bid on the design and development of an R/PA. Effort was expended toward this end in the preparation of a specification describing the proposed operation of the R/PA.

Work following March 1976 has been funded by DMA and is not reported here.

Investigators: The study was carried out by the staff of the Space Development Department under the general direction of Mr. R. W. Larson, Manager of the Space Development Programs.

Reference

1. "Study Report: Combined NAV/GPSPAC Spaceborne Navigation Set," APL/JHU, Space Development Department Report SDO 4221, September 1975.

SUPPORT OF BIOMEDICAL ENGINEERING PROGRAMS

During the past year, five exploratory programs in biomedical engineering were carried out with the help of IR&D funds. An important advance in intracranial pressure sensing has been made, with the design of a device that promises to alleviate problems of reference pressure stability; four units have been constructed and are currently undergoing evaluation in test animals. After projecting the medical information processing needs of the Cancer Center of the Johns Hopkins Hospital, we designed and estimated the cost of a computer system to meet these needs. Pilot support was also obtained for studies of echocardiography of heart wall motion. The fourth and fifth projects were of extremely limited scope; one explored the feasibility of developing a prototype endotracheal tube, and the other supported the preparatory work for an NIH site visit concerned with a proposed Specialized Center of Research in Arteriosclerosis.

INTRACRANIAL PRESSURE MEASUREMENT

The intracranial pressure transsensor previously developed at APL compares cranial pressure to that of an entrapped volume of gas contained within the transsensor itself. The output of this device must be corrected for barometric pressure changes as well as changes in body temperature.

A new type of pressure transsensor has now been developed that measures intracranial pressure more directly by comparing the pressure within the cranium to that immediately outside the skull. This implant has no internal air entrapment and, therefore, no problem of long-term pressure stability. It is also insensitive to barometric pressure and body temperature changes. It is a Lexan cylinder, both ends of which are very thin and capable of transmitting a pressure to the interior of the element with essentially no attenuation. The silicone-oil-filled region within this plastic enclosure is separated into two noncommunicating compartments by a single nickel bellows. As in the case of the previous transsensor, the bellows forms a pressure-sensitive capacitance in a passive circuit whose natural frequency is a function of pressure. The gauge pressure transsensor is mounted in the plane of the skull with one end resting against the dura while the other end is exposed to the subscalp pressure outside the cranium. In this way, the deflection of the bellows is a direct measure of intracranial pressure.

Four gauge pressure transsensors are currently implanted in dogs to determine the length of time that the subscalp pressure

as seen by the outer end of the implant is an acceptable representation of atmospheric pressure.

THE JOHNS HOPKINS CANCER CENTER COMPUTER SYSTEM

A computer system design and funding estimate was prepared for the Cancer Center, which is presently under construction as an addition to the Johns Hopkins Hospital. An examination of the new center's medical information processing needs was carried out and then translated into a computer system designed to automate most of the manual processes. Such areas as doctors' orders, medication logs and schedules, the Cancer Center pharmacy, patient data, supply management, research functions, and interconnection with other computers in the hospital were addressed. A series of working papers were produced and used for a presentation to the Cancer Center management and the Department of Biomedical Engineering.

ECHOCARDIOGRAPHY OF ARTERIAL WALL MOTION

In collaboration with Dr. James Weiss, Frank T. McClure Fellow in Cardiology and Assistant Professor of Cardiovascular Medicine at the Johns Hopkins Medical Institutions (JHMI), echocardiographic data were obtained on both volunteers and patients under exercise conditions, and data processing techniques were developed to quantify left ventricular wall motions. In addition, experiments have been conducted to define appropriate processing techniques for a phased-array cardiac scanning system which will be in operation at JHMI in October 1976. A paper entitled "Evidence of Frank-Starling Effect in Man During Maximal Semisupine Exercise" will be presented at the 49th Scientific Session of the American Heart Association in November 1976.

Principal Investigators: J. G. Chubbuck (intracranial pressure measurement), R. B. McDowell (Cancer Center computer system), and J. B. Garrison (echocardiography). Mr. Chubbuck is a senior engineer and Supervisor of the Medical Systems Section of the Control Systems Group in the Fleet Systems Department. Mr. McDowell is the Group Supervisor of the Computer Engineering Group of the McClure Computing Center. Dr. Garrison is a senior physicist on the Director's staff.

COMPUTER-AIDED HEMODYNAMIC MONITORING UNIT

A small effort was devoted to completing the design and preliminary cost estimate for fabricating a portable computer-aided hemodynamic monitoring unit. The effort was initiated during the last reporting period as an outgrowth of the computerized hemodynamic monitoring system developed by the Laboratory for the Myocardial Infarction Research Unit (MIRU).

Upon completion of preliminary design and the identification of several physicians interested in performing clinical trials of such units in a variety of clinical environments, cost estimates for farbicating from one to four units were made. At that time, it was found that industry was initiating similar studies, that there was considerably less need for exploration efforts, or for demonstration of the units' clinical usefulness, and that accordingly it was difficult to justify the commitment of clinical staff and resources to complete clinical trials with such units not directly related to a commercial prototype. Accordingly, this effort has been terminated with the conclusion that industry shows promise of meeting this need adequately.

OCEAN THERMAL ENERGY SYSTEM

For several years the Laboratory has been engaged in exploring ocean thermal energy conversion as a promising means of utilizing solar energy, primarily through investigations supported by ERDA and the Maritime Administration. During these investigations, technological questions were uncovered for which the support allowed no expenditure of effort to obtain answers. One such question concerns stratification of flow and its effects in OTEC heat exchangers. During the present year, an IR&D project investigated a stratification problem experimentally and found that satisfactory results could be obtained provided that the heat exchanger tubes are slightly tilted.

The tropical oceans develop a temperature difference of about 40°F between the sun-warmed surface waters and the cold water at depth returning from melting arctic ice. OTEC makes use of this stored solar energy temperature gradient to operate a closed Rankine cycle engine for the production of electric power, which, in turn, may be used to manufacture ammonia, aluminum, hydrogen, and other energy-intensive products, resulting in a large saving in energy now required from other sources. Previous reports have described the initiation of the work at APL, the results of two projects sponsored by ERDA, one supported by the Maritime Administration (MARAD), and indirectly funded (IR&D) exploratory investigations. Through this work, and through contributed cooperative effort from Sun Shipyard and Drydock Company, Kaiser Aluminum and Chemical Corporation, Teledyne Corporation, Hydronautics, and other industrial organizations, the Laboratory has achieved a leading position in the OTEC field.

The design of heat exchangers for OTEC systems poses several problems that are different from those usually encountered. For example, the relatively small temperature difference between surface water and deep water falls below the range for which experimental data are available to predict performance. Moreover, since the ocean's thermal energy is available at no intrinsic cost, OTEC heat exchangers are to be optimized for overall plant cost rather than maximum heat transfer efficiency. At the beginning of the present period, a study of least-cost heat exchanger design was completed for ERDA (Ref. 1) based on extrapolations of empirical correlations. The resultant design proposes ammonia as the working fluid and calls for heat exchangers using large diameter aluminum tubes with horizontal tube runs folded in a vertical plane and operating in parallel with similar tube elements to produce piping cover for both the evaporator and condenser. This design allows removal of individual segments for cleaning, repair, or replacement. Figure 1 shows a power module based on this design principle. The

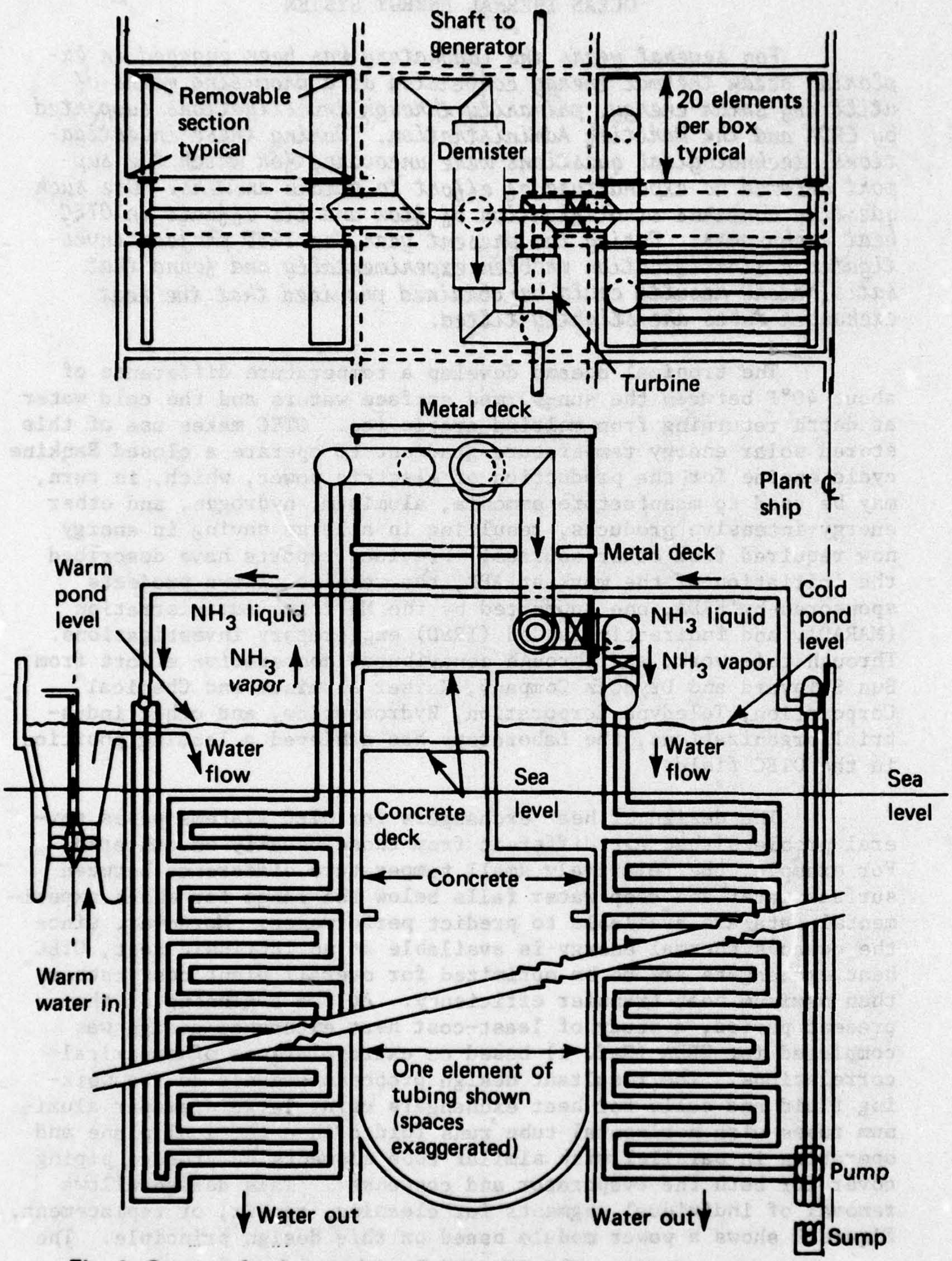

Fig. 1 Concept for Integrating a 5-MW_e (Net) Power Module with Heat Exchangers Made of Nested, Large-Diameter, Multipass Aluminum Tubes with a Modular, Barge-Type Platform for OTEC Plant-Ships

comprehensive study provides the analytical basis from which a rational design of OTEC heat exchangers can be derived.

The correlations used in Ref. 1 were obtained by extrapolation from the literature, where they were generally derived from experiments on smaller diameter tubes, higher temperature differences, and different working media than those proposed for the OTEC heat exchangers. These extrapolated correlations led to quite attractive initial performance estimates, justifying the validity of the APL design approach. Before the analysis could be trusted for actual equipment design considerations, however, it would be necessary to confirm the applicability of the correlations to OTEC conditions, and this could only be done by direct experimentation. Consequently, ERDA sponsored experiments (Refs. 2 and 3) on the two-phase flow of ammonia inside a single horizontal tube with the objective of measuring the overall ammonia-side heat-transfer coefficients for comparison with predicted analytical correlations.

Initial tests revealed significant discrepancies with predicted behavior, and the present IR&D project was initiated to uncover the cause. The explanation was traced to stratification or intermittent flow which occurs to some extent under all conditions appropriate to OTEC. A simple remedy was found by slightly tilting the system by 0.5° or less. Remaining stratification in the tilted configuration does not reduce the overall tube heat transfer greatly, and the Chaddock and Brunneman correlation (used in Ref. 1) was found to predict the two-phase heat-transfer coefficients for ammonia with acceptable precision. However, the stratification flow phenomena should be characterized in more detailed tests at design and off-design operating conditions, which can be done with the existing internal-flow test apparatus by replacing some instrumentation. Also, the occurrence of nucleation in the subcooled flow should be characterized in more detail, especially with respect to the point where it begins. This will require some additional instrumentation. Overall, the IR&D effort has assisted the ERDA-funded program in providing demonstration of generally satisfactory heat exchanger operation in a hitherto unexplored regime.

The IR&D program also contributed to the dissemination of results. Two additional reports on OTEC heat exchangers have been written — Ref. 4, describing the current expected design of the heat exchangers for a plant ship, and Ref. 5, on two-phase-flow heat transfer.

<u>Principal Investigators</u>: H. L. Olsen and R. A. Makofski. Dr. Olsen is a senior engineer on the staff of the Aeronautics Division Office and Mr. Makofski is Group Supervisor of the Transportation Technology Group in the Aeronautics Division.

References

1. H. L. Olsen and P. P. Pandolfini, "Analytical Study of Two-Phase-Flow Heat Exchangers for OTEC Systems," APL/JHU AEO-76-37, November 1975.

2. "Contract N00017-72-C-4401; Technical Program Statement and Cost Estimates for Experimental Studies of Two-Phase-Flow Heat Exchangers for OTEC Systems," APL/JHU AD-6566, 8 January 1976.

3. H. L. Olsen, P. P. Pandolfini, and J. L. Rice, "Internal Heat Transfer Experiments in a Simulated OTEC Evaporator Tube," APL/JHU AEO-76-066, November 1976.

4. H. L. Olsen, P. P. Pandolfini, R. W. Blevins, G. L. Dugger, and W. H. Avery, "Design of Low-Cost Aluminum Heat Exchangers for OTEC Plant Ships," Sharing the Sun Conference, International Solar Energy Society, Winnipeg, Canada, 15-20 August 1976.

5. P. P. Pandolfini, H. L. Olsen, and R. A. Makofski, "Two-Phase-Flow Heat Transfer in Large Diameter Tubes for OTEC," presented at the Two-Phase-Flow and Heat Transfer Symposium-Workshop, 18-20 October 1976, Fort Lauderdale, FL.

COPPER SULFIDE/CADMIUM SULFIDE SOLAR CELLS

Copper sulfide/cadmium sulfide (Cu_2S/CdS) solar cells are potentially important in terrestrial photovoltaic applications due to their ease of fabrication and low cost. Proper encapsulation and empirical optimization of processing methods have done much to improve cell stability and lifetime. Efficiencies of these cells, however, are still low. Important parameters necessary for more complete physical and theoretical understanding and hence improvement in efficiency of the Cu_2S/CdS system include the junction depth (Cu_2S lateral penetration into the CdS columnar grains) and the depth of Cu_2S penetration down the CdS grain boundaries. Sputter-ion source mass spectrometer (SIMS) profiles have been interpreted using a two-component sputtering model to yield estimates of these two properties.

In the current work, prior results on three typical Cu_2S/CdS solar cell samples were reanalyzed. The samples included: (a) an as-deposited CdS layer (No. 1), (b) a Cu_2S/CdS specimen (No. 2) removed immediately following the topotaxial growth of the Cu_2S layer (barrier formation) by dipping in a solution of Cu_2Cl_2, and (c) a Cu_2S/CdS specimen (No. 3) subjected to a simulated grid-ding and encapsulation (lamination) process.

The SIMS beam (defocused beam of 10 keV Ar^+ ions) produces a large flat crater (2 × 3 mm), and the constituent intensity versus time data arise from a constant surface regresstion. Scanning electron microscope (SEM) analysis showed that the original surface topography was essentially preserved after the removal of ~ 9 m, dispelling fears of preferential sputtering. Since a large-area, homogeneous beam was used, the resulting profiles represent the average of approximately 10^6 grains (SEM grain size: 1 to 3 μm). Minor variations in the profiles result from a finite depth resolution (~5%), shadowing from asperities, and instrument memory.

Figure 1 is a linear plot of the surface fraction (Ref. 1) of Cu and Cd versus depth (below the film surface) for sample No. 2. Conversion to depth (from the original intensity time plots) has been made assuming that Cu_2S and CdS sputter at essentially the same rate and that the yield factors for Cu (and S) from Cu_2S and for Cd (and S) from CdS are independent of depth, a two-component sputtering model. This model requires a consistent sulfur stoichiometry (with depth) for validity. Anomalies in the sulfur stoichiometry in a depth range from 0.2 to 2 μm (broad "junction" region) were noted previously (Ref. 2). These variations can be as high as 15%, suggesting the possibility of another constituent such as CdO or the inclusion of debris from the dipping process at the grain boundary-surface intersection point. The importance of these

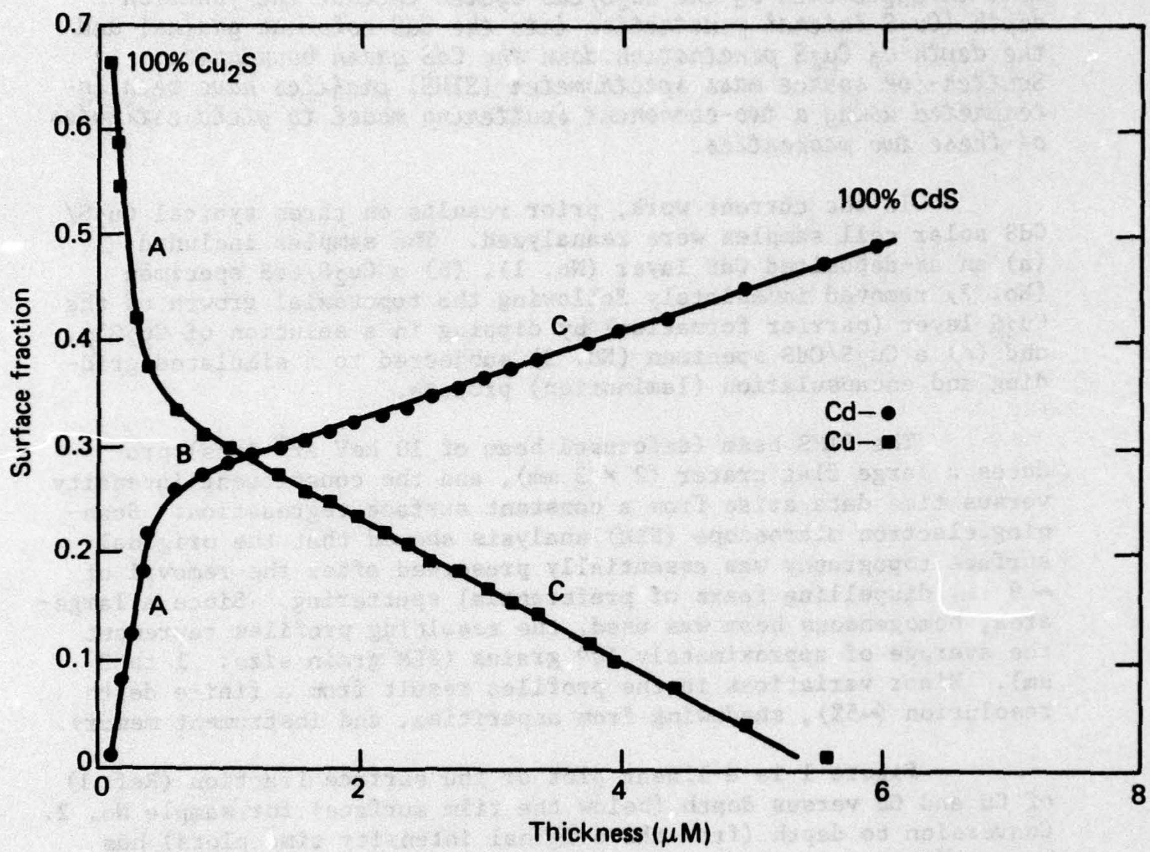

Fig. 1 Cu and Cd Surface Fraction versus Depth, Sample No. 2

factors should not be minimized, but, in the annular ring structure concept considered here, they will be included as one of the factors attributing to the transition region (B) described below.

There are three distinct regions on each curve in Fig. 1, an initial linear region (A), a transition region (B), and another linear region (C). For each material, region A begins at a depth of approximately 0.1 to 0.15 μm and extends to approximately 0.4 μm. Region C begins at 1.8 μm and continues to a depth of 5.7 μm where all traces of Cu_2S disappear. Between regions A and C there is a smooth transition region (B). Region B contains the equal composition point for Cu_2S and CdS (i.e., the point at which the SIMS beam sees 50% CdS and 50% Cu_2S). This occurs for a Cu surface fraction equal to 0.33 and a Cd surface fraction equal to 0.25.

The onset of region A corresponds to the showthrough of the CdS and, hence, gives a good indication of the depth of the Cu_2S layer, i.e., 0.1 to 0.15 μm, at least at the top of the grains. Region C begins approximately at 1.8 μm and continues to almost 6.0 μm. This onset occurs at almost twice the surface roughness estimate (0.5 to 1.0 μm determined from SEM) and suggests that the SIMS beam on the average sees an area composed of CdS grains with Cu_2S surface "rings" of linearly decreasing area (annular ring model). The depth of lateral penetration of the Cu_2S from the CdS grain boundary would then have a square root variation related to the decrease in area with depth. Ultimate grain boundary penetration appears to be limited to approximately 6.0 μm.

Simulated gridding and encapsulation only serve to delay the onset of region A to approximately 0.26 μm and the equal area point occurred at 0.75 μm. The slope of region C was changed slightly but no deeper grain boundary penetration was observed.

Future studies on sulfur stoichiometry anomalies and the resultant Σ (I/Y) deviations (Ref. 1) combined with additional SEM analysis should provide a more detailed picture of the Cu_2S/CdS solar cell structure, providing a basis of understanding for improving their performance.

<u>Principal Investigators</u>: H. K. Charles, Jr., and F. G. Satkiewicz. Dr. Charles is a senior engineer in the Microelectronics Group of the Engineering Facilities Division. Dr. Satkiewicz is a senior chemist in the Solid State Group of the Research Center.

References

1. F. G. Satkiewicz and H. K. Charles, Jr., "SIMS Analysis of Cu_2S/CdS Solar Cell Samples," Proc. of the 24th Annual Conf. on Mass Spectrometry and Allied Topics, San Diego, CA, 9-14 May 1976.

2. F. G. Satkiewicz and H. K. Charles, Jr., "Sputter Ion Mass Spectrometer Analysis of Copper Sulfide/Cadmium Sulfide Solar Cell Samples," APL/JHU TG 1284, October 1975.

AUTOMOTIVE POLLUTION REDUCTION BY WATER INJECTION

The objective of this project was to determine analytically and experimentally the efficacy of the addition of water to the fuel-air mixture used in the conventional automobile engine in reducing the amount of nitrogen oxides in the exhaust. It was concluded that a reduction of 50% or more can be accomplished without detriment to engine operation. Incidental benefits of the water addition include an improvement in effective octane rating of the fuel and provision of convenient means of using a combination of immiscible fuels, such as alcohol and gasoline.

The addition of water to the fuel-air mixture used by the standard automobile engine has been investigated as a means of reducing the pollution of the atmosphere by nitrogen oxides (NO_x) in the engine's exhaust.

Simple equipment, suitable either for retrofit to existing engines or for incorporation as original equipment in new production, was used to introduce regulated amounts of water into the test engine. The procedure used introduces the water into the intake of the engine by means separate from the conventional fuel carburetor (which is retained). The procedure permits instantaneous variation in the water-fuel ratio to meet varying operating conditions and avoids the necessity to mix water and gasoline in their liquid states.

Both analysis and test indicate that the addition of water at a mass rate equal to that of fuel reduces the nitrogen oxides in the exhaust by 50% or more, depending on specific operating conditions.

The unburned hydrocarbon and carbon monoxide content of the exhaust displayed no clear correlation in the tests performed with the presence or absence of the water addition. Specific fuel consumption was unaffected in the test engine by the addition of water, although power output was reduced slightly under some conditions. The antiknock property of water (evidenced by an advance in ignition timing) would permit the use of a lower octane fuel and of a higher compression ratio, both of which could be exploited to obtain economy of operation. The antiknock property could also be beneficial in reducing atmospheric pollution and in ensuring the longevity of catalytic afterburners by facilitating the gradual removal from the market of fuel containing tetraethyl lead.

The use of an ethanol-gasoline mixture as an automotive fuel has been advocated frequently as a means of stabilizing agricultural markets and of reducing the consumption of petroleum.

Current political and economic trends have renewed interest in this proposal. However, since minor contamination of fuel by water is difficult to avoid, the limited mutual solubility of gasoline and slightly aqueous alcohol produces a phase separation of the mixture in the supply tank, thereby resulting in erratic or complete interruption of engine operation. The use of the method reported herein to introduce an alcohol-water solution (rather than only water) would both provide a reduction in NO_x emission and also permit use of the two fuels in any ratio desired without limitation by mutual solubility and water contamination.

This work is more fully documented in internal report SDO-4305, "Benefits Provided by the Injection of Water into the Automobile Engine," December 1975. The results have been presented to ERDA.

<u>Principal Investigator</u>: T. Wyatt. Mr. Wyatt is a senior engineer in the Space Development Department Office.

VESSEL TRAFFIC SYSTEM

Over the past 10 years, the Laboratory has acquired considerable experience in areas of advanced vessel traffic monitoring and control. A new concept for low-cost improvements has evolved and the present IR&D project is aimed at establishing the feasibility of that concept.

The Laboratory had previously designed and constructed a vessel traffic system which was installed in the San Francisco Bay area under U.S. Coast Guard sponsorship. This was followed by a system installed at the U.S. Coast Guard R&D Center in Groton, Connecticut. The initial system utilized relatively expensive radar and computers. It is believed that use of new developments in microprocessor technology could now provide an improved automatic detection and tracking system with low-cost commercial radars.

A small IR&D program was initiated to study a radar video detector using inputs from a low-cost radar together with a microprocessor to assist in preprocessing of data, which would also permit the use of telephone rather than microwave links in handling data from remote sites.

The investigation was later expanded to a study leading to development of a collision avoidance system to interface with existing surface search radars. The proposed collision avoidance system would interface with a variety of existing surface search radars, providing an inexpensive yet capable system that could be used by both military and commercial vessels as an aid to maritime navigation. Such a system would be particularly applicable to the high-speed surface effect vessels ("flying ships").

Existing surface search radars, such as the AN/SPS-10 and Type B commercial radars, possess an untapped capability in that the video output from the radar receiver could be processed and used to implement a semiautomatic collision avoidance system. A combined analog and digital front-end would preprocess the incoming video to achieve a data rate compatible with a state-of-the-art microprocessor, which would perform additional digital signal processing. Ultimately, a track file of all surface targets would be developed, and from the track file the microprocessor would produce a display to assist the helmsman in maneuvering the ship. This could be a PPI type display on which synthetic tracks would be shown, or a tabular display on which tracks would be ranked according to some predetermined criteria, or a combination of the two. In addition, the system also would provide alerts that would warn of possible collisions and provide instructions to avert them. The microprocessor, a key element in this system to process

the video output from the radar receiver, was procured along with some interface equipment as a start to building up an inexpensive prototype.

Principal Investigator: D. B. Staake. Mr. Staake is Supervisor of the Operational Systems Development Branch in the Fleet Systems Department.

AIR TRAFFIC SAFETY AND CONTROL

During the past six years, the Laboratory has been applying its expertise derived primarily from Navy programs to the requirements of the Federal Aviation Administration. As a result of this work, several new areas have been identified as being worthy of exploratory investigations. Several IR&D-supported investigations related to the safety and capacity of the National Aviation System are highlighted in the following paragraphs.

AEROSAT-DOD SATCOM COMPATIBILITY

The objective of this project was to examine the consequences to the U.S. Department of Defense of the existence of the AEROSAT system. AEROSAT is a prospective international satellite system intended to provide civil aviation over-water air traffic control and ground-air communications. It was concluded that it would be advantageous to design the AEROSAT system so as to provide interoperability with DoD aircraft and to preclude interoperability or interference of civil aircraft and AEROSAT with the DoD satellite communications systems.

Oceanic air traffic control and ground-air communications are presently conducted over high-frequency radio circuits that operate with poor reliability and are nearly saturated on the heavily traveled routes. No system of airspace surveillance exists. Separation and control are based on pilots' reports of aircraft positions as determined from onboard navigation equipment.

Air traffic control and ground-air communications on ocean routes require improvement to permit smaller aircraft separations in order to handle future increases in traffic volume, particularly along North Atlantic routes. The United States, Canada, and Western European nations have agreed to cooperate in producing this improvement in air traffic control over the North Atlantic. The new system, which is named AEROSAT, will consist of two synchronous equatorial satellites located above the Atlantic Ocean, with ground stations on the North American Atlantic coast, in the United Kingdom, and on the European Atlantic coast, and aircraft equipment. The AEROSAT system will provide VHF and L-band ground-air communications and ground station determination of the position of aircraft over the North Atlantic by a radio-ranging technique. The positional information will be used for air traffic control and will also be provided to aircraft for use as a navigational aid. AEROSAT service is planned to begin in 1980.

The Department of Defense has several present and projected satellite communication systems that are used by military aircraft, ships, and land stations for message, voice, and data, typically at UHF and S-band. The DoD has no plans to produce a ground-station operated navigation system analogous to that of AEROSAT. It is U.S. policy that military aircraft be compatible with the existing air traffic control and communications systems.

AEROSAT will be designed, built, and operated by an international consortium. The detailed technical characteristics of the military systems are classified and cannot be shared with the consortium, even though the member nations of the initial North Atlantic segment are NATO allies. The expected expansion of the AEROSAT system to the other ocean areas will require a cooperative effort involving nations not allied militarily with the U.S.

Design of the AEROSAT system so as to provide interoperability of DoD aircraft with AEROSAT and to preclude interoperability or interference of civil aircraft and AEROSAT with the DoD satellite communications systems would provide the following benefits:

1. Safety, efficiency, and economy of North Atlantic air traffic control by vesting control of both military and civil aircraft in a single agency.

2. Responsiveness of North Atlantic air traffic control system in a military emergency.

3. Convenience of hand-off of North Atlantic air traffic to NATO air traffic control in military emergency.

4. Facility of use by the Civil Reserve Air Fleet.

5. Provision of means for air-sea coordination in the North Atlantic.

6. Reduction in risk that a civil system may interfere with existing and planned military systems.

7. Ease of extension of all above to South Atlantic, Pacific, and Indian Oceans, and the Mediterranean.

The Laboratory is qualified to provide technical assistance to the Federal Aviation Administration and to the Department of Defense in the coordination of the AEROSAT program and the DoD communication satellite programs.

<u>Principal Investigator</u>: T. Wyatt. Mr. Wyatt is a senior engineer in the Space Development Department Office.

AIRSPACE SAFETY ENHANCEMENT

One of the primary missions of the Federal Aviation Administration (FAA) is to meet the requirement of safe air travel. Many programs within the FAA and elsewhere have contributed to the maintenance of a good safety record for the current levels of aviation activity. However, projections of aviation activity indicate that by 1986 the FAA must be prepared to meet safety requirements with a traffic volume that is twice the current volume.

The present safety program conducted by the FAA, the National Transportation Safety Board (NTSB), and the National Aeronautics and Space Administration (NASA) covers many aspects of general aviation and scheduled air carrier operations within the National Aviation System (NAS). The FAA's programs range from the certification of pilots and aircraft to the flammability characteristics of the uniforms worn by flight attendants. This combined program relies to a large degree on the occurrence of mishaps (accidents/incidents) to determine where unsafe conditions exist.

In order to improve the performance of any complex system, it is necessary to quantify the exhibited performance on a recurring basis, isolate existing problem areas, and institute corrective feedback. The Laboratory has concluded that this approach can be advantageously applied to the improvement of NAS safety through the implementation of a recurring, comprehensive, nonpunitive safety enhancement program. The program would have as its hallmark the determination and implementation of required corrective actions before the need is demonstrated by a fatal aircraft accident. The type of engine speed settings that may have contributed to the National Airlines DC-10 accident near Albuquerque, New Mexico, on 3 November 1973 might have been uncovered by this type of investigation. It is conceivable that this and other similar accidents might have been prevented by procedural changes that could result from a safety enhancement program as described here. Initiation of such a program would also allow the FAA to demonstrate continuing responsiveness to recommendations from Department of Transportation Task Forces, the NTSB, and the General Accounting Office.

The Laboratory has compiled the following concepts for consideration as a nucleus during the formulation of an Airspace Safety Enhancement Program (ASEP) of the type indicated here:

1. At the initiation of the program, some mechanism must be devised to assure complete anonymity of the personnel involved in the NAS operations being evaluated. This would permit the ASEP to be nonpunitive (that is, the ASEP would constitute a nofault evaluation).

2. The digital flight data recorder (DFDR) and the cockpit voice recorder (CVR) should be the main sources of data initially. The data from each recorder would be systematically evaluated independent of data from the other. If this process indicates that a problem of sufficient importance exists, a correlated evaluation of the data from the DFDR and CVR for the same flight would be performed.

3. Initially, the ASEP would concentrate on the approach and landing phase of aircraft operations as the areas of greatest potential payoff.

4. This analysis would allow a quantified statistical description of NAS operations to be generated.

5. In the future, other sources of NAS data such as Automated Radar Terminal System (ARTS III) and NAS Stage A data extracts and audio recordings could be utilized, and the evaluation could be extended to other phases of NAS operations. Again, complete anonymity should be maintained.

6. The complete cooperation of personnel in all areas of NAS operations must be obtained initially and maintained continuously.

7. A mechanism must be devised to assure high-level FAA review of any recommendations that result from this program and implementation of those recommendations that are approved. Timeliness of action is important.

Principal Investigator: J. P. Berry. Mr. Berry is the Assistant Project Manager for the Surveillance Systems Project Office, Fleet Systems Department.

ELECTROSTATICS INVESTIGATION

The Laboratory has investigated the possible application of electrostatic measurements to the detection of aircraft wake vortices. The possible application of the same techniques to the detection of wind shear was also briefly studied. If successful, these techniques could enhance air safety.

Wake vortices (extremely high energy rotating "tubes" of air trailing behind an aircraft) are produced during the generation of lift by the aircraft. The diameter and energy of the

vortices are functions of aircraft size. The vortices are particularly violent during short intervals at takeoff and landing of heavy aircraft. If a small aircraft is trailing a heavy aircraft too closely, the small aircraft is subject to major perturbations in its flight path and, in certain circumstances, to overturning. To avoid this hazard, the Federal Aviation Administration (FAA) increases the spacing between aircraft with a consequent loss of capacity of the airport runway.

Electrical charge separation processes are generally associated with the exhausts from jet aircraft engines. It was hypothesized that electrically charged particles in engine exhausts may be trapped within the vortices, giving rise to concentrated tubes of electrical charge. Such tubes of charged particles could generate electric fields that may be detected at some distance from the core of the tube. By extension, it was believed that if these electric fields could be detected by electrostatic measurements, then a mechanism would exist for the detection of the wake vortices that could be applied by the FAA to reduce aircraft separation under the proper circumstances and thereby increase airport capacity without compromising safety.

A rudimentary electrostatic measurement detector was assembled and installed in the public parking area near the end of a runway at Washington National Airport. For a limited number of "targets of opportunity," some signatures were obtained that indicated the passage of aircraft. The results were somewhat promising but far from conclusive. In order to establish the validity of the hypothesis, it would be necessary to improve the instrumentation and to collect systematically a large body of data for a variety of aircraft types.

An extension of this idea was also briefly considered in connection with the detection of wind shear. The term wind shear is applied to rapid variations of wind speed and direction over very short distances. These rapid variations in wind produce rapid variations in lift that can have catastrophic effects on aircraft during takeoff and landing operations. Severe boundary layer shear and turbulence are frequently associated with thunderstorm activity. It was hypothesized that space charge excesses associated with thunderstorm activity might be entrained in downward convection within the storm cell and that these downdrafts containing the space charge might turn and flow parallel to the earth's surface, giving rise both to horizontal wind shear conditions and to a space charge excess remote from the storm that could be detected by an electrostatic measurement.

A Faraday cage containing a radioactive ionizer detector was installed on the top of one of the Laboratory buildings to test

this idea. The instrument was found to be sensitive to atmospheric phenomena during local and distant thunderstorm activity as evidenced by pulses correlated with lightning and more slowly varying signals probably indicative of large changes in space charge. No strong wind gusts occurred during the period of the experiment and the possible existence of high concentrations of space charge in horizontal wind shear flows was not confirmed. Additional investigation with an improved detector is warranted to test the hypothesis further; such investigations could also lead to new information about the fundamental electrical properties of thunderstorms.

Principal Investigator: M. L. Hill. Mr. Hill is the Supervisor of the Aerophysics and Flight Research Group.

AIRCRAFT FIRE EXTINGUISHMENT

Safety within the National Aviation System is of paramount concern to the Federal Aviation Administration (FAA). The Laboratory has investigated methods for the containment and extinguishment of both inflight and postcrash aircraft fuselage fires as one mechanism for improving the safety of air transportation.

The occurrence of inflight or postcrash fuselage fire may be a major cause of casualties, particularly in large commercial aircraft that carry hundreds of passengers. While much has been done to reduce the incidence of serious inflight engine and fuel fires, it appears that less has been accomplished to minimize the hazard of fuselage fires.

Much of the current FAA effort on reducing the hazard of fuselage fires is concentrated in the area of fire-resistant materials. It is frequently true that, when fire-resistant materials burn, they generate more toxic fumes than the less resistant materials. Moreover, current procedures that call for shutting down the ventilation system onboard the aircraft tend to increase the level of fumes. Descent from higher altitudes to lower altitudes tends to increase the amount of oxygen available to sustain a fire. Since smoke and toxic fumes are key ingredients in the lethality of cabin fires, improvements in the present methods for coping with these inflight fires and reducing the concentration of smoke and toxic fumes would help the FAA increase the level of safety. Studies of civilian fire casualties by the Laboratory in cooperation with the State of Maryland Medical Examiner and the Johns Hopkins School of Hygiene and Public Health have shown that the principal cause of fire casualties is inhalation of toxic substances.

Fires that almost inevitably follow aircraft crashes result in injury or death to aircraft occupants who might otherwise

have come through unscathed. After a crash, it is only a matter of minutes before a fire can reach an intensity that would prevent occupants from escaping the aircraft. Except for the hand fire extinguishers located in the aircraft cabin and the fire extinguishing system located in the engine compartments, aircraft carry no fire extinguishing equipment with which to combat a serious fire of the type resulting from the impact of a crash.

The Laboratory has considered a potential approach to the control of fire and the removal of toxic fumes for high-altitude (long-range) flights by exploiting the difference in pressure between the interior of the aircraft and the outside atmosphere. If appropriate modifications were made to the existing ventilation system to allow exhausting the air to the outside, the amount of oxygen in the aircraft could be reduced to a level that is insufficient to support combustion, and the amounts of harmful fumes produced by the fire could be reduced to tolerable levels. Specifically, oxygen concentrations of 10% would sustain life for short periods, but would not support the combustion of most materials. Use of this technique must take into account human tolerance to rapid changes and extremes in temperature and pressure, and to smoke, toxic fumes, and lack of oxygen, and the capabilities of existing emergency breathing equipment.

It has also been concluded that the following efforts would help to develop an effective onboard system for the immediate control of postcrash fires to gain time for the aircraft occupants to escape:

1. Select an appropriate extinguishing agent or a combination of agents (from, for example, carbon dioxide, liquid nitrogen, Halon 1301, and mechanical foams);

2. Develop and test an effective means for deploying these agents in the event of an incident;

3. Evaluate the quantities of extinguishing agents that the aircraft must carry as a function of the additional time they would provide for the escape of the occupants and for getting firefighting equipment to the aircraft; and

4. Evaluate the use of protective covers and/or shields for aircraft occupants to use during the evacuation of the aircraft.

Principal Investigator: F. K. Hill. Dr. Hill is Supervisor of the Fluid Mechanics Group.

SIGNAL PROCESSING INVESTIGATIONS I

One of the primary areas of investigation for improved air traffic control has been the processing of both broadband (video) signals and digitized information. These investigations have uncovered several areas which appear to merit exploratory development. Investigations in one such area are highlighted here.

Simple Air Traffic Control Automatic Advisory System

Based on experience derived to date, a simple, automatic Air Traffic Advisory System (ATAS) appears to be realizable. Currently, automated aircraft tracking systems such as the Federal Aviation Administration's (FAA's) Automated Radar Terminal System (ARTS) establish new or update existing tracks by correlating the relative positions of centroided raw surveillance system signal returns with the stored track data. After track updating, this relative position information is then deleted from the computer stores. At the same time, this very same information is provided to aircraft pilots by the ground-based traffic controllers in the form of air traffic advisories. If the above operation were automated, three direct and important benefits could accrue:

1. The air traffic controllers work load would be reduced (a productivity increase);

2. The use of the ground-to-air voice communications channels for air traffic advisories would be decreased (a capacity increase); and

3. The reliance on the human factor to ensure airspace separation of aircraft would be decreased (a safety increase).

The suggested ATAS would ultimately consist of a cockpit display of air traffic relative to each aircraft. The display would receive its input over a digital ground-to-air data link driven by the ground-based airspace surveillance system. Figure 1 is a block diagram of the ground-based portion of such an ATAS as interfaced with the FAA's ARTS III system. The corresponding airborne system is depicted in Fig. 2.

Since the key to the success of such a system is the development of an easy to use (by the pilot) low-cost airborne subsystem, work to date has concentrated on this aspect. The display (see Fig. 3) consists of a matrix of light-emitting diodes, one of

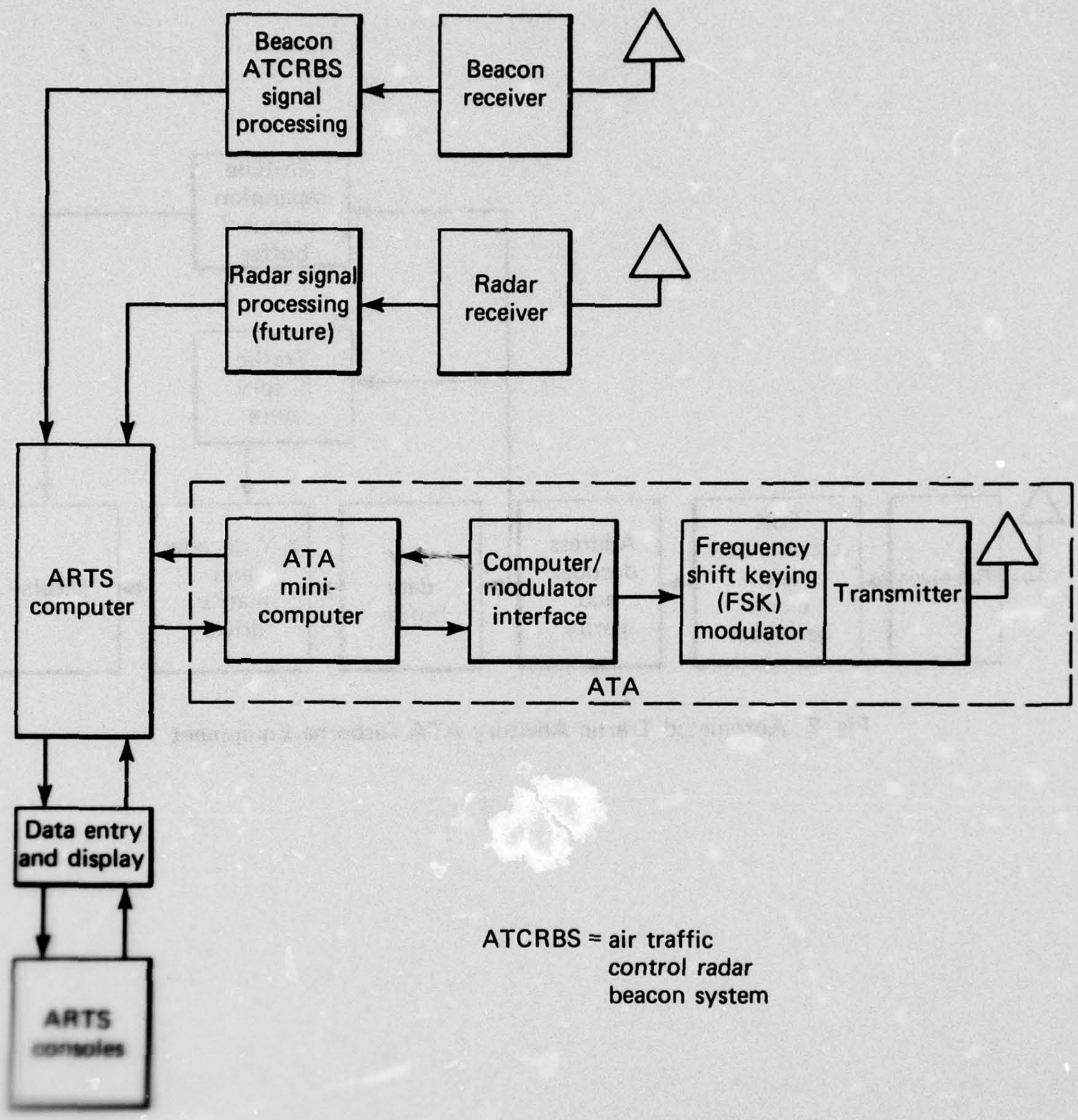

Fig. 1 Automated Traffic Advisory Ground Equipment

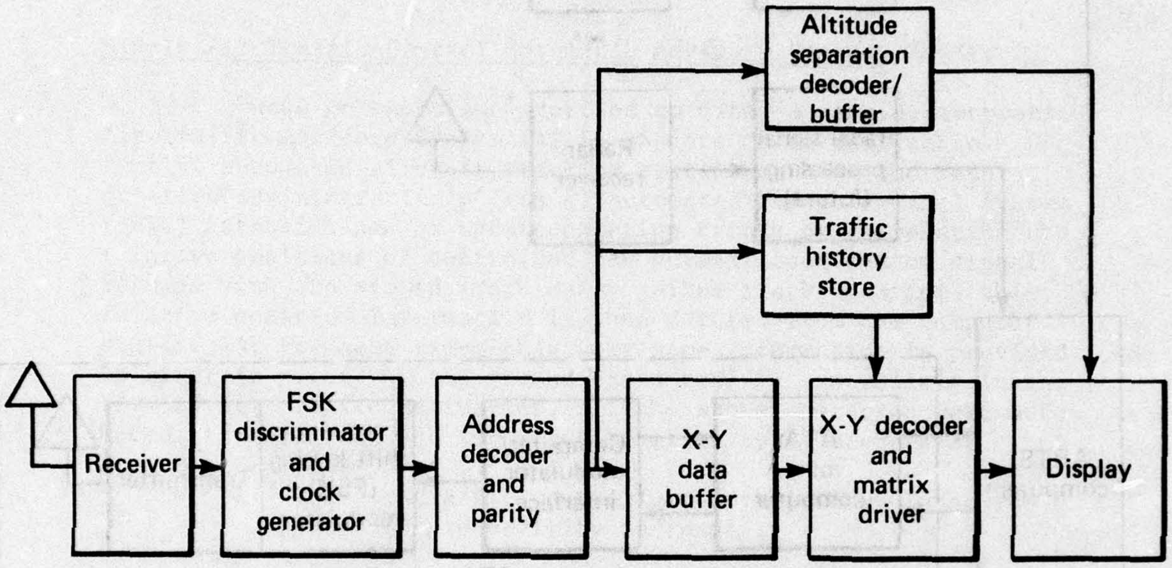

Fig. 2 Automated Traffic Advisory ATA Airborne Equipment

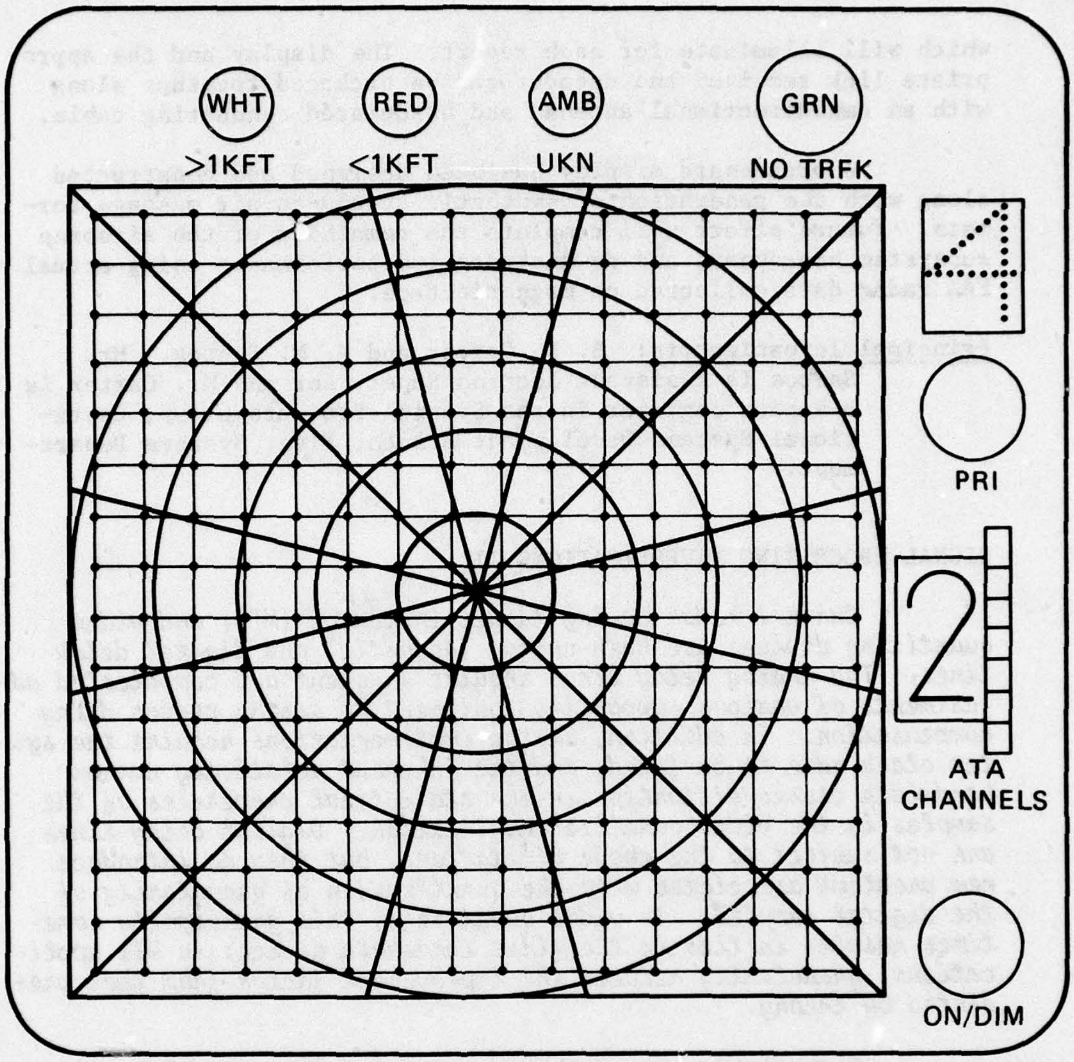

Description

Main Display: 16 x 16 LED matrix with polarized red filter and etched, edge-lighted plastic graticule. Range rings = 1 nmi, azimuth lines = 30^{o}.
Traffic Altitude Separation Lamps: White = >1Kft, red = <1Kft, amber = unknown separation.
No TRFK Lamp: Green = no traffic.
PRI (priority): Unit normally displays altitude separation and scan history of priority *one* (closest) traffic. Rotating PRI knob will light LED digit 2, 3, or 4; depressing knob will provide altitude separation and scan history display for that priority.
ATA Channel: Selects appropriate ATA(RF) channel.
ON/DIM: Turns unit on or off and controls illumination brightness.

Fig. 3 ATA Display (size X2)

which will illuminate for each report. The display and the appropriate link receiver and decoder can be packaged together along with an omnidirectional antenna and associated conducting cable.

A breadboard display has been designed and constructed along with the generation of synthetic ground-to-air message formats. Future effort will complete the remainder of the airborne subsystem breadboard and demonstrate its performance using actual FAA radar data collected on magnetic tape.

Principal Investigators: B. K. Carter and A. M. Santos. Mr. Santos is Assistant Section Supervisor and Mr. Carter is a senior engineer in the Special Projects Group, Operational Systems Development Branch, Fleet Systems Department.

SIGNAL PROCESSING INVESTIGATIONS II

Current radar moving target indicator (MTI) and video quantizing devices use both analog (acoustic) and digital delay lines. The analog delay lines require frequent and complicated adjustments of various supporting equipment to assure proper delay compensation. In addition, analog implementations require the system clock rate to be fixed, and the inherent relatively narrow bandwidth causes distortion in the statistical properties of the samples in the video quantizer application. Digital delay lines are not subject to the above limitations, but they do introduce new problems associated with the quantization of granularity of the digital samples. In video quantizers, this granularity sometimes results in ties in the first threshold device; in MTI applications, granularity reduces the improvement factor from that predicted by theory.

Recently developed charge-coupled devices (CCD's) offer a potential solution to these shortcomings of analog and digital delay lines. CCD's provide analog sampling with digital shifting capability. The adjustments required appear to be minimal, shift rates are variable, and speeds are comparable to those required for video processing techniques used in radar signal processing applications. An evaluation of a commercial grade tapped analog delay line (CCD) was conducted to determine on an empirical basis the actual performance capabilities of such a device in a rank order video quantizer. Based on a survey of available and most promising CCD's, a pair of Reticon Corporation tapped analog delay lines (TAD-112) was purchased for this investigation. This device, which is functionally a discrete-time tapped analog delay line with 12 output taps, was tested using the configuration shown in Fig. 1 to determine the following characteristics:

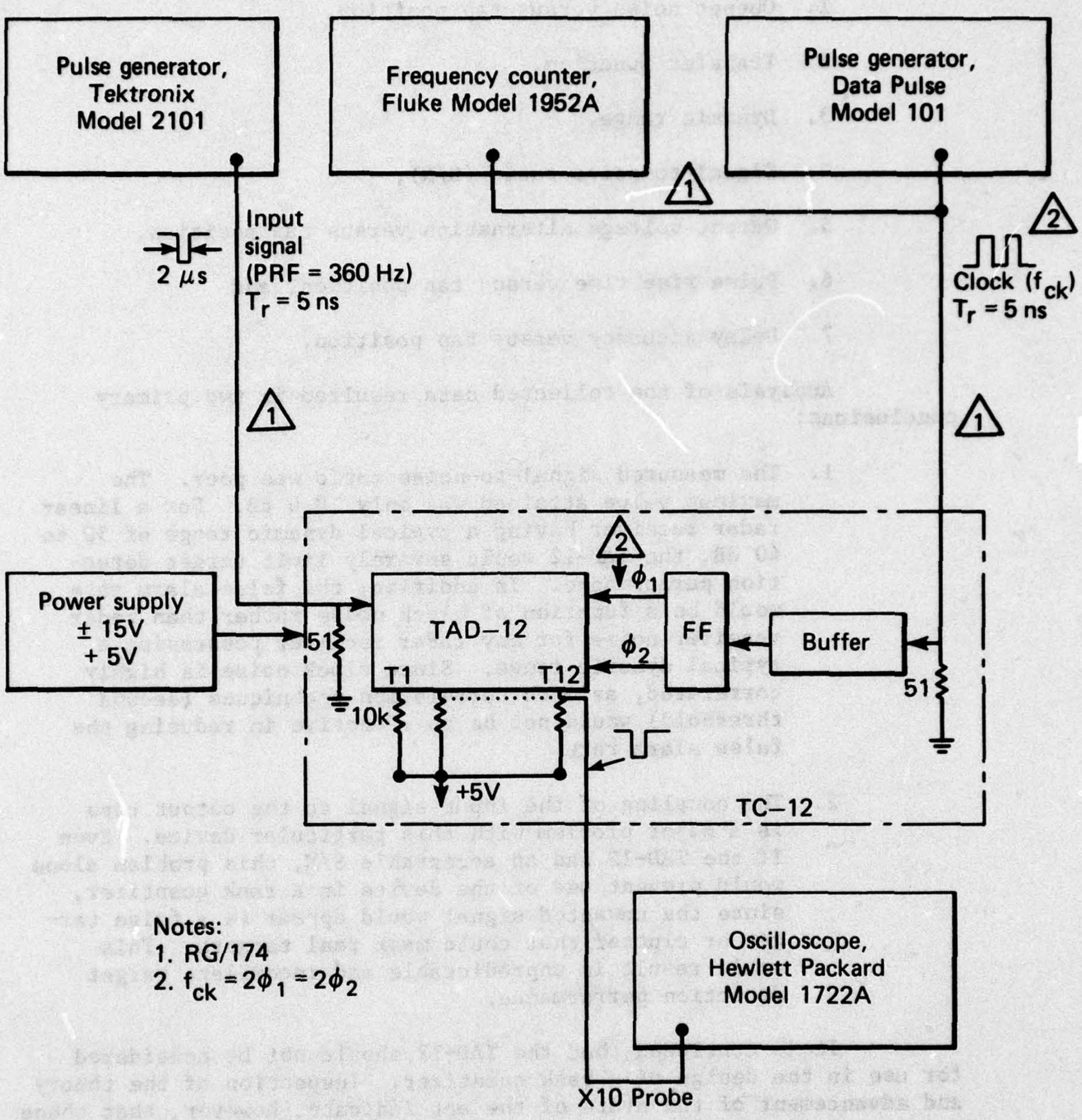

Fig. 1 CCD Test Configuration

1. Output noise versus tap position,
2. Transfer function,
3. Dynamic range,
4. Signal-to-noise ratio (S/N),
5. Output voltage alternation versus tap position,
6. Pulse rise time versus tap position, and
7. Delay accuracy versus tap position.

Analysis of the collected data resulted in two primary conclusions:

1. The measured signal-to-noise ratio was poor. The maximum value attained was only 18.6 dB. For a linear radar receiver having a typical dynamic range of 30 to 40 dB, the TAD-12 would severely limit target detection performance. In addition, the false alarm rate would be a function of clock noise rather than radar receiver noise for any radar receiver possessing a typical dynamic range. Since clock noise is highly correlated, azimuth correlation techniques (second threshold) would not be as effective in reducing the false alarm rate.

2. The coupling of the input signal to the output taps is a major problem with this particular device. Even if the TAD-12 had an acceptable S/N, this problem alone would prevent use of the device in a rank quantizer, since the unwanted signal would appear as a false target or clutter that could mask real targets. This would result in unpredictable and incomplete target detection performance.

It is concluded that the TAD-12 should not be considered for use in the design of a rank quantizer. Inspection of the theory and advancement of the state of the art indicate, however, that these devices should not be discounted for future applications without performing further investigation.

Principal Investigator: R. J. Erdahl. Mr. Erdahl is a senior engineer, Special Projects Group, Operational Systems Development Branch, Fleet Systems Department.

RESEARCH CENTER PUBLICATIONS

1 October 1975 - 30 September 1976

F. J. Adrian and V. A. Bowers, "g-Tensor and spin doubling constant in $^2\Sigma$ molecules CN and C_2H," Chem. Phys. Lett., Vol. 41, No. 3, 1976, p. 517.

F. J. Adrian, H. M. Vyas, and J. K. S. Wan, "Magnetic field and concentration dependence of CIDP in some quinone photolyses: Further evidence for an Overhauser mechanism," J. Chem. Phys., Vol. 65, No. 4, 15 August 1975, pp. 1454-1461.

R. J. Bartlett and D. M. Silver, "Some aspects of diagrammatic perturbation theory," Int. J. Quantum Chem. Symp., Vol. 9, December 1975, pp. 183-198.

R. J. Bartlett and D. M. Silver, "Erratum: Many-body perturbation theory applied to electron pair correlation energies. I. Closed-shell first row diatomic hydrides (J. Chem. Phys. 62, 1975)," J. Chem. Phys., Vol. 64, No. 3, February 1976, p. 1260.

R. J. Bartlett and D. M. Silver, "Erratum: Pair-correlation energies in sodium hydrides with many-body perturbation theory (Phys. Rev. A, 10, 1974, 1927)," Phys. Rev. A., Vol. 13, No. 2, February 1976, p. 912.

R. J. Bartlett and D. M. Silver, "Many-body perturbation theory applied to electron pair correlation energies. II. Closed shell second-row diatomic hydrides," J. Chem. Phys., Vol. 64, No. 11, June 1976, pp. 4578-4586.

J. F. Bird, "An elemental phenomenon of vision-suprafusion transients: General theory retinal-cortical manifestations, Potential application," J. Theor. Biol., Vol. 55, No. 2, 1975, pp. 553-557.

N. A. Blum and C. Feldman, "The crystallization of amorphous Germanium films," J. Non-Cryst. Solids, Vol. 22, 1976, pp. 29-35.

N. A. Blum and R. B. Frankel (MIT), "Hyperfine interactions in antiferromagnetic EuTe using the Te-125 Mossbauer resonance, magnetism and magnetic materials, 1975," eds. J. J. Becker et al., AIP Conf. Proc. No. 29, AIP, New York, 1976, pp. 416-417.

J. Bohandy and B. F. Kim, "Optical spectra of Ni Porphin, Pd Porphin and free base Porphin in single crystal Triphenylene," Spectrochim. Acta 32A, August 1976, pp. 1083-1088.

N. J. Brown and D. M. Silver, "Reactive and inelastic scattering of H_2+D_2 using a London-type potential energy surface," J. Chem Phys., Vol. 65, No. 1, 1 July 1976, pp. 311-325.

F. L. Carter (NRL) and C. Feldman, Fifth International Symposium on Boron and Borides, ONR London Conference Report C-12-76, 27 May 1976, pp. 1-6.

J. Davidson (USN), V. G. Sigillito, and JHU Evening College, "A basic-to-APL translator," APL Quote Quad, Vol. 6, No. 4, winter 1976, pp. 8-13.

L. W. Ehrlich and M. M. Gupta, "Some difference schemes for the biharmonic equation," SIAM J. Num. Anal., Vol. 12, No. 5, October 1975, pp. 773-790.

R. A. Farrell and R. L. McCally, "On corneal transparency and its loss with swelling," J. Opt. Soc. Am., Vol. 66, No. 4, April 1976, pp. 342-345.

R. A. Farrell and R. L. McCally, "On the interpretation of depth dependent light scattering measurements in normal corneas," Acta Ophthalmol., Vol. 54, August 1976, pp. 261-270.

C. Feldman, H. K. Charles, Jr., F. G. Satkiewicz, and J. Bohandy, "Electrical properties of carbon-doped amorphous boron film," J. Less-Common Metals, Vol. 47, 1976, pp. 141-145.

D. W. Fox, "Transient solutions for stratified fluid flows," J. Res. Nat. Bur. Stand., Sec. B., Vol. 80B, No. 1, January-March 1976, pp. 79-88.

M. H. Friedman, "Self-consistent analysis of arterial uptake of cholesterol from perfusing serum," Circ. Res., Vol. 38, No. 3, March 1976, pp. 215-216.

M. H. Friedman, "Transport through a growing boundary layer to a permeable wall," AIChE J., Vol. 22, No. 2, March 1976, pp. 407-409.

M. H. Friedman and L. W. Ehrlich, "Effect of spatial variations in shear on diffusion at the wall of an arterial branch," Circ. Res., Vol. 37, October 1975, pp. 446-454.

S. K. Ghatak (C.N.R.S., Grenoble) and K. Moorjani, "Structurally disordered Heisenberg ferromagnet," Solid State Commun., Vol. 17, 1975, pp. 293-295.

S. K. Ghatak (C.N.R.S., Grenoble) and K. Moorjani, "Spin glasses: Beyond the molecular field approximation," J. Phys. C: Solid State Phys., Vol. 9, June 1976, pp. L293-295.

S. Green and L. Monchick, "Validity of approximate methods in molecular scattering: Thermal HCl-He Collisions," J. Chem. Phys., Vol. 63, No. 10, 15 November 1975, pp. 4198-4205.

B. F. Hochheimer and R. Flower, "Simultaneous choroidal and retinal angiography," Johns Hopkins Med. J., Vol. 138, 1976, p. 33.

L. W. Hunter, C. Grunfelder, and R. M. Fristrom, "The effect of CF_3Br on a CO-H_2-O_2-Ar diffusion flame," Halogenated Fire Suppressants, 1975, ACS Symposium Series #16, Am. Chem. Soc., pp. 234-255.

B. F. Kim, "Low Angle Light Scattering Apparatus," Rev. Sci. Instrum., Vol. 47, No. 9, September 1976, pp. 1039-1043.

B. F. Kim and J. Bohandy, "Site selective spectra of Zn Porphin in Triphenylene," Opt. News, September 1975 (received in October, not reported in FY 75).

T. J. Kistenmacher, T. E. Phillips, D. O. Cowan, A. N. Bloch, and T. O. Poehler, "Crystal Structure and Diffuse X-Ray Scattering in the 1.3:2 Salt of 4,4', 5,5' Tetramethyl-$\Delta^{2.2'}$-bis-1,3-Dithiole (TMTTF) and 7,7,8,-Tetracyano-p-quinodimethane (TCNQ), a Non-Stoichiometric Quasi-One-Dimentional Organic Conductor," Acta Crystallog., Vol. B32, 1976, p. 539.

H. A. Kues, J. C. Murphy, P. R. Zarriello, and L. C. Aamodt, "Convenient electron spin resonance/optically detected magnetic resonance spectrometer," Rev. Sci. Instrum., Vol. 46, No. 11, November 1975.

R. L. McCally and R. A. Farrell, "The depth dependence of light scattering from the normal rabbit cornea," Exp. Eye Res., Vol. 23, July 1976, pp. 69-81.

R. A. Meyer, R. E. Walker, and V. Mountcastle, "A laser stimulator for the study of cutaneous thermal and pain sensations," IEEE Trans. Biomed. Eng., Vol. 23, No. 1, January 1976, pp. 54-60.

K. Moorjani and S. K. Ghatak (C.N.R.S., Grenoble), "Bethe-Peierls-Weiss Approximation in disordered ferromagnets," AIP Conference Proceedings, Magnetism and Magnetic Materials, Vol. 29, May 1976, pp. 152-153.

G. H. Mowbray, R. W. Flower, and J. F. Bird, "Visual cortex responses to abrupt changes in the periodicity of rapidly intermittent light," Electroencepholog r. Clin. Neurophysiol., Vol. 39, No. 4, October 1975, pp. 305-312.

V. O'Brien, "Pulsatile fully-developed flow in rectangular channels," J. Franklin Inst., Vol. 300, No. 3, September 1975, pp. 225-230.

V. O'Brien, "Reply by Author to D. P. Telionis," AIAA J., Vol. 13, No. 12, December 1975, p. 1680.

V. O'Brien, L. W. Ehrlich, and M. H. Friedman, "Unsteady flow in a branch," J. Fluid Mech., Vol. 75, Pt. 2, May 1976, pp. 315-336.

J. G. Parker, "Reduction of total coliform counts of natural water samples by means of laser radiation," Water and Sewage Works, Vol. 123, No. 5, May 1976, pp. 52-53.

T. O. Poehler, R. Gemmer, D. O. Cowan, and A. N. Bloch, "Chemical purity and the electrical conductivity of Tetrathiofulvalenium Tetracyanoquinodimethanide," Org. Chem., Vol. 40, No. 24, November 1975.

T. O. Poehler et al., "The organic state," Mol. Cryst. Liq. Cryst., Vol. 32, 1976, pp. 223-225.

F. G. Satkiewicz and H. K. Charles, Jr., "SIMS analysis of Cu_2S/CdS solar cell samples," Proceedings of the 24th Annual Conference on Mass Spectrometry and Allied Topics, May 1976, San Diego, CA.

J. A. Schetz, F. S. Billig, and S. Favin, "Simplified analysis of supersonic base flows including injection and combustion," AIAA J., Vol. 14, No. 1, January 1976, pp. 7-8.

J. A. Schetz, S. Favin, and F. S. Billig, "Analytical comparison of the performance of different base burning modes," AIAA J., Vol. 14, No. 9, September 1976, pp. 1337-1338.

V. G. Sigillito, "A priori inequalities and the Dirichlet problem for a pseudoparabolic equation," SIAM J. Math. Anal., Vol. 7, No. 2, April 1976, pp. 222-229.

V. G. Sigillito, "A priori inequalities and approximate solutions of the first boundary value problem for $\Delta^2 u = f$," SIAM J. Num. Anal., Vol. 13, No. 2, April 1976, pp. 251-260.

D. M. Silver and R. J. Bartlett, "Modified potentials in many-body perturbation theory," Phys. Rev. A, Vol. 13, No. 1, January 1976, pp. 1-12.

G. A. Thomas et al., "Electrical Conductivity of Tetrathiofulvalenium Tetracyanoquinodimethanide (TTF-TCNQ)," Phys. Rev. B, Vol. 13, June 1976, p. 5105.

G. W. Turner, H. K. Charles, Jr., and C. Feldman, "Switching in amorphous boron films under single pulse conditions," J. Appl. Phys., Vol. 47, No. 8, 1976, pp. 3618-3624.

R. Turner and R. A. Murphy, "The Far Infrared Helium Laser," Infrared Phys., Vol. 16, 1976, pp. 197-200.

R. Turner and T. O. Poehler, "Electrically initiated pulsed chemical DF-CO_2 and DF laser," J. Appl. Phys., Vol. 47, No. 7, July 1976, pp. 3038-3041.

A. A. Westenberg and N. deHaas, "Rate of the reaction $O + SO_2M \rightarrow SO_3M^*$," J. Chem. Phys., Vol. 63, No. 12, 15 December 1975, pp. 5411-5415.

S. Wilson, "The group function model. A set of orthogonality conditions," J. Chem. Phys., Vol. 64, No. 4, February 1976, pp. 1692-1696.

RESEARCH CENTER PAPERS ACCEPTED FOR PUBLICATION

1 October 1975 - 30 September 1976

F. J. Adrian and V. A. Bowers, "ESR Spectrum of Xe Cl in Argon at 4.2 °K," J. Chem. Phys.

N. A. Blum and C. Feldman, "The Crystallization of Amorphous Germanium Films," J. Non-Cryst. Solids.

D. W. Fox and V. G. Sigillito, "Steady State Oscillations in a Buoyant Fluid," J. Appl. Math. Phys.

B. F. Hochheimer and J. Calkin, "The Irradiance of Flashbulbs," Opt. Eng.

A. N. Jette and F. J. Adrian, "Theoretical Investigation of the Hyperfine Structure Constants of the V_K and $(XY)^-$ Centers Using a Valence Bond Wave Function for the Halogen Molecule Anions," Phys. Rev.

R. I. Joseph and R. A. Farrell, "High Temperature Series for the Spin-One Ising Model for Arbitrary Biquadratic Exchange, Field and Anisotropy," Physics.

K. Moorjani and S. K. Ghatak (C.N.R.S., Grenoble), "Critical Behavior of a Structurally and Chemically Disordered Ferromagnet," J. Phys. C: Solid State.

V. O'Brien, "Steady and Unsteady Flow in Non-Circular Straight Ducts," ASME J. Appl. Mech.

T. O. Poehler and J. W. Leight, "DF-CO_2 and DF Chemical Waveguide Laser," J. Appl. Phys.

D. M. Silver, S. Wilson, and R. J. Bartlett, "Modified Potentials in Many-Body Perturbation Theory: Three-Body and Four-Body Contributions," Phys. Rev. A.

L. H. Viehland, E. A. Mason, T. H. Stevens, and L. Monchick, "Test of the H_2^+ - He Interaction Potential. Comparison of the Interactions of He with H^+, H_2^+, and H_3^+," Chem. Phys. Lett.

S. Wilson, R. J. Bartlett, and D. M. Silver, "Many-Body Effects in the $X^1\Sigma^+$ States of the Hydrogen Fluoride, Lithium Fluoride and Boron Fluoride Molecules," Molec. Phys.

S. Wilson and D. M. Silver, "Diagrammatic Perturbation Theory: Many-Body Effects in the $X^1\Sigma^+$ States of First-Row and Second-Row Diatomic Hydrides," J. Chem. Phys.

EXPLORATORY DEVELOPMENT PUBLICATIONS

1 October 1975 - 30 September 1976

T. P. Armstrong and S. M. Krimigis, "Interplanetary acceleration of relativistic electrons observed with IMP-7," J. Geophys. Res., Vol. 81, 1976, p. 677.

W. M. Cronyn, S. D. Shawhan, F. T. Erskine, A. H. Huneke, and D. G. Mitchell, "Interplanetary scintillation observations with the COCOA-Cross radio telescope," J. Geophys. Res., Vol. 81, 1976, p. 695.

J. P. Doering, W. K. Peterson, C. O. Bostrom, and T. A. Potemra, "High resolution daytime photoelectron energy spectra from AE-E," Geophys. Res. Lett., Vol. 3, 1976, p. 129.

T. Iijima and T. A. Potemra, "The amplitude distribution of field-aligned currents at northern high latitudes observed by TRIAD," J. Geophys. Res., Vol. 81, 1976, p. 2165.

E. P. Keath, E. C. Roelof, C. O. Bostrom, and D. J. Williams, "Fluxes of ≥ 50 keV protons and ≥ 30 keV electrons at ~ 35 R_e. 2. Morphology and flow patterns in the magnetotail," J. Geophys. Rev., Vol. 81, 1976, p. 2315.

S. M. Krimigis, J. W. Kohl, and T. P. Armstrong, "The magnetospheric contributions to the quiet-time low energy nucleon spectrum in the vicinity of earth," Geophys. Res. Lett., Vol. 2, 1975, p. 457.

S. M. Krimigis, E. T. Sarris, and T. P. Armstrong, "Observations of Jovian electron events in the vicinity of earth," Geophys. Res. Lett., Vol. 2, 1975, p. 561.

D. G. Mitchell and E. C. Roelof, "A Mathematical analysis of the theory of interplanetary scintillation in the weak-scattering approximation," J. Geophys. Res., Vol. 81, 1976, p. 5071.

H. L. Olsen and P. P. Pandolfini, "Analytical study of two-phase-flow heat exchangers for OTEC Systems," AEO-76-37, November 1975.

H. L. Olsen, P. P. Pandolfini, R. W. Blevins, G. L. Dugger, and W. H. Avery, "Design of low-cost aluminum heat exchangers for OTEC plant ships," Proceedings, Sharing the Sun Conference, International Solar Energy Society, Winnipeg, Canada, 15-20 August 1976.

E. C. Roelof, E. P. Keath, C. O. Bostrom, and D. J. Williams, "Fluxes of $\geq$ 50 keV protons and $\geq$ 30 keV electrons at $\sim$ 35 R_e. 1. Velocity anisotropy and plasma flow in the magnetotail," J. Geophys. Res., Vol. 81, 1976, p. 2304.

E. C. Roelof, S. M. Krimigis, W. M. Cronyn, S. D. Shawhan, and P. S. McIntosh, "Solar wind and energetic particle events of June 20-30, 1974 analyzed using measurements of interplanetary radio scintillations at 34.3 MHz," Space Res. XVI, ed. M. J. Rycroft and R. D. Reasenberg, Akademie-Verlag (Berlin), 1976, p. 727.

E. T. Sarris, S. M. Krimigis, and T. P. Armstrong, "Observations of a high-energy ion shock spike in interplanetary space," Geophys. Res. Lett., Vol. 3, 1976, p. 133.

E. T. Sarris, S. M. Krimigis, and T. P. Armstrong, "Observations of magnetospheric bursts of high energy protons and electrons at $\sim$ 35 R_e with IMP-7," J. Geophys. Res., Vol. 81, 1976, p. 2341.

E. T. Sarris, S. M. Krimigis, T. Iijima, C. O. Bostrom, and T. P. Armstrong, "Location of the source of magnetospheric energetic particle bursts by multispacecraft observations," Geophys. Res. Lett., Vol. 3, 1976, p. 437.

F. G. Satkiewicz and H. K. Charles, Jr., "Sputter ion mass spectrometer analysis of Copper Sulfide/Cadmium Sulfide solar cell samples," APL/JHU TG 1284, October 1975.

F. G. Satkiewicz and H. K. Charles, Jr., "SIMS analysis of Cu_2S/CdS solar cell samples," Proceedings of the 24th Annual Conference on Mass Spectrometry and Allied Topics, San Diego, CA, 9-14 May 1976 (see Research Center Publications).

M. Sugiura and T. A. Potemra, "Net field-aligned currents observed by TRIAD," J. Geophys. Res., Vol. 81, 1976, p. 2155.

AD-A048 852 JOHNS HOPKINS UNIV LAUREL MD APPLIED PHYSICS LAB F/G 20/12
INDIRECTLY FUNDED RESEARCH AND EXPLORATORY DEVELOPMENT AT THE A--ETC(U)
JUL 77 R W HART N00017-72-C-4401
UNCLASSIFIED APL/JHU/SR-77-2 NL

3 OF 3
AD
A048852

END
DATE
FILMED
2-78
DDC

INITIAL DISTRIBUTION EXTERNAL TO THE APPLIED PHYSICS LABORATORY*

The work reported in SR 77-2 was done under Task X8 of Contract N00017-72-C-4401 with the Department of the Navy.

ORGANIZATION	LOCATION	ATTENTION	No. of Copies
DEPARTMENT OF DEFENSE			
Harry Diamond Lab.	Washington, DC 20438	A. Renner, 1040	1
DDC	Alexandria, VA		12
Department of the Navy			
Assistant Secretary, R&D	Washington, DC 20350		1
Office of the Assistant Secretary, R&D	Washington, DC 20360	Dr. S. Koslov	1
Commands			
NAVSEASYSCOM			
Commander	Washington, DC 20360	SEA-00	1
Assistant Deputy Dir./Tech. Dir. R&T	Washington, DC 20360	SEA-03B	1
Chief Engineer	Washington, DC 20362	SEA-00E	1
	Washington, DC 20360	SEA-06Gb	1
	Washington, DC 20360	SEA-0253W	1
	Washington, DC 20360	SEA-0341	1
	Washington, DC 20360	RADM W. Dedrick	1
NAVAIRSYSCOM	Washington, DC 20360	AIR-310B	1
Offices			
Naval Research	800 N. Quincy St.	ONR-420	1
	Arlington, VA 22217	ONR-470	1
NAVPLANTREPRO	Laurel, MD 20810		1
Defense Contract Audit Agency	Laurel, MD 20810		1
Laboratories			
Naval Research Lab.	Washington, DC 20390	NRL-6000	1
Department of the Army			
USA Electronics Command	Ft. Monmouth, NJ 07703	Proj. Mgr., NAVCON	1
			1
USA Research Office	Physics Dept. Box CM, Duke Station Durham, NC 27706	Dr. C. Boghosian	1
Department of the Air Force			
Deputy Chief of Staff, R&D	Washington, DC 20330	LGEN A. D. Slay	1
Office of Scientific Research	Washington, DC 20330	Dr. Max Swerdlow	1
HQ ASD	Wright-Patterson AFB	C. H. Marshall, ASD/RWDE	1
Avionics Lab., Guid. and Nav. Anal. Office	Wright-Patterson AFB Dayton, OH	J. W. Chin, NVA/666A	1
L. G. Hanscom Field	Bedford, MA 01730	L. Higginbotham, ESD/DCL Stop 43	1
U.S. GOVERNMENT AGENCIES			
NASA	Washington, DC 20546	Code RRC	1
National Science Foundation	1800 G St., N.W. Washington, DC 20550	Dr. R. Silberglitt	1
		Dr. H. W. Etzel	1
		Dr. W. E. Wright	1
		Dr. T. Kitchens	1

Requests for copies of this report from DoD activities and contractors should be directed to DDC, Cameron Station, Alexandria, Virginia 22314 using DDC Form 1 and, if necessary, DDC Form 55.

*Initial distribution of this document within the Applied Physics Laboratory has been made in accordance with a list on file in the APL Technical Publications Group.

INITIAL DISTRIBUTION EXTERNAL TO THE APPLIED PHYSICS LABORATORY*

SR 77-2

ORGANIZATION	LOCATION	ATTENTION	No. of Copies
UNIVERSITIES			
JHU Center for Metro. Planning and Research	Shriver Hall Baltimore, MD 21218	J. Fischer, Dir.	1
CONTRACTORS			
Woods Hole Oceanographic Institution	Woods Hole, MA 02543	Paul Fye, Dir.	1

*Initial distribution of this document within the Applied Physics Laboratory has been made in accordance with a list on file in the APL Technical Publications Group.